Freie Universität Berlin

Freie Universität Berlin, Institute of Geological Sciences, Workgroup Hydrogeology

Integrated Watershed Management - Geogenic and anthropogenic impact on the ground- and surface water quality in the Krom Antonies River-Valley, South Africa

Master Thesis

Submitted by

Heinrich Hecht, Matriculation Number: 4200638

February 2015

1. Referee: Prof. Dr. Michael Schneider

2. Referee: Prof. Dr. Brigitta Schütt

Content

List of Figures VI

List of Tables X

List of Abbreviations XI

Summary XII

Zusammenfassung XIII

1 Introduction 1

1.1 Project - IWM Research & Development Capacity Building 1

1.2 Objectives of the study 3

1.3 Study Area 4

1.3.1 Climate 5

1.3.1 Landuse 5

1.3.2 Drainage 6

2 Geology and Hydrogeology 7

2.1 Geology 7

2.1.1 Geological history of the study area 10

2.1.2 Alluvium 12

2.1.3 Malmesbury Group 12

2.1.4 Table Mountain Group 13

2.1.5 Riviera Granite 14

2.1.6 Structural geology 15

2.2 Hydrogeology 17

2.2.1 Groundwater recharge 17

2.2.2 Groundwater Level 20

3 Methodology 21

3.1 Sampling and onsite measurements 21

3.1.1 Preparation of the samples 21

3.1.1 Onsite measurements 23
3.2 Hydrochemical analyses 24
3.3 Water classification 25
3.3.1 Nomenclature 25
3.3.2 WHO maximum permissible values 27
4 Results 28
4.1 Cross-sections 28
4.1.1 Cross-section A - A´- B 29
4.1.2 Cross-section C - D 30
4.1.3 Cross-section E - F 31
4.1.4 Cross-section G - H 32
4.1.5 Cross-section I - I´- J 33
4.2 Groundwater dynamics 34
4.3 Hydrochemistry 35
4.3.1 Cations 35
4.3.2 Anions 36
4.3.3 Ionic balance error 37
4.4 Hydrochemical distribution maps 39
4.4.1 Conductivity 41
4.4.2 pH 42
4.4.3 Sodium 43
4.4.4 Calcium 44
4.4.5 Chlorine 45
4.4.6 Bicarbonate 46
4.4.7 Magnesium 47
4.4.1 Ammonium 48
4.4.2 Nitrite 49
4.4.1 Nitrate 50

4.4.2 Manganese 51
4.4.3 Fluorine 52
4.4.4 Sulfur 53
4.4.5 Sulfate 54
4.4.6 Phosphate 55
4.4.7 Arsenic 56
4.4.8 Bromine 57
4.4.9 Potassium 58
4.4.10 Iron 59
4.4.11 Strontium 60
4.4.12 Silicon 61
4.5 Piper- and Schoeller plots 62
4.6 Classification of waters 64
5 Interpretation 65
5.1 Geology and groundwater 65
5.1.1 Riviera Granite aquifer 67
5.1.2 Malmesbury Rock aquifer 68
5.1.3 Table Mountain Rock aquifer 68
5.1.4 Special locations 68
5.1.5 Krom Antonies River 69
5.2 Anthropogenic influence on the groundwater 70
5.2.1 Ammonium 70
5.2.2 Nitrate 71
5.2.3 Phosphate 71
5.2.4 Manganese 71
5.2.5 Arsenic 71
6 Conclusion 72
6.1 Geology and groundwater 72

6.2 Anthropogenic influence on the groundwater 72
6.3 Henceforward water quality 73
6.4 Discussion 74
6.5 Recommendations for future research 75
7 Appendix 76
7.1 Appendix A: Glossary of Terms 76
7.2 Appendix B: Timeline 78
7.3 Appendix C: Measuring points 80
7.4 Appendix D: Maps 109
7.5 Appendix E: Acknowledgments 112
7.6 Appendix F: References 114

List of Figures

Fig. 1: Title Image: View of the hills and mountains formed by quartzitic sandstones of the Table Mountain Group inside the Krom-Antonies catchment. Line of sight: NE. ccby, H.Hecht. I

Fig. 2: Western Cape Province, source: GoogleEarth. 4

Fig. 3: Roadmap near Moutonshoek Valley (red square), source: GoogleEarth. 4

Fig. 4: A center pivot irrigation system in central Montana. ccby-sa: Montanabw. 5

Fig. 5: Geology of the Piketberg area (after De Beer 1990 and Rozendaal 1994). The red outline point out the study area. 7

Fig. 6: Geological map of the Moutonshoek Valley (after De Beer 1990 and Rozendaal 1994). The estimated shape of the Riviera Granite is not representative. Imagery: LANDSAT prepared with ARCGIS 10.1. 8

Fig. 7: Topographic map of the Moutonshoek Valley. 9

Fig. 8: Geological map of the western Cape, showing the distribution of the Malmesbury Group, its formations, the overlying Cape Supergroup and the Cape Granite Suit. The red rectangle shows the position of the study area in Moutonshoek Valley (after BELCHER 2003, modified from ROZENDAAL ET AL1994). 10

Fig. 9: Geological cross-section of the Riviera granite dome (ROZENDAAL ET AL. 1994) 14

Fig. 10: Geological cross-sections in the Piketberg area showing the structural relationship and spatial position of the Riviera pluton (After ROZENDAAL ET AL 1994). 16

Fig. 11: Geology of the Piketberg area (after DE BEER 1990 & ROZENDAAL 1994). 16

Fig. 12: Groundwater recharge of the area (CONRAD 2012, GEOSS-REPORT 2006). 18

Fig. 13: Mean Annual Effective Recharge (mm/a) from Rainfall (VISSER 2009). 19

Fig. 14: Selection of the Observation points in the study area. The black crosses are showing the position of shallow boreholes which only reaches the first aquifer about up to 20 m depth as well as river- and dam samples. The red dots are the positions of the boreholes deeper than about 20 m which reaches below the clay layer into the second aquifer. The blue dots are

additive boreholes as part of the documentation for the DWA. The map is based on LANDSAT images, edited with ArcGIS and photoshop. 22

Fig. 15: Geological map including cross sections. 28

Fig. 16: Vertical exaggerated cross section A - A´ - B. 29

Fig. 17: Vertical exaggerated cross section C-D. 30

Fig. 18: Vertical exaggerated cross section E-F. 31

Fig. 19: Vertical exaggerated cross section G-H. 32

Fig. 20: Vertical exaggerated cross section I - I´ - J. 33

Fig. 21: Map of the estimated groundwater flow in Moutonshoek Valley. 34

Fig. 22: Observation points of the master thesis in Moutonshoek Valley (Sa01 - Sa30). 39

Fig. 23 and 24: Spatial distribution maps of the conductivity. 40

Fig. 25 and 26: Spatial distribution maps of the pH. 41

Fig. 27 and 28: Spatial distribution maps of Sodium. 42

Fig. 29 and 30: Spatial distribution maps of Calcium. 43

Fig. 31 and 32: Spatial distribution maps of Chlorine. 44

Fig. 33 and 34: Spatial distribution maps of Bicarbonate. 45

Fig. 35 and 36: Spatial distribution maps of Magnesium. 46

Fig. 37 and 38: Spatial distribution maps of Ammonium. 47

Fig. 39 and 40: Spatial distribution maps of Nitrite. 48

Fig. 41 and 42: Spatial distribution maps of Nitrate. 49

Fig. 43 and 44: Spatial distribution maps of Manganese. 50

Fig. 45 and 46: Spatial distribution maps of Fluorine. 51

Fig. 47 and 48: Spatial distribution maps of Sulfur. 52

Fig. 49 and 50: Spatial distribution maps of Sulfate. 53

Fig. 51 and 52: Spatial distribution maps of Phosphate. 54

Fig. 53 and 54: Spatial distribution maps of Arsenic. 55

Fig. 55 and 56: Spatial distribution maps of Bromine. 56

Fig. 57 and 58: Spatial distribution maps of Potassium. 57

Fig. 59 and 60: Spatial distribution maps of Iron. 58

Fig. 61 and 62: Spatial distribution maps of Strontium. 59

Fig. 63 and 64: Spatial distribution maps of Silicon. 60

Fig. 65: Piper Plot of the measuring points. 61

Fig. 66: Schoeller Plot of the measuring points. 62

Appendix:

Image Sa01: Moutonshoek rainwater-dam, line of sight: W, 25.02.2013. 79

Image Sa02: Krom-Antonies River near Moutonshoek, line of sight: S, 27.02.2013. 80

Image Sa03: Krom-Antonies River near Moutonshoek, line of sight: S, 28.02.2013. 81

Image Sa04: Dam near Moutonshoek, line of sight: SE, 01.03.2013. 82

Image Sa06: Tributary of the Krom-Antonies River, line of sight: E, 05.03.2013. 83

Image Sa07: Kromvlei irrigantion well, Boorgat I, line of sight: NE, 05.03.2013. 84

Image Sa08: Kromvlei irrigantion well, Boorgat II, 06.03.2013. 85

Image Sa09: Jan´s irrigantion well, line of sight: N, 06.03.2013. 86

Image Sa10: Kromvlei irrigantion well, Boorgat VI, line of sight: W, 06.03.2013. 87

Image Sa11: Rugby-field irrigantion well, line of sight: SW, 07.03.2013. 88

Image Sa12: Karookop irrigantion well, line of sight: W, 07.03.2013. 89

Image Sa13: Krom Antonies River, line os sight: W, 08.03.2013. 90

Image Sa14: Arthesian borehole near the Krom Antonies River, 08.03.2013. 91

Image Sa15: Little brook near Namaquasfontaine, line of sight: W, 09.03.2013. 92

Image Sa16: Konkelbos irrigation well 1, line of sight: N, 11.03.2013. 93

Image Sa17: Konkelbos irrigation well 2, line of sight: NE, 11.03.2013. 94

Image Sa18: Konkelbos animal drinking water, line of sight: NE, 11.03.2013. 95

Image Sa21: Irrigation well, line of sight: N, 13.03.2013. 98

Image Sa23: Volgersbosdrift well, line of sight: NE, 21.03.2013. 100

Image Sa24: Vrede Farm well, line of sight: NE, 14.03.2013. 101

Image Sa25: Vrede Farm irrigation well, line of sight: N, 21.03.2013. 102

Image Sa26: Vrede Farm irrigation pumps inside Krom Antonies River, line of sight: W, 21.03.2013. 103

Image Sa27: Pumping well of the northest borehole inside the study area, line of sight: NNW, 14.03.2013. 104

Image Sa28: Krom Antonies passage at the Riviera Farm, line of sight: SW, 15.03.2013. . 105

Image Sa29: Krom Antonies upstream, line of sight: S, 17.03.2013. 106

Image Sa30: Volgersbosdrift well, 19.03.2013. 107

List of Tables

Tab. 1: Water classes with respect to the TDS. 26

Tab. 2: Water classes with respect to the conductivity. 26

Tab. 3: WHO maximum permissible values of drinking water (2015). 27

Tab. 4: Analytical results of the cations. 35

Tab. 5: Analytical results of the anions. 36

Tab. 6: Ionic balance error. 37

Tab. 7: Water classification of the samples. 63

Tab. 8: WHO maximum permissible values of drinking water (2015) compared to the maximum values in the study area. 72

List of Abbreviations

DAAD	German Academic Exchange Service
DWA	Department of Water Affairs
DWAF	Department of Water Affairs in Forestry (nor replaced by DWEA)
GW	Groundwater
IWM	Integrated Watershed Management
mamsl	Metres above mean sea level
NWA	National Water Act (Act No. 36 of 1998)
UCT	University of Cape Town
WUA	Water User Assossiation
mS/cm	Milli-Siemens per centimetre
µS/cm	Micro-Siemens per centimetre
ΔIB	Total dissolved solids

Summary

Hydrogeological investigations are the instrument for understanding interactions between groundwater and geology. Based on this, statements about water availability and -quality can be made as well as the influence of agricultural use and settlements.

Within the project *Integrated Watershed Management Research & Development Capacity Building* as part of the program *Welcome to Africa* by the German Academic Exchange Service, a field trip has taken place into the Moutonshoek Valley, a small catchment in the western part of South Africa in spring 2013. In close cooperation with the University of Cape Town, the responsible authorities and local residents, 30 water samples were taken out of the ground- and surface water, prepared and transferred to Germany. In addition to physical parameters such as the pH, the temperature and the electrical conductivity, which were taken on site, a considerable anion and cation analysis was implemented.

Through the analysis and comparison of chemical distribution maps, geographical and hydrogeological cross-sections and geological maps, it was possible to determine the natural composition of groundwater to make an assessment of the impact of agricultural land use and settlement onto the groundwater quality.

It has been found out, that the groundwater in the area of Riviera granite and downstream in the valley is characterized by high amounts of sulfate, silicon, chlorine, bromine, magnesium and strontium, with an electrical conductivity of up to 2400 µS/cm. Water from the Malmesbury Group are generally brackish with high concentrations of chlorine and calcium. The human or anthropogenic influence were discovered in the concentration distributions of ammonium, nitrate, phosphate and manganese.

Zusammenfassung

Hydrogeologische Untersuchungen sind das Mittel zum Verständnis der Interaktionen zwischen Grundwasserkörper und Geologie. Auf Grundlage dessen können Aussagen über die Wasserverfügbarkeit und -qualität ausgearbeitet- und der Einfluss landwirtschaftlicher Nutzung und menschlicher Besiedlung getroffen werden.

Im Rahmen des Projektes *Integrated Watershed Management, Research & Development Capacity Building*, als Teilprojekt des Programmes *Welcome to Africa* vom Deutschen Akademischen Austausch Dienst, wurde im Frühjahr 2013 eine Exkursion in das Moutonshoek Valley, einem kleinen Einzugsgebiet im westlichen Teil Südafrikas durchgeführt. In enger Absprache mit der Universität Cape Town, den verantwortlichen Behörden sowie den Anwohnern, wurden 30 Wasserproben aus dem Grund- und Oberflächenwasser entnommen, entsprechend präpariert und nach Deutschland überführt. Neben physikalischen Parametern wie dem pH-Wert, der Temperatur und der elektrischen Leitfähigkeit, die direkt vor Ort gemessen wurden, wurde im Anschluss eine umfangreiche Anionen- und Kationenanalyse umgesetzt.

Durch die Auswertung und den Vergleich von chemischen Verteilungskarten, geo- und hydrogeologischen Profilschnitten sowie geologischen Karten war es möglich, die natürliche Zusammensetzung des Grundwassers zu bestimmen, eine Einschätzung zum Einfluss der landwirtschaftlichen Nutzung und der Besiedlung auf die Grundwasserbeschaffenheit im Einzugsgebiet zu treffen und Aussagen zu formulieren, die auf durch den Klimawandel bedingte Änderungen in der Wasserchemie eingehen.

Es wurde ermittelt, das sich das Grundwasser im Bereich des Riviera Granites und stromabwärts durch hohe Mengen an Sulfat, Silizium, Chlor, Brom, Magnesium und Strontium bei einer elektrischen Leitfähigkeit von bis zu 2400 µS/cm charakterisieren lässt. Wässer aus der Malmesbury Group hingegen in der Regel brackig, mit hohen Anteilen an Chlor und Kalzium sind. Der menschliche oder anthropogene Einfluss zeigt sich überwiegend in den Konzentrationsverteilungen von Ammonium, Nitrat, Phosphat und Mangan.

1 Introduction

1.1 Project - IWM Research & Development Capacity Building

Since the United Nations Conference (Earth Summit) in Rio de Janeiro in 1992, the concept of IWM (Integrated Watershed Management) received increasing international importance. Basically it provides effective and sustainable management of natural resources (such as water and soil) within catchments in coordination with the local population. The catchment areas are to be considered as a coherent system, including the man as a part of it (FÖRCH AND SCHÜTT 2004).

The approach is highly interdisciplinary. At the beginning natural scientists investigate the current situation and possible future developments. On this basis social scientists involve the stakeholders (competent authorities, water user associations and residents) in the project to jointly develop ideas for improving the situation in the catchment. The buildup of local expertise and the sustainable implementation of the concepts developed by IWM is a little more complicated due to the different interests of the stakeholders, but should nevertheless be realized with a clear description of possible threats and opportunities.

The project in which context this master-thesis is written, is part of the program *Welcome to Africa* by the German Academic Exchange Service - DAAD (www.daad.de) in cooperation with universities in Germany, Kenya, Cameroon and South Africa. It is called: *Integrated Watershed Management, Research & Development Capacity Building*.

Project management:

Prof. Dr. Brigitta Schütt brigitta.schuett@fu-berlin.de

Project coordination:

Anette Stumptner anette.stumptner@fu-berlin.de

Stefan Thiemann stefan.thiemann@fu-berlin.de

Partner universities:

Kenyatta University, Department of Geography, Nairobi, Kenya

University of Yaounde I, Higher Teachers´ Training College, Cameroon

University of Cape Town, Freshwater Research Unit, South Africa

United Nations University, Istitute for Environment and Human Security, Bonn (Germany)

"The international university project ´Integrated Watershed Management Research & Development Capacity Building´ is designed as an interdisciplinary research, development and capacity building project of Freie Universität Berlin, United Nations University, Kenyatta University, University of Cape Town, University Yaoundé and the consultancy IWM Expert. Integrated Watershed Management is our days a wide accepted concept to sustainable manage human and natural resources of a watershed in order to keep and increase livelihood of the local population. However, management and development competences in the sector of IWM are lacking, not only due to missing capacity building opportunities, but due to a severe communication gap among the different IWM stakeholders: researchers, regulatory authorities, water resources users associations and other community based organizations interact too little but communicate dominantly within their stakeholder group. The overall objective of this project aims at strengthening information and knowledge transfer among the different stakeholder groups with regard to IWM. Thus, the project contributes to reach the MDGs 7 (ensure environmental sustainability) and MDG 1 (eradicate extreme poverty and hunger) and supports international exchange in research and education." (ETZOLD 2012)

The regional person in charge for the project in South Africa is Prof. Jenny Day, Co-founder and Director of the Freshwater Research Unit at the University of Cape Town. During the period of this master thesis the project was in the initial phase (first information evaluation of the catchment area).

1.2 Objectives of the study

The ambition of the master thesis is to improve the implementation of the concept of Integrated Watershed Management (IWM) into a catchment with an already established water management infrastructure. Therefore a fieldtrip to the Krom Antonies catchment (also known as Moutonshoek Valley) in South Africa has taken place from 11th February to 23th March 2013. Without specified information of the catchment beforehand, a geohydrological overview should be provided to get an idea of the mineral composition of the groundwater in general, compared to the man made impact on the natural groundwater quality. In particular it was planned to collect up to 30 water samples of the Krom Antonies River itself, wells (boreholes) and springs distributed equally from up- to downstream and points of interest for an anion-cation-analyses and to gather physical parameters.

During the fieldtrip three major questions where developed:

- How does the geology in the catchment look like and what kind of waters are present?
- Comparing the up- and downstream- waters: What is the geogenic and anthropogenic impact on the water-mineral composition?
- What about the water-quality, if there would be less (ground-) water available depending on climate change or other impacts and could anything be done to keep the water quality in its state?

Finally, the contribution of this master thesis is to sensibilise the local farmers on their natural resource water and to provide gathered information to the stakeholders.

1.3 Study Area

The Moutonshoek Valley is situated 150 km north of Cape Town and 40 km to the east of the Atlantic Ocean (Fig.2). The nearest town, Piketberg, is situated approximately 23 km to the south of the study area. Located in the Western Cape Province of South Africa, it is part of the *Quatenary catchment G30 D* and includes approximately 500 km^2 (Fig.3). The altitudes are 65 m (mamsl) in the north up to approximate 1400 m (mamsl) at the Piketberg Mountains in the southeastern part (Topographic map, Fig.7).

Figure 2: Western Cape Province. The red outline points out the study area. Source: GoogleEarth.

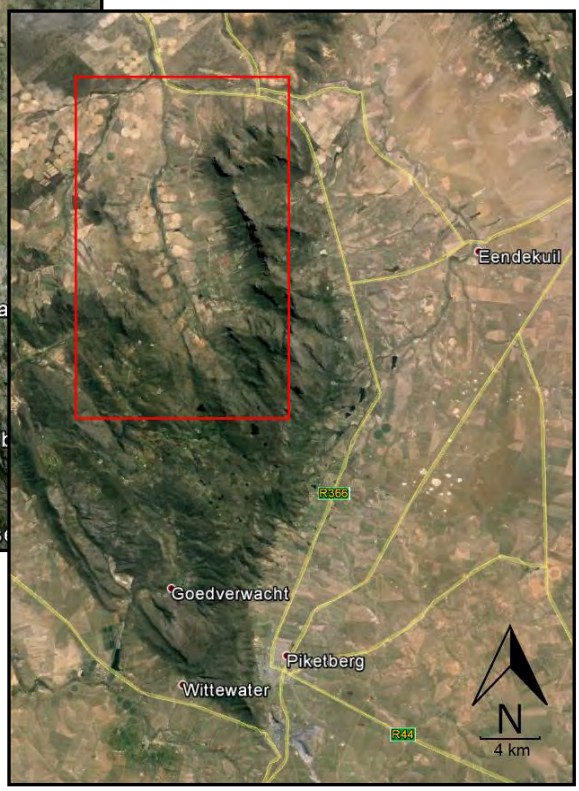

Figure 3: Roadmap near Moutonshoek Valley (red outline). Source: GoogleEarth.

1.3.1 Climate

The climate of the region is Mediterranean with an average temperature of 19,6 °C and the majority of the rain falling during May to August (with the peak rainfall month July), the winter months of the southern hemisphere. The average mean annual precipitation in the study area is about 370 mm/a. Depending on the topography (Fig.7) the annual precipitation ranges from 250 mm/a in the lowest parts of the study area, to an order of about 380 mm/a in the topographically higher areas, up to 600 mm/a in the Piketberg Mountains in the south-east (CONRAD 2012, SCHULZE 1997). Depending on a model, the mean annual potential evaporation ranges from 1800 mm/a to 2400 mm/a (SCHULZE 1997).

Climate change models for the Sandveld-Area indicate warmer and drier conditions also resulting in reduced groundwater recharge (CONRAD 2012).

1.3.1 Landuse

The study area is fit for agricultural use and the main income of the local farmers is out of harvesting grapes and potatoes. In the upper valley in addition some smaller Rooibos fields are cultivated and fallow lands as well as grass fields for feeding horses are most common. Except of the grain fields, where drip irrigation is applied, the farmer are using center pivot irrigation systems (Fig.4) with electrical pumps, rarely solar- and windmills. The irrigation requirement is sourced from both, primary unconfined aquifers and the underlying fractured (and in places confined) aquifers (CONRAD 2012) (see also in chapter geohydrology on page 17).

Figure 4: A center pivot irrigation system in central Montana. ccby-sa: Montanabw.

1.3.2 Drainage

The major drainage of the catchment is by the north-westerly flowing Krom Antonies River. The Krom Antonies- as well as the Kruismans- and Eselshoek Rivers, which are part of the upper Krom Antonies River catchment G30D, merge in the north into the Verlorenvlei River with a mean annual runoff estimated at 4.3 Mm^3/a (VISSER ET AL 2009). About 25 water-reservoirs for agricultural usage, essentially set for the sedimentation of turbidity, are providing enough water specially in the dry seasons.

2 Geology and Hydrogeology

2.1 Geology

The study area is bounded in the east, west and south by hills and mountains formed by quartzitic sandstones of the Table Mountain Supergroup, namely the Piekenier-, Graafwater- and Penisula Formation (BELCHER AND KISTERS 2003, VISSER 2009). Due to the high resistance to weathering, the Table Mountain Rocks builds up the topographically highest areas of the study area (Fig.7).

The basement, which is overlain by a few tens of meters of unconsolidated alluvial and clay deposits, is composed out of the lithologies of the Malmesbury Group (Piketberg Formation), a low to medium-grade metasedimentary sequence alternating Chloride Schist, interbedded diverse calcareous rocks and altered marble (ROZENDAAL ET AL 1994, Council for Geoscience South Africa). North-westerly trending faults in this basement induced the intruding of the Riviera Granite Pluton in at least one part of the study area (ROZENDAAL ET AL 1994) (Fig.5, 6 and 7).

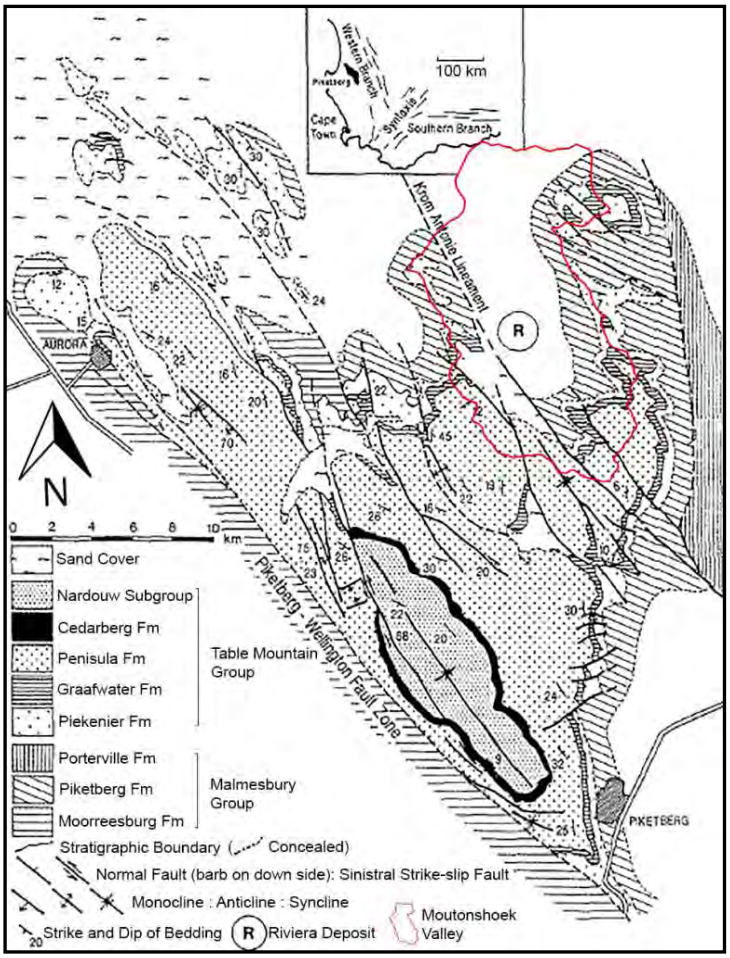

Figure 5: Geology of the Piketberg area (after De Beer 1990 and Rozendaal 1994). The red outline point out the study area.

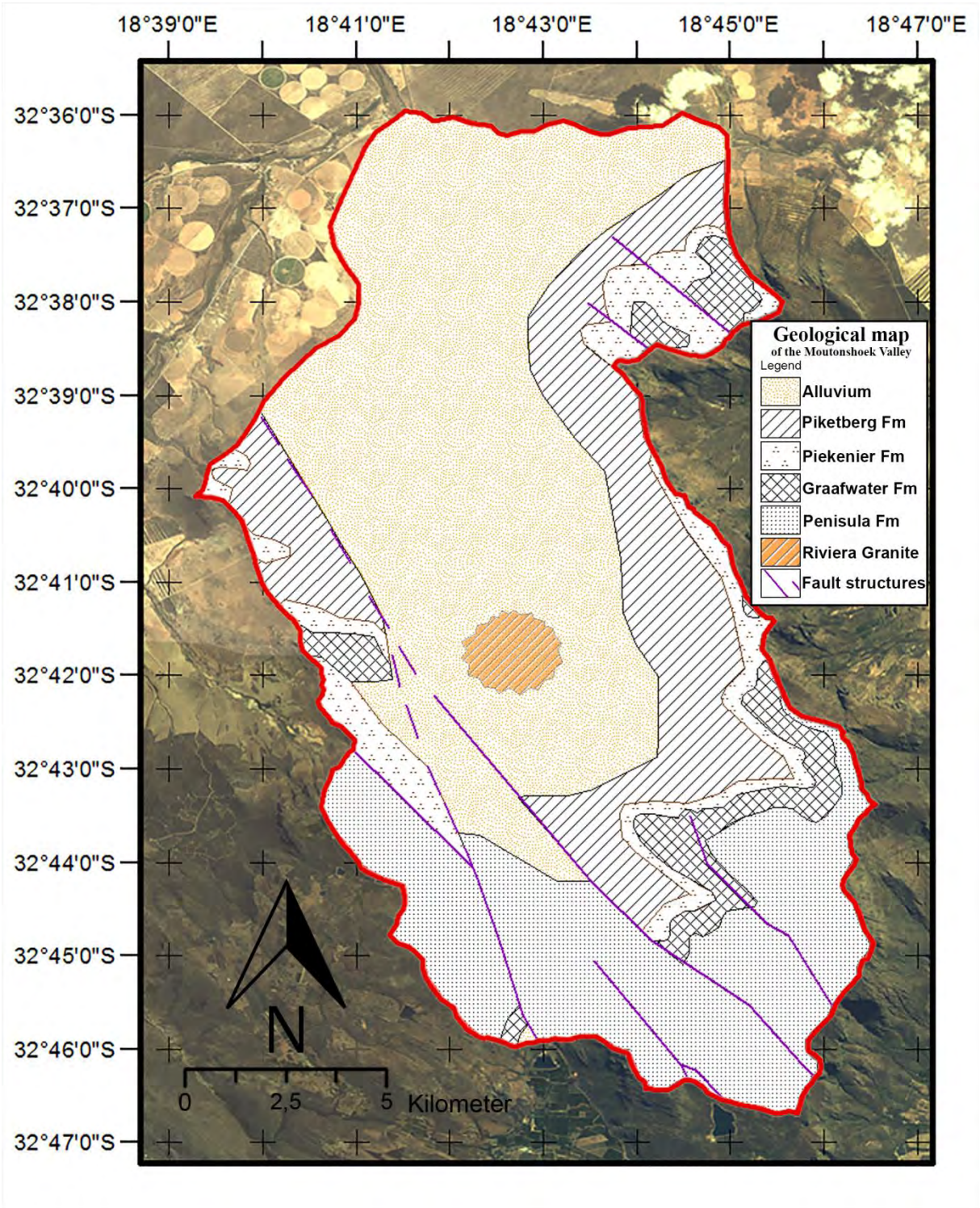

Figure 6: Geological map of the Moutonshoek Valley (after DE BEER 1990 and ROZENDAAL 1994). The estimated shape of the Riviera Granite is not representative. Imagery: LANDSAT prepared with ARCGIS 10.1.

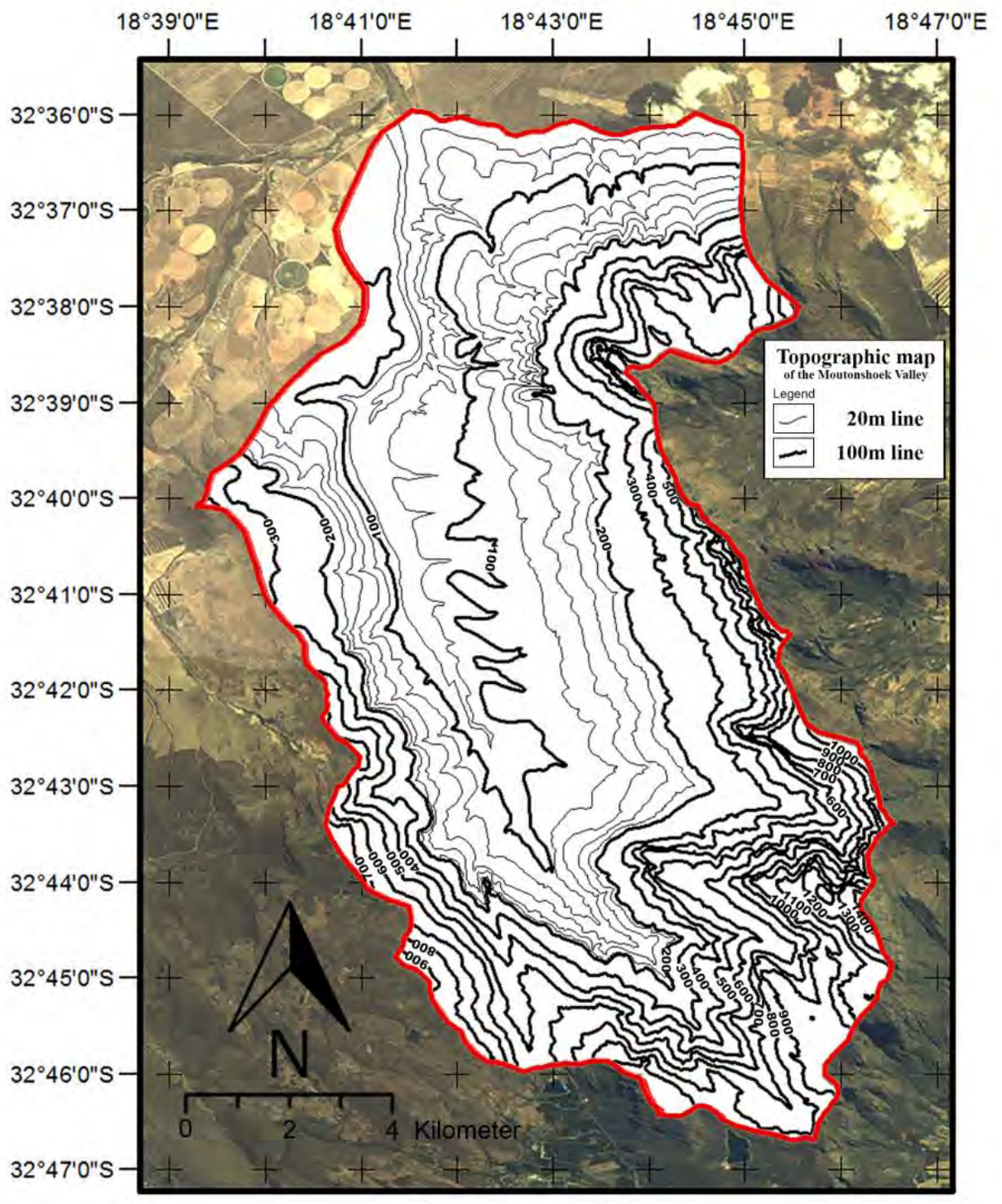

Figure.7: Topographic map of the Moutonshoek Valley. Imagery: LANDSAT prepared with ARCGIS 10.1.

2.1.1 Geological history of the study area

The rocks of the Malmesbury Group (Piketberg-, Tygerberg- and Porterville Formation) are the oldest in the Western Cape. They were formed as part of the Malmesbury Supergroup (Swartland-, Malmesbury- and Klipheuwel Group) in the late Precambrian age between 1,2 Gy and 600 My ago in form of continental slope sediments and turbidity currents (THERON ET AL 1992, BELCHER AND KISTERS 2003). During the Vendian closure of the Adamastor Ocean, when the South American and the Antarctic continents collided with Africa around 600 My ago, the rocks got slightly metamorphosed and experienced an uplift (FRIMMEL AND FÖLLING 2004). Huge batholites, relics of this subduction, intruded into the Malmesbury Supergroup and formed the plutons of the Cape Granite Suit (Fig.8), which emerged near the surface all over Western Cape due to erosion processes (THERON ET AL 1992, VILLAROS 2006). The Riviera Granite Pluton located in the study area originated about 520 Ma as a part of the Cape Granite Suit (ROZENDAAL ET AL 1994).

About 510 My ago a rift developed through the weakened zone of the Malmesbury Series, separating the south of Gondwana from the Falkland Plateau. The rift, flooded by the Aghulas Sea for a period of about 200 My, filled up with an up to 10 km thick layer of sediments which consolidated to the Cape Soupergroup (VOS AND TANKARD 1980, MCCARTHY AND RUBRIDGE 2005). Forced by another subduction the closure of the rift appears about 330 My ago and the Falkland-Plateau drift back towards South Gondwana, creating the Cape Fold Montains. Unaffected of this process the collision of Laurussia and Gondwana in the north 30 My later results in the new supercontinent Pangaea, which separates about 200 My ago, creating the Altlantic ocean and forming the recent shape of the African and South American continents.

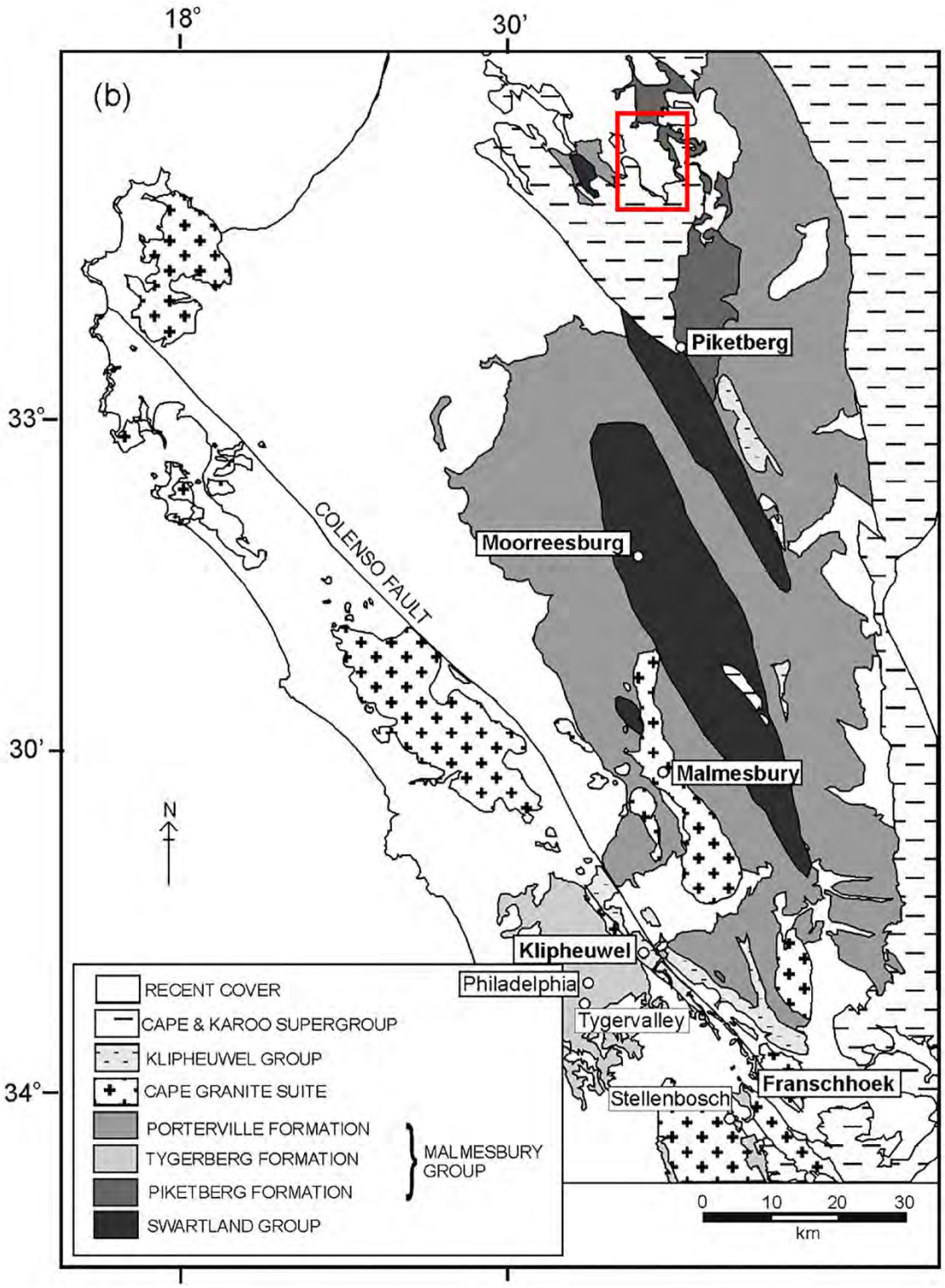

Figure 8: Geological map of the western Cape, showing the distribution of the Malmesbury Group, its formations, the overlying Cape Supergroup and the Cape Granite Suit. The red rectangle shows the position of the study area in Moutonshoek Valley (after BELCHER 2003, modified from ROZENDAAL ET AL1994).

2.1.2 Alluvium

The basement of the study area is overlain by 10 - 30 m tertiary to recent unconsolidated alluvial- and clay deposits (VISSER 2009). The clay layer varies in thickness of about 3 to 25 m, depending on its position in the valley. In the area of the Riviera Granite thicknesses of about 30 m could be verified in borehole examination and due to transport-processes it is supposed that the clay layer in the lower valley is more abundant than in the higher areas.

2.1.3 Malmesbury Group

The nomenclature of the Malmesbury sequences changed in 2003, because long accepted lithostratigraphic subdivisions and correlations of formations as well as the poorly constrained age of the deposition, deformation and metamorphism leads to the problem of identifying coherent stratigraphic packages (BELCHER AND KISTERS 2003). Nowadays the Malmesbury Group is divided into the Klipheuwel- , the Malmesbury- and the Swartland Group, based on the recognition of two major tectonostratigraphic units, namely the Colenso- and Piketberg-Wellington Fault (Fig. 8).

The Malmesbury Group is subdivided into the Porterville-, Tygerberg- and Piketberg Formation, of whom only the Piketberg Formation is present in the study area (Fig. 6) and which is exposed as weathered outcrops in stream gullies, road-cuts and against hill slopes. The Malmesbury Group is typically a monotonous sequence of phyllites, schist, shale and greywacke.

<u>Piketberg Formation</u>

The base of the Piketberg Formation is composed of conglomerates and small grain-sized gravel or rather grits which are interbedded with minor shales. Theese shale beds become more prominent in the upper parts of the Piketberg Formation and indicates a generally fining-upward trend (BELCHER AND KISTERS 2003). The conglomerate is composed of quartz and ferruginous clays. Due to the vein-quartz dominated clast population and their most likely proximal source, as indicated by the subrounded nature, the conglomerates were possibly derived from the underlying rocks of the Swartland Group (BELCHER 2003).

2.1.4 Table Mountain Group

In the western Cape Province over 4000 m of mainly quartz arenitic sandstone and conglomerate comprise the Table Mountain Group at the base of the Cape Supergroup (VOS AND TANKARD 1980). As described in the Geological history (page 10), the depot for the Cape Supergroup was an elongate basin in the Aghulas Sea, trending parallel to the present coast around 510 My ago. Due to the opening of the Sea, different facies were formed over time, which led to the Piekenier-, the Graafwater- and the Penisula Formation. Except of a area in the western part of the study area, the Formations of the Table Mountain Group are generally flat lying or dips at low angles on top of the Piketberg Formation, Malmesbury Group (VOS AND TANKARD 1980).

Piekenier Formation:

The Piekenier Formation is the stratigraphically lowest Formation of the Table Mountain Group in the study area and overlays the Piketberg Formation of the Malmesbury Group. It was sedimentated as part of an braided alluvial plain complex, influenced by a moderate to high runoff and includes conglomerates as well as coarse-grained sandstones (VOS AND TANKARD 1980).

Graafwater Formation:

The Graafwater Formation interfingers with the Piekenier Formation and is interpreted as a tidally dominated sequence out of a tidal flat lagoon (VOS AND TANKARD 1980). Interbedded quartz arenite (sandstone), siltstone, mudstone and minor shale are the main compounds of this Formation (VOS AND TANKARD 1980, VISSER 2009).

Penisula Formation:

The Penisula Formation builded up near the coast in a barrier complex, where medium- to coarse-grained quartz arenites sedimentated in a shallow tide-dominated shelf (VOS AND TANKARD 1980).

2.1.5 Riviera Granite

The Riviera Granite, as part of the Cape Granite Suit, intruded the Malmesbury Rocks around 520 My ago (as described in the geological history of the study area on page 10). It is positioned in the upper-central valley, easterly of the Krom Antonies River (Fig.5 and 6). Though initially intruded at great depth, the granite exposed at the surface due to prolonged erosion processes (COMPTON 2004).

Discovered in 1975 by Union Carbide Exploration Company by stream sediment sampling, the contents tungsten (scheelite) and molybdenum were soon identified. Analyses of the rocks establishes the marginal grades of 0,216 % tungsten and 0,02 % molybdenum (WALKER 1993). The dome-shaped structure is subalkaline to K-calcalkaline, conforms to the characteristics of I-type granites and comprises a suite of metaluminous (Na2O+K2O+CaO > Al2O3, in mole percent) to slightly peraluminous (Na2O+K2O+CaO < Al2O3, in mole percent) granitoids (ROZENDAAL AND MOYEN 2009). „Close up, the granite is a coarse-grained rock consisting of large (2–5 cm) white or pink feldspar crystals, glassy brown quartz and flakes of black mica, and containing inclusions of dark Malmesbury hornfels“ (THEORON 1992).

Due to the occurrence of diagnostic minerals such as vesuvianite, hornblende and hedenbergite, the surrounding rocks define a typical endo-skarn association (ROZENDAAL AND MOYEN 2009). Skarns are most often formed at the contact zone between intrusions of granitic magma bodies and carbonate sedimentary rocks. Hot waters derived from the granitic magma are rich in silica, iron, aluminium and magnesium. These fluids mix in the contact zone, dissolve calcium-rich carbonate rocks, and convert the host carbonate rock to skarn deposits in a metamorphic process called metasomatism.

The position and shape of the Rivera Granite Dome is described in ROZENDAAL ET AL 1994 (Fig.9).

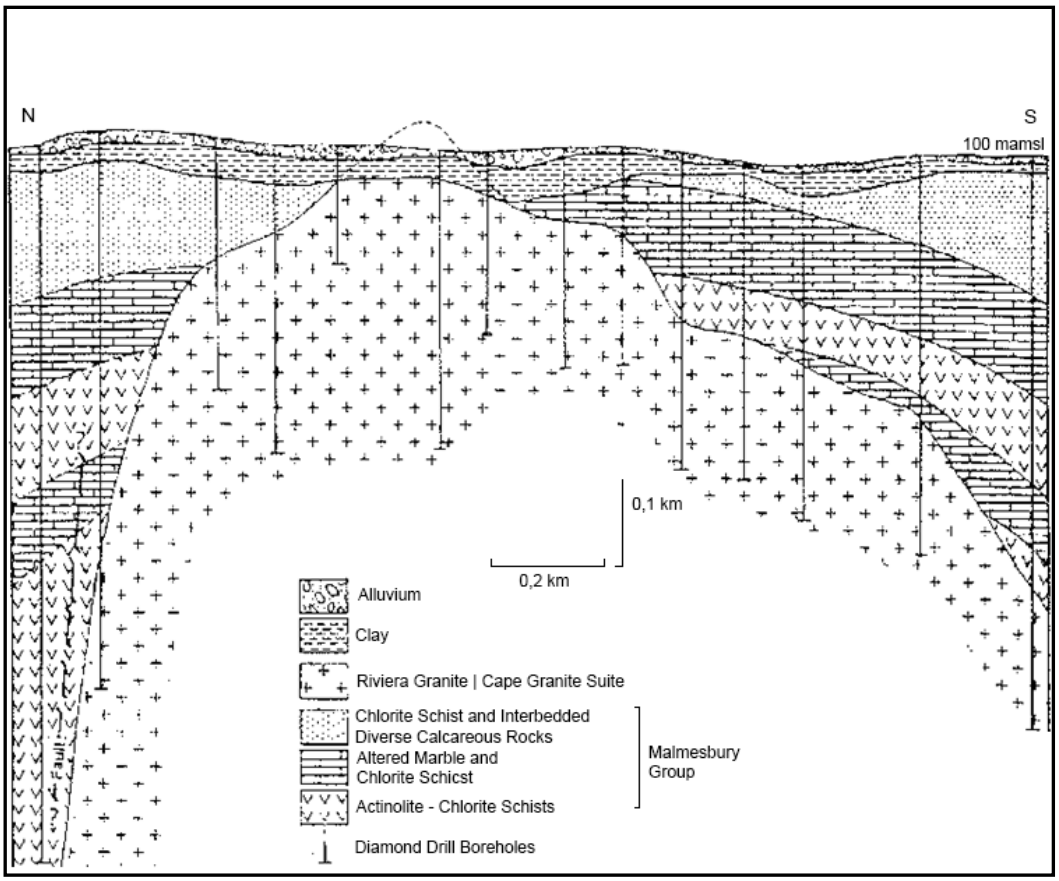

Figure 9: Geological cross-section of the Riviera granite dome (ROZENDAAL ET AL. 1994).

2.1.6 Structural geology

Due to the geological history of the area, there are many structural displacements. The late Precambrian tectonics resulted in a swarm of steeply dipping north-west trending normal faults, forming graben-horst structures and showing significant displacements along some faults (CONRAD 2012) (Fig.10 and 11).

The granite pluton is terminated on its western edge by a major fault, called the Krom-Antonies Fault, which has a downthrow of about 450 m to the west (ROZENDAAL ET AL. 1994). The Malmesbury Group is a low to medium-grade metasedimentary sequence with many local folds and compressive tensions.

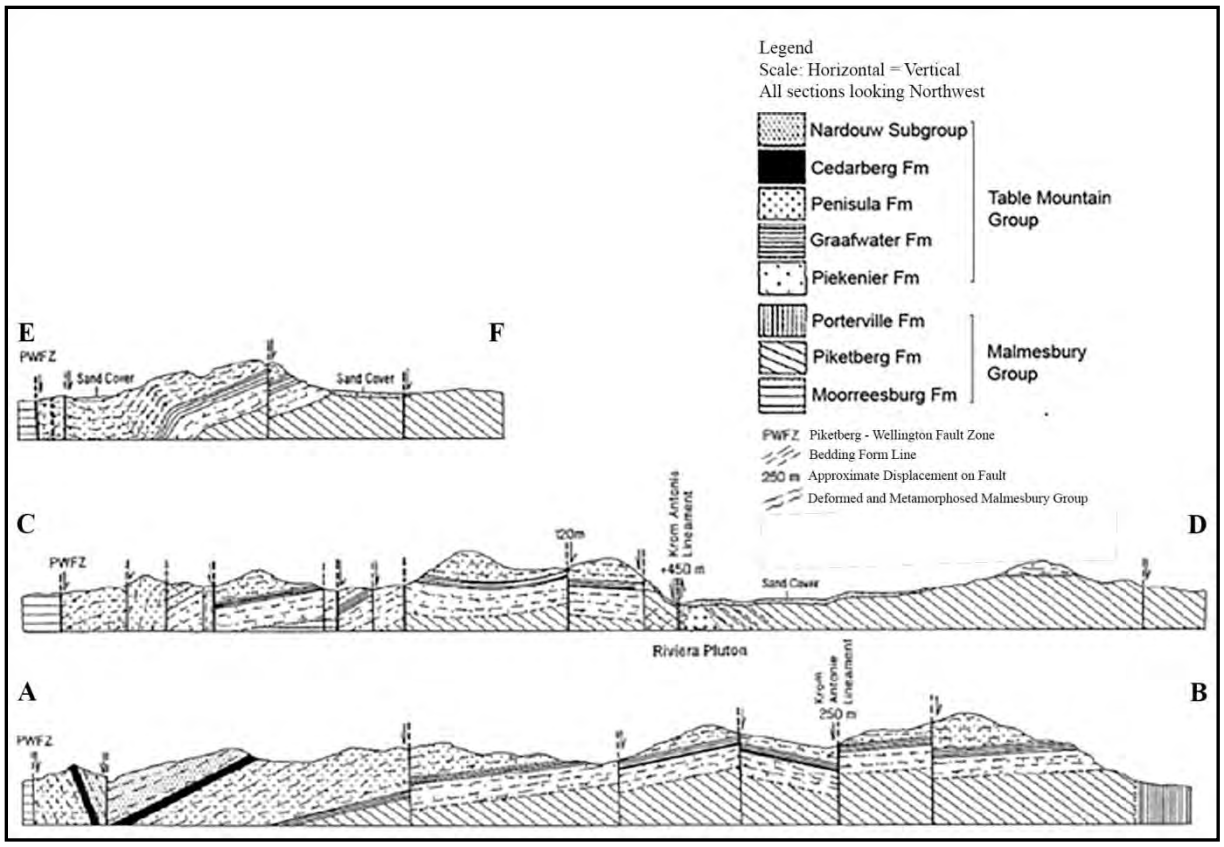

Figure 10: Geological cross-sections in the Piketberg area showing the structural relationship and spatial position of the Riviera pluton (After ROZENDAAL ET AL 1994).

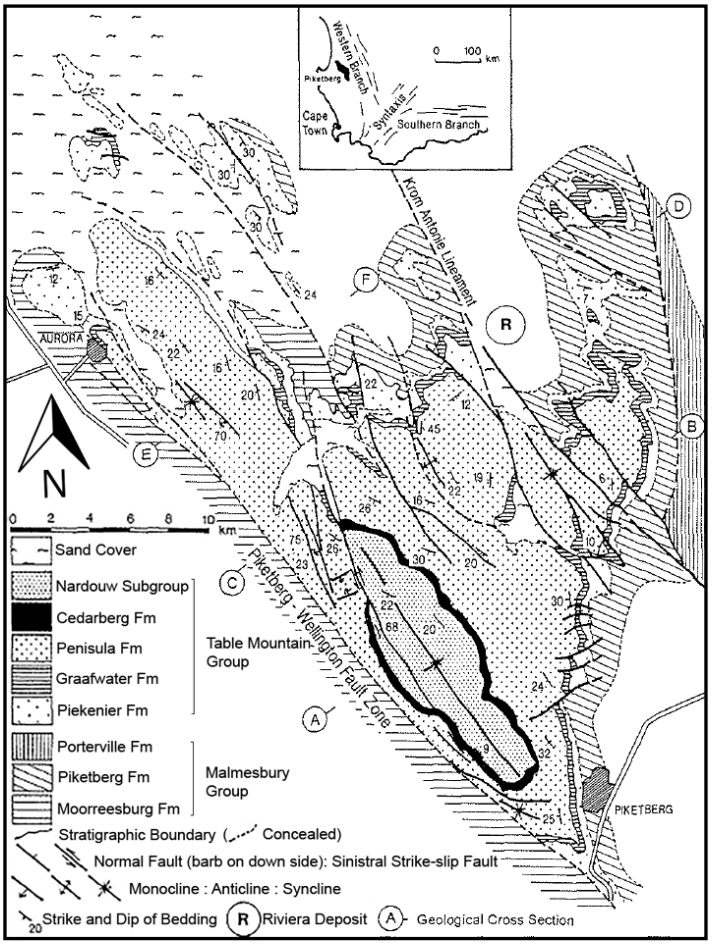

Figure 11: Geology of the Piketberg area (after DE BEER 1990 & ROZENDAAL 1994).

2.2 Hydrogeology

Two aquifer types can be identified in the study area:

1. unconfined primary aquifer

2. semi-confined secondary fractured rock aquifer

The unconfined primary aquifer is build out of the alluvial sand cover, which, in many parts of the study area, is underlain by a clay layer with a thickness up to 30 m (ROZENDAAL ET AL 1994). It is supposed that it is directly recharged by precipitation (CONRAD 2012) and possibly by the secondary aquifer in parts of good connectivity between the primary and secondary aquifer (CONRAD 2004).

The secondary aquifer is partly covered by the clay-layer of the alluvium and is present within secondary openings due to faulting, fractures, joints and possibly solution cavities in the Piketberg Formation. Near the Riviera Granite intrusion a well developed fractured rock aquifer, yielding large amounts of groundwater, is expected (VISSER 2007). Recharged by the surrounding Table Mountain rocks it is partly confined, resulting in higher piezometric heads than the water table itself (CONRAD 2004). Thereof artesian boreholes can be found in the study area like the measuring point Sa14.

According to the Department of Water Affairs and local farmers, the typical borehole yield is about 0,5 - 5,0 l/s, depending on the location and depth of the borehole. Some dry and abandoned boreholes where discovered, which were either drilled to shallow or in an unfortunate spot without sufficient fractures (CONRAD 2012).

2.2.1 Groundwater recharge

Due to a report of GEOSS - Groundwater and GIS Consultants, a GIS based approach was used to determine the groundwater recharge distribution, using lithology- and rainfall data. According to the report, the mean annual recharge is up to 90 mm/a with a vertical recharge about 12,8 mm/a for the catchment G30E, Moutonshoek Valley (Conrad 2012) (Fig.12). Results made from Bongani Minerals (Pty) Ltd in June 2009 differs significantly. They assumed a mean annual effective recharge up to 37,5 mm/a in the topographically higher areas of the study area (Fig.13).

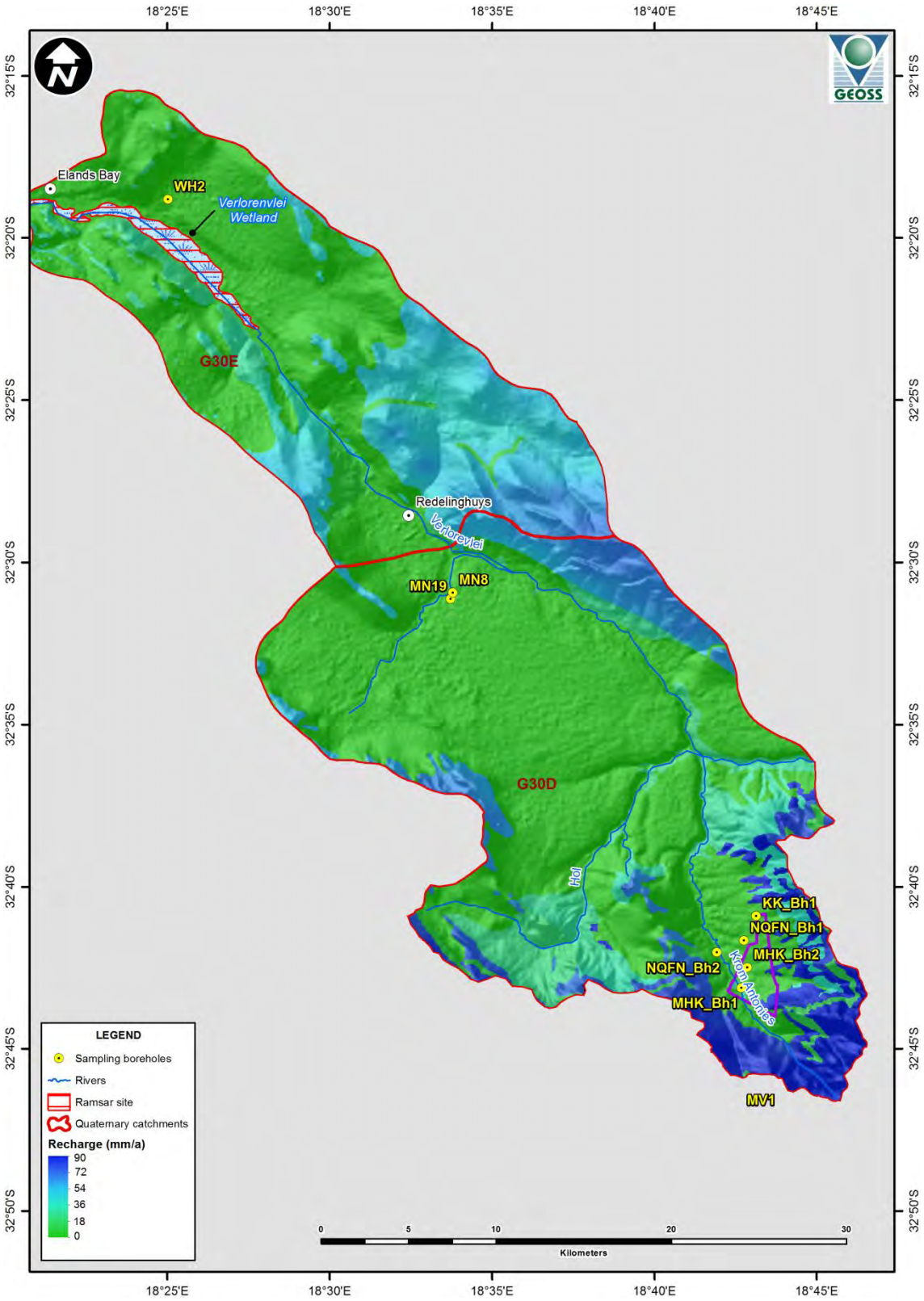

Figure 12: Groundwater recharge of the area (CONRAD 2012, GEOSS-REPORT 2006).

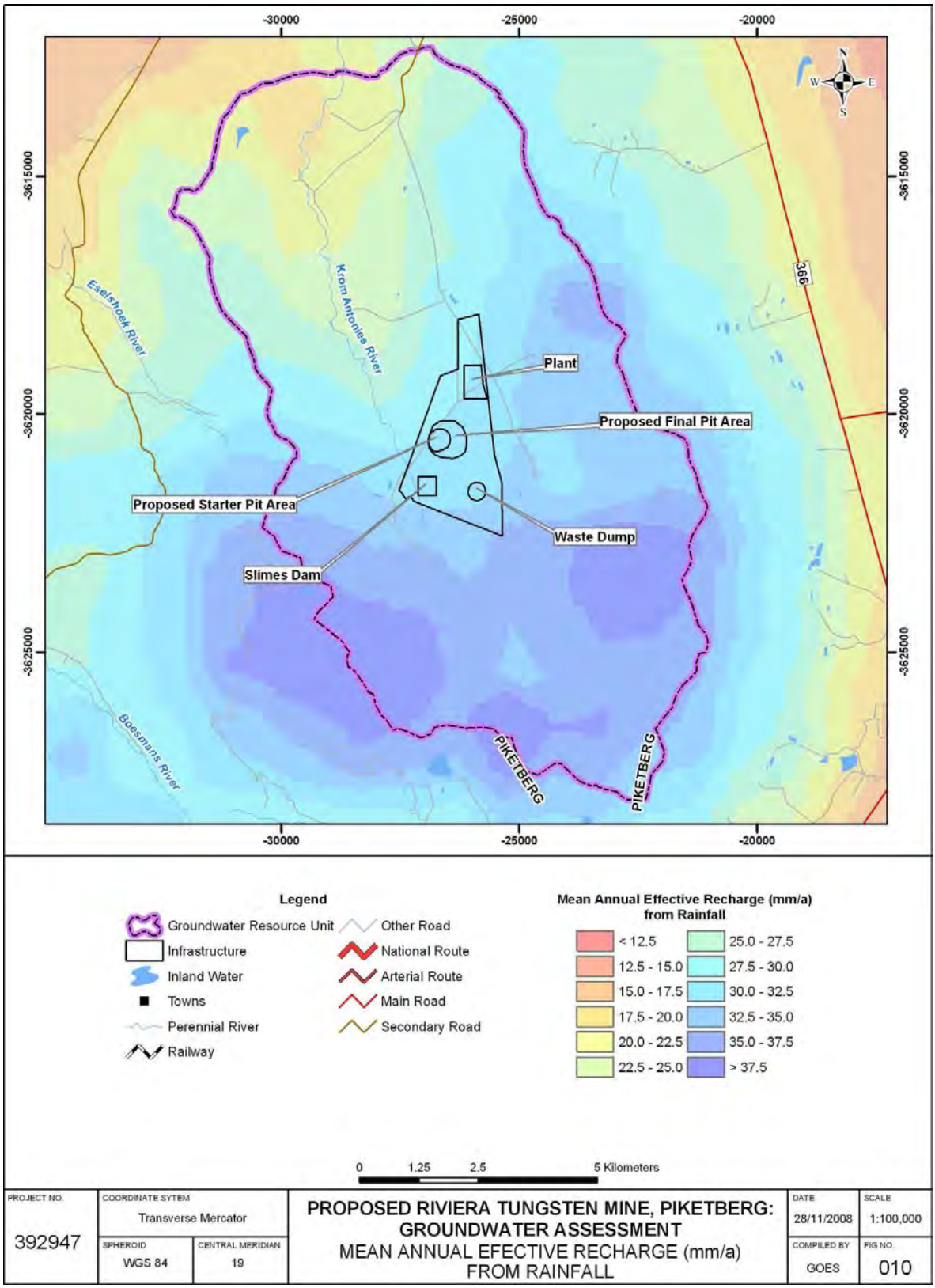

Figure 13: Mean Annual Effective Recharge (mm/a) from rainfall (VISSER 2009).

2.2.2 Groundwater Level

After VISSER 2009, the Groundwater level depth ranges from approximately 21 m on the flanks of the catchment to about 1 m in the valley floor near the Krom Antonies River. Only few data for the groundwater level could be found in literature and measurements during the field trip were limited due to the fact that the sampled boreholes were in use for irrigation. Therefore the groundwater level of the study area had to be estimated by a handful of measured groundwater levels of unused boreholes, the topography, geological maps and regions where the groundwater edge the surface (swampy regions, drain away of the Krom Antonies River). These water-levels are illustrated in five cross-sections of the study area (see on page 28).

3 Methodology

On the following pages the procedure of selecting, analyzing and preparing (visualization) of the samples will be subscribed to ensure the reproduction-ability of the data collection.

3.1 Sampling and onsite measurements

Due to limited equipment and time in the field, a maximum count of 30 measuring points for an accurate survey were prepared. To get an general overview of the study area, the distribution of these points where selected while taking geographical- (up- and downstream), geological- (different rock types) and geohydrological (different aquifers) circumstances in mind (Fig.14).

In case of the river samples particular days without rain beforehand where chosen to get fewest rainfall affected base flow samples. To ensure to get unmodified groundwater-samples out of boreholes, the water pumps had worked for at least five minutes or until the electrical conductivity received a steady value, before the samples were taken.

3.1.1 Preparation of the samples

For every measuring point two sample-bottles of 75 ml for the anion and cation analyses in the laboratory had been carefully filled up with the gathered water, avoiding gas inclusions which would have caused chemical reactions with the atmosphere. Beforehand the water-samples have been filtered with an low pressure hand pump including a filter mesh size of not more than 0,4 µm. For every sample a new filter was used. The cation-samples had been acidified using Nitritic-acid (HNO_3) to an pH of about 2,0 to avoid precipitation of solved minerals during the storage. Prepared samples were stored in a fridge at a temperature of about 5 °C until the departure.

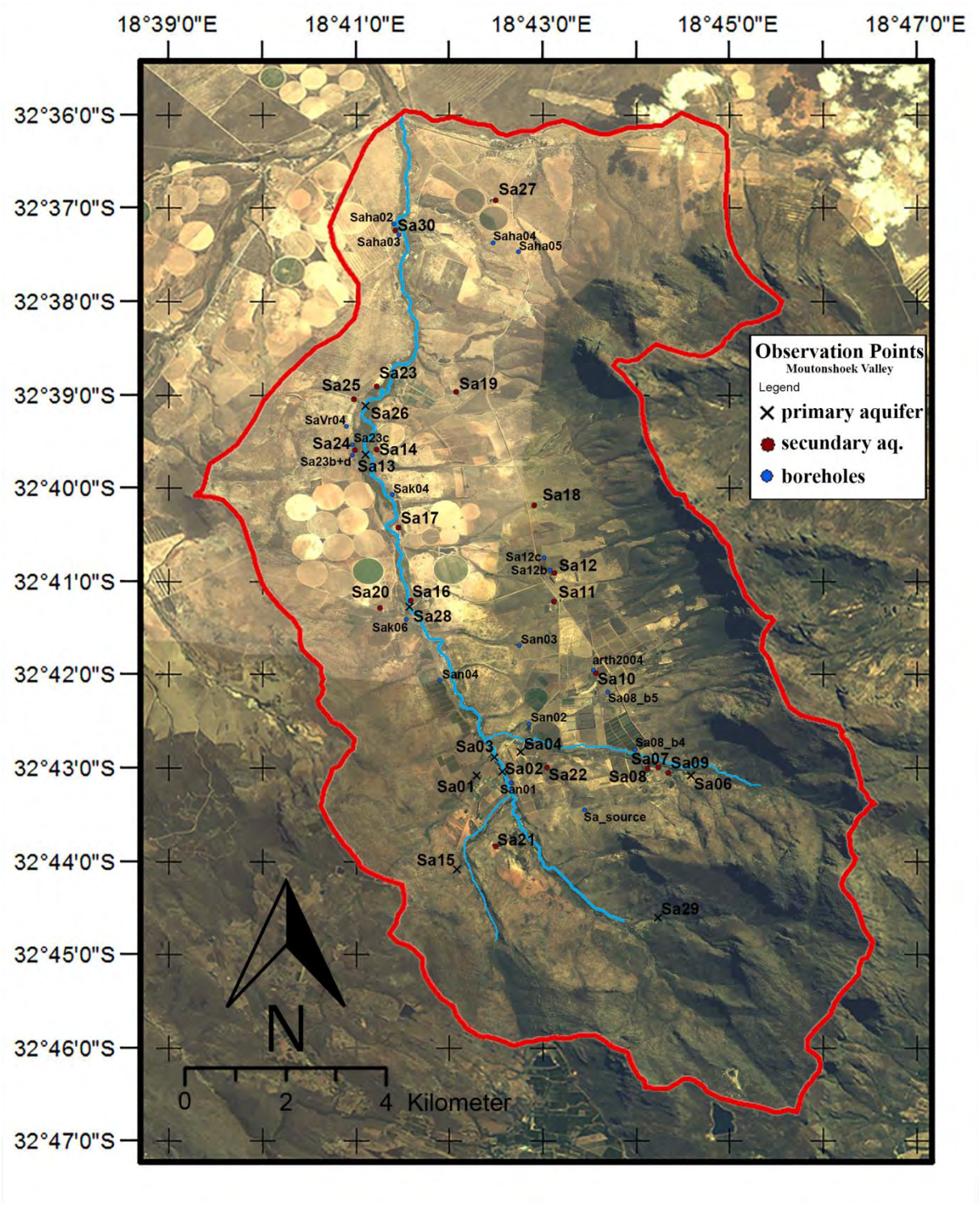

Figure 14: Selection of the Observation points in the study area. The black crosses are showing the position of shallow boreholes which only reaches the first aquifer about up to 20 m depth as well as river- and dam samples. The red dots are the positions of the boreholes deeper than about 20 m which reaches below the clay layer into the second aquifer. The blue dots are additive boreholes as part of the documentation for the DWA. The map is based on LANDSAT images, edited with ArcGIS and image editing software.

3.1.1 Onsite measurements

Beside the documented smell, color, weather, coordinates, date and time of the samples, some further quick-tests had to be processed in the field. To get an overview during the investigation of the study area at first hand, some Easy-Test-strips (for pH, Nitrite, Nitrate, hardness of water and carbonate) of JBL were used. Although they turned out as a very useful tool, none of these results have been taken into count in this thesis.

pH and conductivity

The pH and temperature were measured in situ with an pH-meter of Hanna Instruments (HI9124) directly in the river or respectively inside the sample-bucket, like the conductivity, which was measured with an Conductivity Portable Meter (HI87314). Once a week the pH- and conductivity-meter had been calibrated, although there haven´t been any unconformabilities during the field trip.

NO_2^-

A Nitrite MColortest by MERCK including a color card and a sliding comparator was used. In this procedure nitrite ions react with sulfanilic acid to form a diazonium salt in acidic solutions, which in turn reacts with N-(1-naphthyl)ethylenediamine dihydrochloride to form a red-violet azo dye. By visual comparison of the color of the measurement solution with the color fields of a color card the nitrite concentration is measured semiquantitatively (Merck Millipore, information and direction for use).

NO_3^-

A Nitrate MColortest by MERCK was used to determine the quantitative amount of Nitrate in the water samples. Nitrate ions react in acidic solution with sulfanilic acid to form a diazonium salt. An orange-yellow color occur within the reaction of a benzoic acid. The color strength is proportional to the concentration of Nitrate and can be measured semiquantitatively by visual comparison of the color of the measurement solution with the color fields of a color card (Merck Millipore, information and direction for use).

NH_4^+

The determination of ammonium was realized by the usage of a *MColortest Ammonium Test* of MERCK. In this procedure Neßler´s reagent reacts with ammonium ions to form a yellow-brown compound, which can be measured semiquantitatively by visual comparison of the color of the measurement solution with the color fields of a color card (Merck Millipore, information and direction for use).

S_2^-

Also the Sulfide was determined colorimetric by a MColortest of MERCK. A pH-dependent equilibrium exists between dissolved hydrogen sulfide ($H2_S$), hydrogen sulfide ions (HS^-), and sulfide ions (S_2^-) when aqueous solutions are present. In the acidic range of dissolved hydrogen sulfide, it reacts with dimethyl-p-phenylenediamine and iron(III) ions to form methylene blue which can be measured semiquantitatively by visual comparison of the color of the measurement solution with the color fields of a color card (Merck Millipore, information and direction for use).

HCO_3^-

A titrimetric with dropping bottle MColortest by MERCK was used to determine the quantity of the carbonate hardness. The carbonate ions are titrated with hydrochloric acid against a mixed indicator. At the titration end-point (at pH 4.3) the color changes to red. The carbonate hardness (acid capacity) is determined from the consumption of titration solution (Merck Millipore, information and direction for use).

3.2 Hydrochemical analyses

The samples were analyzed in the laboratory of the Freie Universität Berlin by Elke Heyde. The anions were analyzed by ion chromatography (Dionex DX 500), described by WEISS 1995, and the cations by inductively coupled plasma optical emission spectrometry (ICP OES, Perkin Elmer 2100), as descibed by NÖLTE 2002.

Spatial chemical distribution maps

Divided in the first- (river samples and shallow boreholes) and second aquifer, the spatial distribution of the anions and cations were interpolated with ArcGIS 10.1 using the Inverse Distance Weighting method. The results could only be used as a first idea of the distribution, because the method didn´t include basic boundary conditions like the topology, the groundwater flow direction or connectivity between groundwater and river. These factors were included afterwards by image editing (see on page 38).

3.3 Water classification

Piper- and Schoeller plots:

The Piper and Schoeller Plots were generated by AquaChem 4.0 (see results on page 61 and 62).

Cross-sections:

To get an geohydrological overview five vertical exaggerated cross sections were made. Therefore the topography and geology was digitalized. The expected groundwater head is based on a few available groundwater heads, recorded swampy regions (used as an indicator for the connectivity between the groundwater-head and the surface) and the vanishing Krom Antonies River, interpreted as the intersects between river and groundwater head (see results on page 28).

3.3.1 Nomenclature

The water classification is realized with reference to the equivalent percent of the anions and cations. The regulations to classify the water are:

1. All anions and cations whose amount exeed 20% of the sum of all come into count.
2. When the percentages of a single cation or anion exceeds 60%, the other cations or anions are not included in the name.
3. The cations are always called before the anions.

Total hardness:

The total hardness of a water-sample is defined as the sum of the mol-equivalence-ions of Calcium and Manganese (other earth alkali are not included).

Bicarbonate- hardness:

The content of Bicarbonate in the sample.

Non-carbon-hardness (permanent-hardness):

Total hardness without bicarbonate- hardness.

Total dissolved solids:

The total amount of dissolved ions (cations and anions) is also known as TDS. The TDS is quantified by the specific electrical conductivity, which is the rate of the total mineralization of the water.

Water classes described by the TDS:

Class	**TDS [mg/l]**
fresh water	- 1000
brackish water	1000 -10000
saltwater	10000 - 100000
brine	>100000

Table 1: Water classes with respect to the TDS.

Water classes describet by the conductivity:

Class	**LF [µS/cm] [1/Ω]**
fresh water	- 1500
brackish water	1500 - 15000
saltwater	15000 - 150000
brine	>150000

Table 2: Water classes with respect to the electrical conductivity.

3.3.2 WHO maximum permissible values

To compare the measurements of the anions and cations, a list of the maximum permissible values in drinking water by the World Health Organisation (WHO) is shown below. Some are not listed, because they were proved to be "not of health concern at levels found in drinking water" (WHO 2011). These are the total dissolved solids (principally calcium, magnesium, potassium, sodium, bicarbonates, chlorides and sulfates) and small amounts of organic matter as well as Bromine, Fluorine, Sulfur, Sodium and Strontium.

WHO maximum permissible values:

Ion	**WHO-Guideline value**
Ammonium	1,5 mg/l
Arsenic	0,01 mg/l
Chlorine	no value (detectable taste: 250 mg/l)
Fluoride (Fluorine)	1,5 mg/l
Nitrate	50 mg/l
Phosphate	no value (6,7 mg/l until 2003)
pH	6,5 - 8,5 (European Drinking Water Directive, 1998)

Table 3: WHO maximum permissible values of drinking water (date: January 2015) (WHO 2011)

4 Results

4.1 Cross-sections

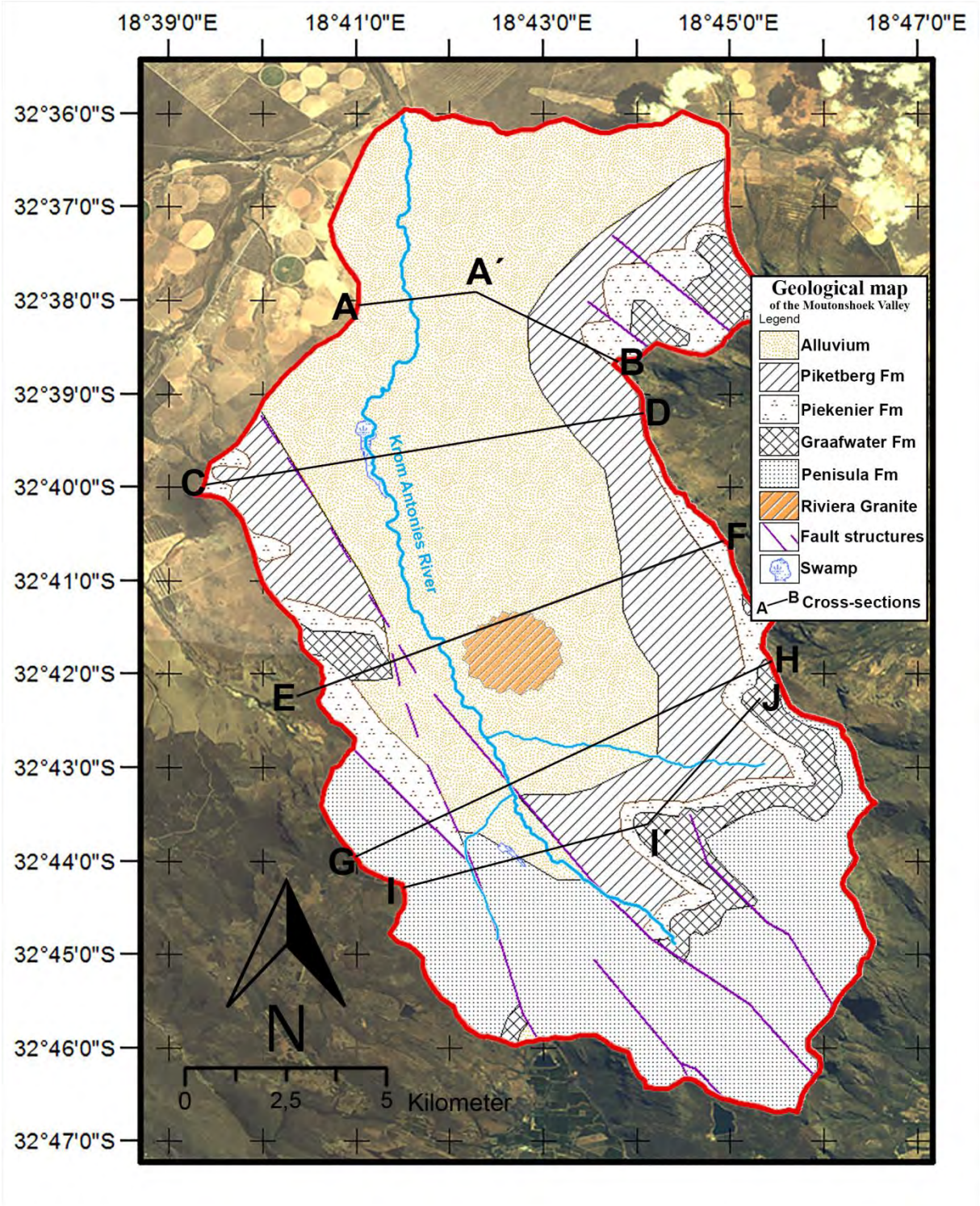

Figure 15: Geological map including cross sections and faults**.** Imagery: LANDSAT prepared with ARCGIS 10.1.

4.1.1 Cross-section A - A´- B

The vertical exaggerated cross section A - A´- B was modeled on the basis of the topography (Fig.7) and geology (Fig.6). The expected groundwater head is based on a few available groundwater heads (and its interpolation), known borehole-depths and recorded swampy regions as well as the vanishing Krom Antonies River interpreted as the intersect between river and groundwater head.

Due to the fact that the Krom Antonies River actually lose water as it flows towards the Verlorenvlei River in the northern part of the valley, it is supposed to be an influent stream. Therefore the river and the groundwater head are not connected directly. The clay layer isn´t present, because the origin of the clay is supposed to be out of chemical interactions between the host rocks and geothermal waters, described in PEROLD AND THEART 2007. The thickness of the Alluvium varies between 1 - 15 m, flattening towards the Krom Antonies River in the central valley. The underlain Piketberg Formation hosts the unconfined secondary aquifer.

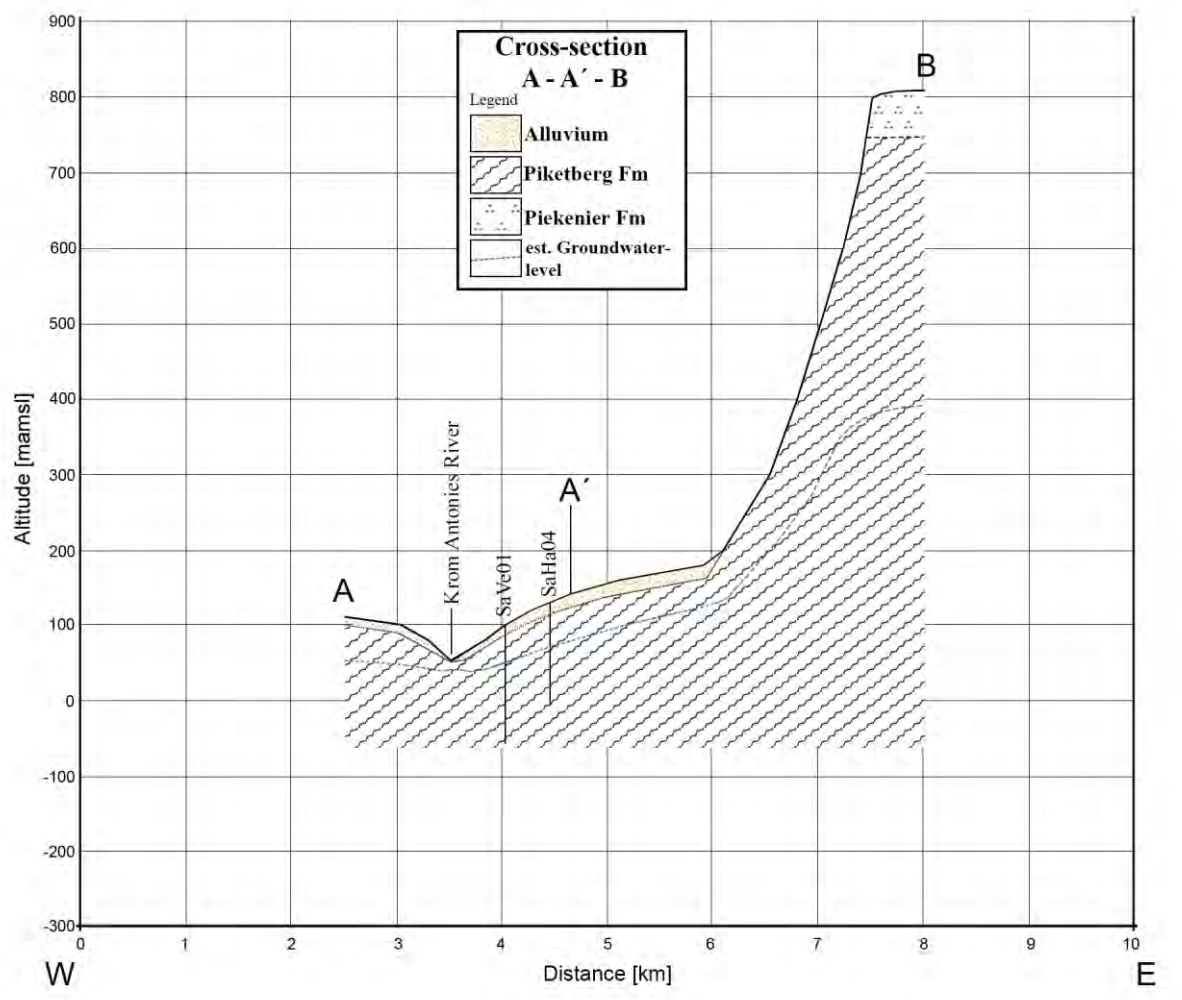

Figure 16: Vertical exaggerated cross section A - A´ - B.

4.1.2 Cross-section C - D

The vertical exaggerated cross section C - D was modeled on the basis of the topography (Fig.7) and geology (Fig.6). The expected groundwater head is based on a few available groundwater heads (and its interpolation), known borehole-depths and recorded swampy regions as well as the vanishing Krom Antonies River interpreted as the intersect between river and groundwater head.

The angle of the surface in the region of cross-section C - D is much lower than in the region of cross-section A - A´- B. For this reason the layer of the Alluvium is proposed to be more prominent. Due to the reduced flow velocity of the groundwater and the spatial proximity to the Riviera Granite and its formal geothermal waters, the occurrence of a well developed clay layer is supposed. The presence of an artesian borehole (Sa14) supports this assumption as well. In the western part the Krom-Antonies-Fault leads to an topographically step, described as an graben-horst structure by ROZENDAAL ET AL 1994.

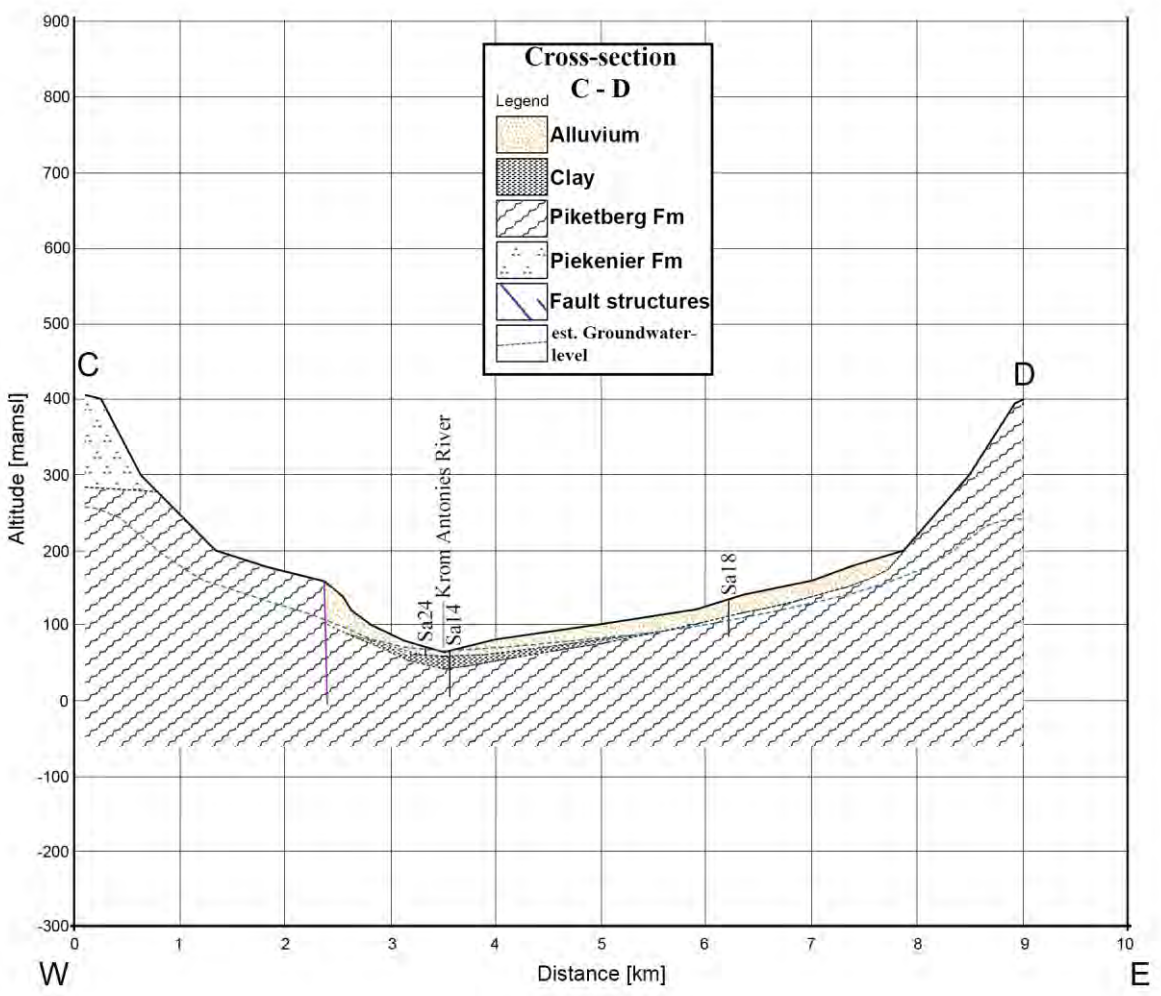

Figure 17: Vertical exaggerated cross section C - D.

4.1.3 Cross-section E - F

The vertical exaggerated cross section E - F was modeled on the basis of the topography (Fig.7) and geology (Fig.6). The expected groundwater head is based on a few available groundwater heads (and its interpolation), known borehole-depths and recorded swampy regions as well as the vanishing Krom Antonies River interpreted as the intersect between river and groundwater head.

Cross-section E - F cuts through the well described Riviera Granite Pluton and the thickness of the clay layer was proofed by core drillings beforehand (ROZENDAAL ET AL 1994). The Krom Antonies River is directly connected to the primary aquifer, so in this region the river is effluent due to it get its water from the primary aquifer. The graben-horst structures on the western part leads to the declaration, that the groundwater recharge area is greater than the topographically developed study area itself and reaches in the Hol River valley.

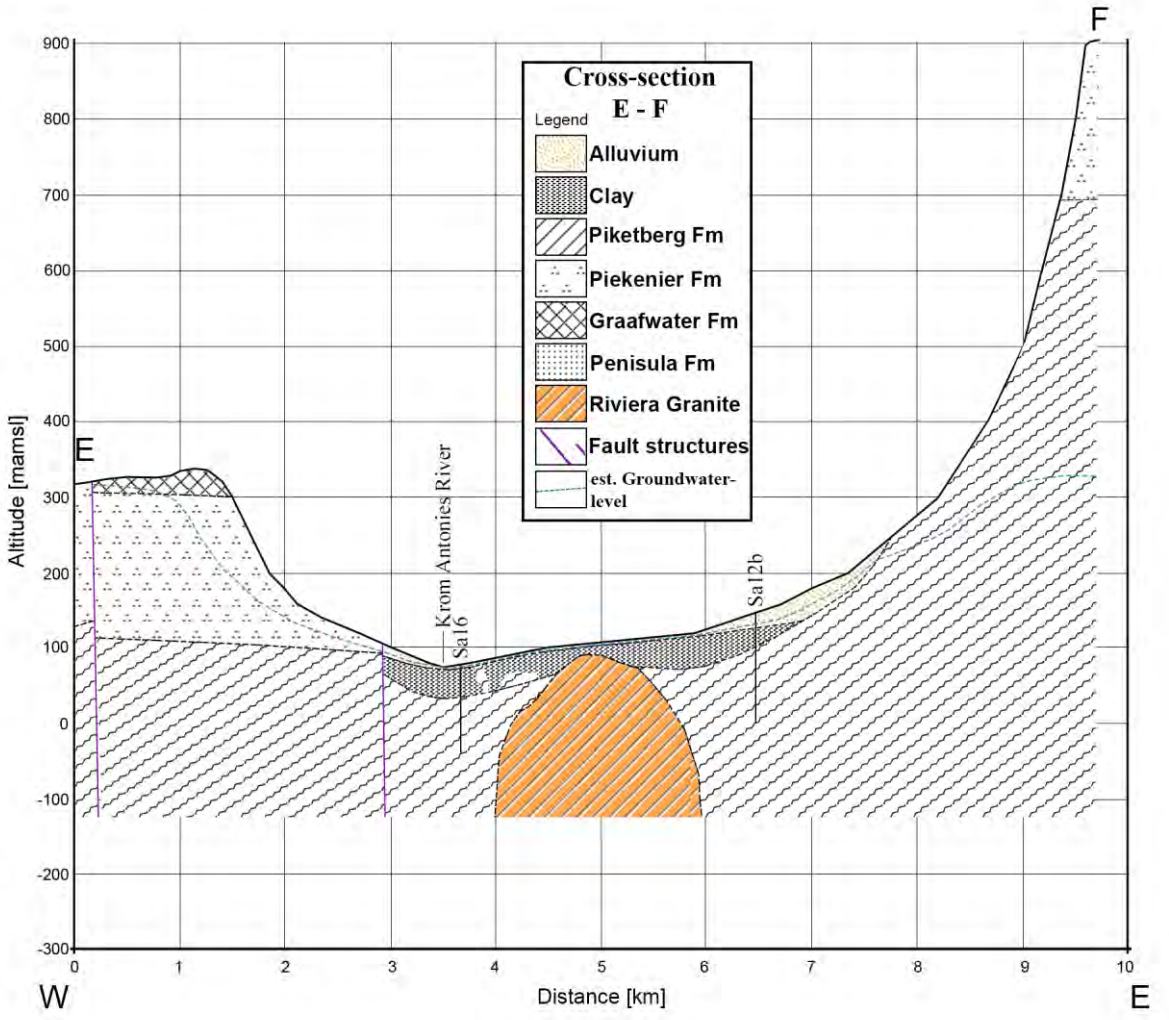

Figure 18: Vertical exaggerated cross section E - F.

4.1.4 Cross-section G - H

The vertical exaggerated cross section E - F was modeled on the basis of the topography (Fig.7) and geology (Fig.6). The expected groundwater head is based on a few available groundwater heads (and its interpolation), known borehole-depths and recorded swampy regions.

Cross-section G - H is characterized by the high altitudes in the eastern as well as in the western part of the valley of about 700 m [mamsl] and its distinctive fault systems like the Krom-Antonies-Fault. It cuts through both rivers, the Krom Antonies River in the west and the Eselshoek River in the east. Borehole Sa22 just got a depth of about 20 m, but has got a yield of up to 100 qm/h. Therefore the Piketberg Formation in this area got a great aquifer with many fractures and a groundwater head near the surface. Due to the pronounced fault system in the western part associated with geothermal waters, a clay layer occurs in the central valley as well.

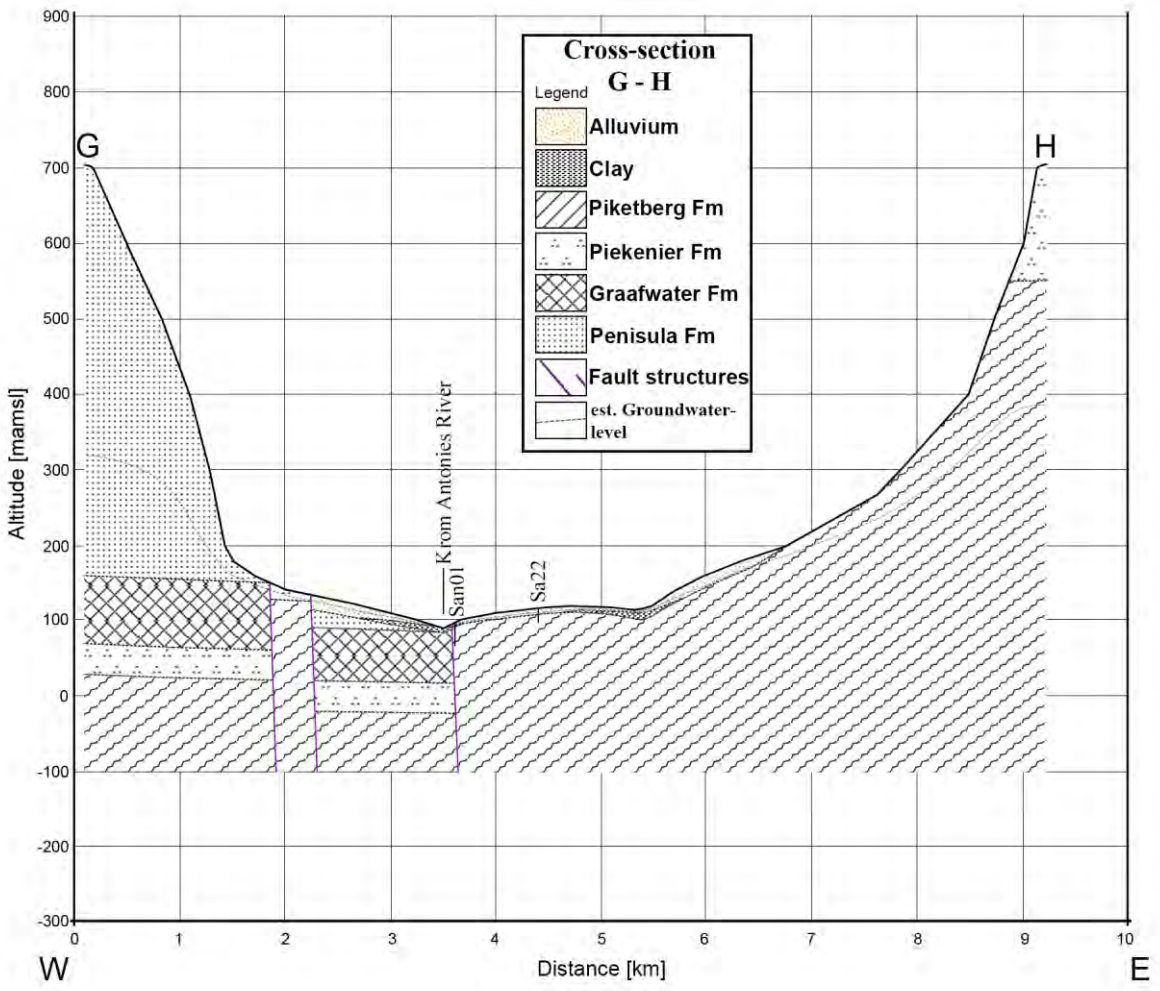

Figure 19: Vertical exaggerated cross section G - H.

4.1.5 Cross-section I - I´- J

The vertical exaggerated cross section I - I´- J was modeled on the basis of the topography (Fig.7) and geology (Fig.6). The expected groundwater head is based on a few available groundwater heads (and its interpolation), known borehole-depths and recorded swampy regions (Sa21).

In cross-section I - I´- J both valleys, either formed by the Krom-Antonies River and Eselshoek River, can be identified greatly. Caused by the Krom-Antonies-Fault the western aquifers are mainly hosted by the Penisula Formation of the Table Mountain Group. The groundwater head of Sa21 was only 2,8 m below the surface and a nearby dam was told to fill up progressively. This could be due to unconformabilities in the Penisula Formation or an unrecognized clay layer, impounding the interflow.

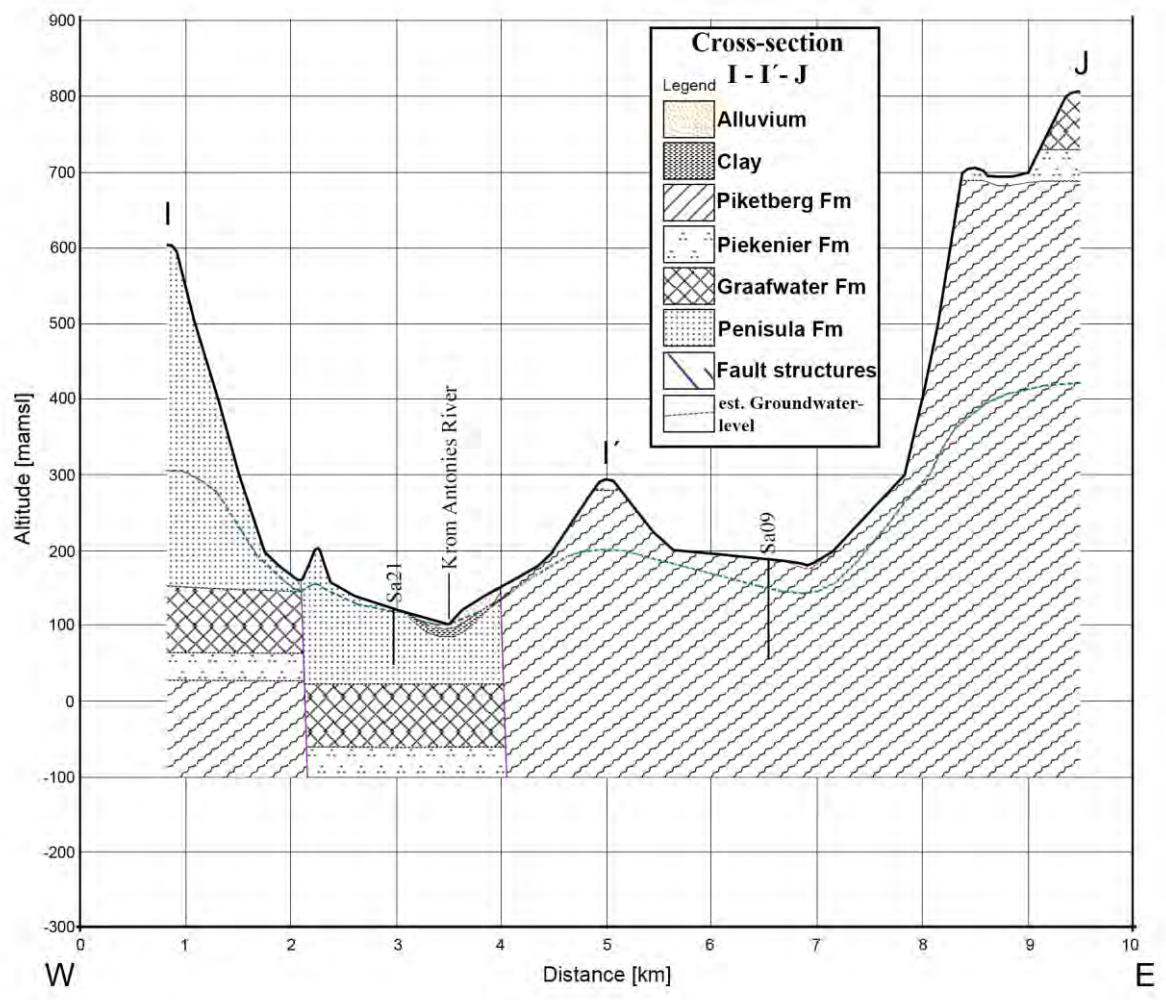

Figure 20: Vertical exaggerated cross section I - I ´- J.

4.2 Groundwater dynamics

The direction of the groundwater flow was estimated due to the topography and geochemical distributions. Large-scale interpolations of groundwater heads were resulting in an more north-westerly streaming groundwater flow in the northern part of the study area (CONRAD 2012). This was not take into account due to respect of the influences of the graben-horst-structures described on page 31, Fig.18.

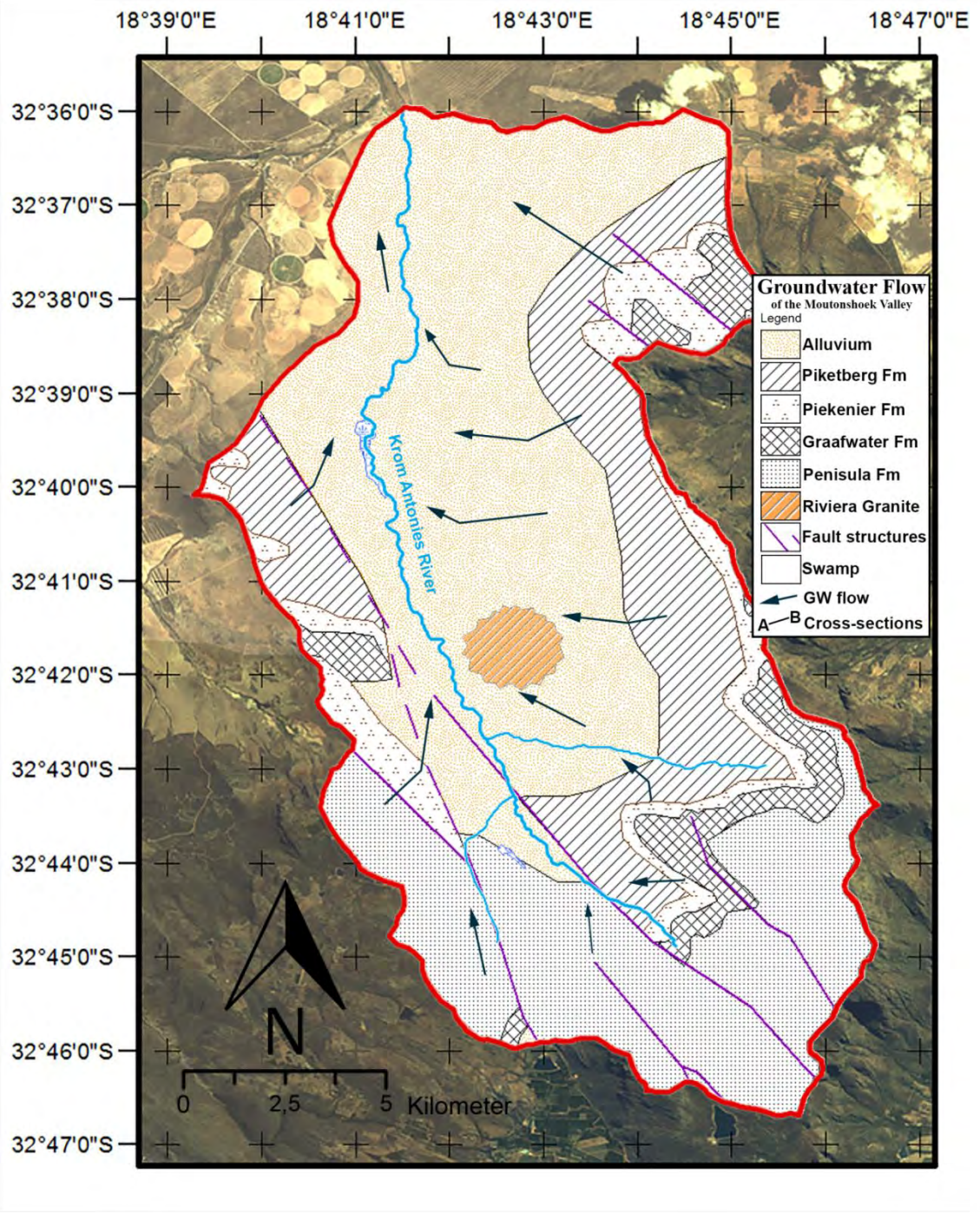

Figure 21: Map of the estimated groundwater flow in Moutonshoek Valley.

4.3 Hydrochemistry

4.3.1 Cations

Table 4 is showing the analytical results of the cation analyzes, described on page 24.

ID	LF [µS/cm]	pH	Ca [mg/l]	Mg [mg/l]	Na [mg/l]	K [mg/l]	Fe [mg/l]	Mn [mg/l]	As [µg/l]	Sr [mg/l]	NH4 [mg/l]
Sa01	66	7,51	6,2	2,7	13,6	0,8	0,64	0,5	0	0,03	0,1
Sa02	248	7,61	32,9	6,6	26,2	1,2	0,2	0,04	2	0,19	0,1
Sa03	237	7,64	30,1	6,7	26,9	1,1	0,03	0,02	1	0,18	0,025
Sa04	163,3	-	20,2	5,4	25,2	1,2	0	0,003	2	0,12	0,1
Sa06	29,2	6,8	2,1	0,95	6,2	0,08	0,07	0,01	0	0,001	0,025
Sa07	261	7,07	33,8	5,2	28,5	2,4	0,07	0,14	0	0,21	0,075
Sa08	288	7,84	31,9	6,6	32,3	2,6	0,1	0,004	0	0,21	0,05
Sa09	91,4	6,49	7,6	4,5	15,4	2,4	0,25	0,02	0	0,05	0,025
Sa10	972	7,01	87,8	17,5	71,3	3	1	0,2	0	0,5	0
Sa11	2400	7,09	167	66	141	3,6	4,7	0,2	8	0,97	0,025
Sa12	2160	6,3	87	51	207	3,7	9	0,4	29	0,52	0
Sa13	976	7,28	40	19,7	128	0,8	0,13	0,2	0	0,2	0
Sa14	1157	7,38	87	23	115	1	1,5	0,2	4	0,5	0
Sa15	31,4	5,76	27,8	1,1	8,5	0,02	0,01	0,005	0	0,006	0
Sa16	2370	7,25	63,2	46,5	199	1,5	0,94	0,2	9	0,72	0,025
Sa17	1086	7,29	1,4	24	113	1,1	0,96	0,14	9	0,39	0,05
Sa18	2370	7,52	136	57,3	196	3,1	0,02	0,3	0	0,85	0,025
Sa19	513	7,26	57	13	61,8	1	1,9	0,7	2	0,2	0,025
Sa20	528	4,39	141	14,6	73,4	0,8	0,02	0,06	0	0,04	0,025
Sa21	46,1	6,65	2,1	1,1	9,5	0,4	4,8	0,3	0	0,009	0,025
Sa22	613	7,55	59,5	10,5	49,2	2,1	0,02	0,03	0	0,41	0,025
Sa23	751	7,73	4,3	7,7	51	1,6	0	0,02	0	0,04	0,075
Sa24	318	4,13	42,2	17,1	69,6	2,3	0,1	0,007	0	0,29	0,05
Sa25	1040	7,33	24,8	18,4	117	1,05	0,5	0,05	0	0,19	0
Sa26	1450	7,25	33,9	29,8	177	0,6	0,48	0,08	1	0,26	0,05
Sa27	3310	7,09	184	75	282	7,6	0,03	0,01	0	1,26	0
Sa28	1294	7,38	45,7	27,6	151	0,8	0,21	0,35	0	0,28	0,05
Sa29	25,3	7,65	1,7	0,8	6,1	0,1	0,04	0,008	0	0,007	0,025
Sa30	467	6,74	19,8	13,1	50,2	2,4	0	0,1	0	0,13	0

Table 4: Analytical results of the cations.

4.3.2 Anions

Table 5 is showing the analytical results of the anion analyzes, described on page 24.

ID	Cl [mg/l]	SO4 [mg/l]	NO3 [mg/l]	PO4 [mg/l]	HCO3 [mg/l]	F [mg/l]	Br [mg/l]	Si [mg/l]	S2 [µg/l]
Sa01	22	2	0,1	0	12,2	1	0,1	3,1	0,02
Sa02	42	24	0,4	0,4	122	0,3	0,1	7,9	0
Sa03	43	23	0	0	91,5	0,25	0,1	7,6	0,02
Sa04	44	11	0,07	0	73,2	0,4	0,1	3,3	0,02
Sa06	11	1,7	0,02	0,02	12,2	0,9	0,04	3,6	0,02
Sa07	45	10	1,2	0	128,1	0,8	0,1	13,5	0
Sa08	53	13,7	0,08	0	115,9	0,2	0,1	9,3	0
Sa09	32	5,5	0,65	0	30,5	0,3	0,07	10	0
Sa10	152	54	0	0	237,9	0,4	0,4	16,4	0,02
Sa11	478	204	0	0	158,6	0,2	1,3	16,4	0
Sa12	460	166	0	0	85,4	0,3	1,3	12,8	0
Sa13	215	31	1	0	103,7	0,1	0,6	4,4	0
Sa14	230	55	0,6	0	164,7	0,1	0,6	6	0,02
Sa15	15	1,7	0,1	0,05	12,2	0	0,05	4	0,02
Sa16	540	95	0	0	201,3	0,15	1,4	10,8	0
Sa17	228	53	0,05	0	146,4	0,1	0,6	7,4	0
Sa18	422	223	0,15	0	298,9	0,2	1,1	10,3	0,02
Sa19	117	36	0	0	67,1	0,4	0,3	7,1	0,02
Sa20	152	5,5	30	0	12,2	0,2	0,4	4,7	0,01
Sa21	13	0,9	0,25	0	0	0,9	0	2,8	0,02
Sa22	100	26	0	0	195,2	0,4	0,2	11,5	0
Sa23	100	10,8	2,8	0	0	0,4	0,2	4,9	0,01
Sa24	185	22	0,06	0	85,4	0,08	0,5	5,8	0
Sa25	243	30	4,6	0	48,8	0,1	0,6	5,5	0
Sa26	344	42	0,6	0,26	122	0,07	1	4,4	0
Sa27	726	245	12,2	0	298,9	0,05	2,3	6,5	0
Sa28	280	43	1,1	0	219,6	0,16	0,8	5,1	0
Sa29	11	1,4	0	0	12,2	0	0,03	4,6	0
Sa30	116	26	0,6	0	36,6	0,2	0,3	2,8	0,02

Table 5: Analytical results of the anions.

4.3.3 Ionic balance error

The ionic balance error ΔIB results from the difference in equivalent-concentrations (eq / L) of cations and anions according to the following equation:

$$\Delta IB = \frac{\sum cations - | \sum anions |}{\sum cations + | \sum anions |} \text{ x } 100$$

So the ΔIB is a output in percent and corresponds to the "relative error" based on the total ion concentration.

Since there is no electrically charged water in nature, the ΔIB value should be exactly zero. This ideal case is unlikely to be achieved in practice and water analysis including an error less than 5% are tolerable. The ionic balance error of a water analysis can also be incomplete by not measured or sampled ions. Other causes of error are:

- analysis or measurement error in the laboratory
- one or more dissolved species (primary ions) were not sampled
- using unfiltered samples containing particulate matter, which (for preservation purposes) dissolve in addition of acid.

Sample	**IB [%]**	**Sample**	**IB [%]**
Sa01	-12,02	Sa17	17,36
Sa02	4,8	Sa18	3,21
Sa03	-0,78	Sa19	12,54
Sa04	2,1	Sa20	-39,21
Sa06	13,22	Sa21	-18,3
Sa07	2,89	Sa22	4,33
Sa08	1,11	Sa23	-0,13
Sa09	1,96	Sa24	3,49
Sa10	1,74	Sa25	2,94
Sa11	0,84	Sa26	3,0
Sa12	0,56	Sa27	4,83
Sa13	-4,43	Sa28	5,37
Sa14	-4,29	Sa29	12,43
Sa15	-47,35	Sa30	1,35
Sa16	13,34		

Table 6: Ionic balance error.

4.4 Hydrochemical distribution maps

The hydrochemical distribution maps are based on the results of the hydrochemical analyses of the observation points. Divided in the primary- and secondary aquifer, the samples Sa01 to Sa30 were take into account. Additional boreholes have been listed for possible future investigations as well. Divided in the first- (river samples and shallow boreholes) and second aquifer (samples Sa01 to Sa30), the spatial distribution of the anions and cations were interpolated with ArcGIS 10.1 using the Inverse Distance Weighting method. The results could only be used as a first idea of the distribution, because the method didn´t include basic boundary conditions like the topology, the groundwater flow direction or connectivity between groundwater and river. These factors were included afterwards by image editing.

Due to limited measuring points it is not possible to interpolate confident concentrations at the borders of the study area. With respect to this fact, zones of an "unclear state" were added, visualized by transparent cross lines in the maps.

The order of the distribution maps is based on the importance (pH, conductivity), the main constituents (sodium, calcium, chlorine, bicarbonate, magnesium), followed by the nitrogen compounds (ammonium, nitrite, nitrate), the sulfur compounds (sulfur, sulfate, phosphate) and the further analyzed ingredients (arsenic, bromine, potassium, iron, strontium, silicon).

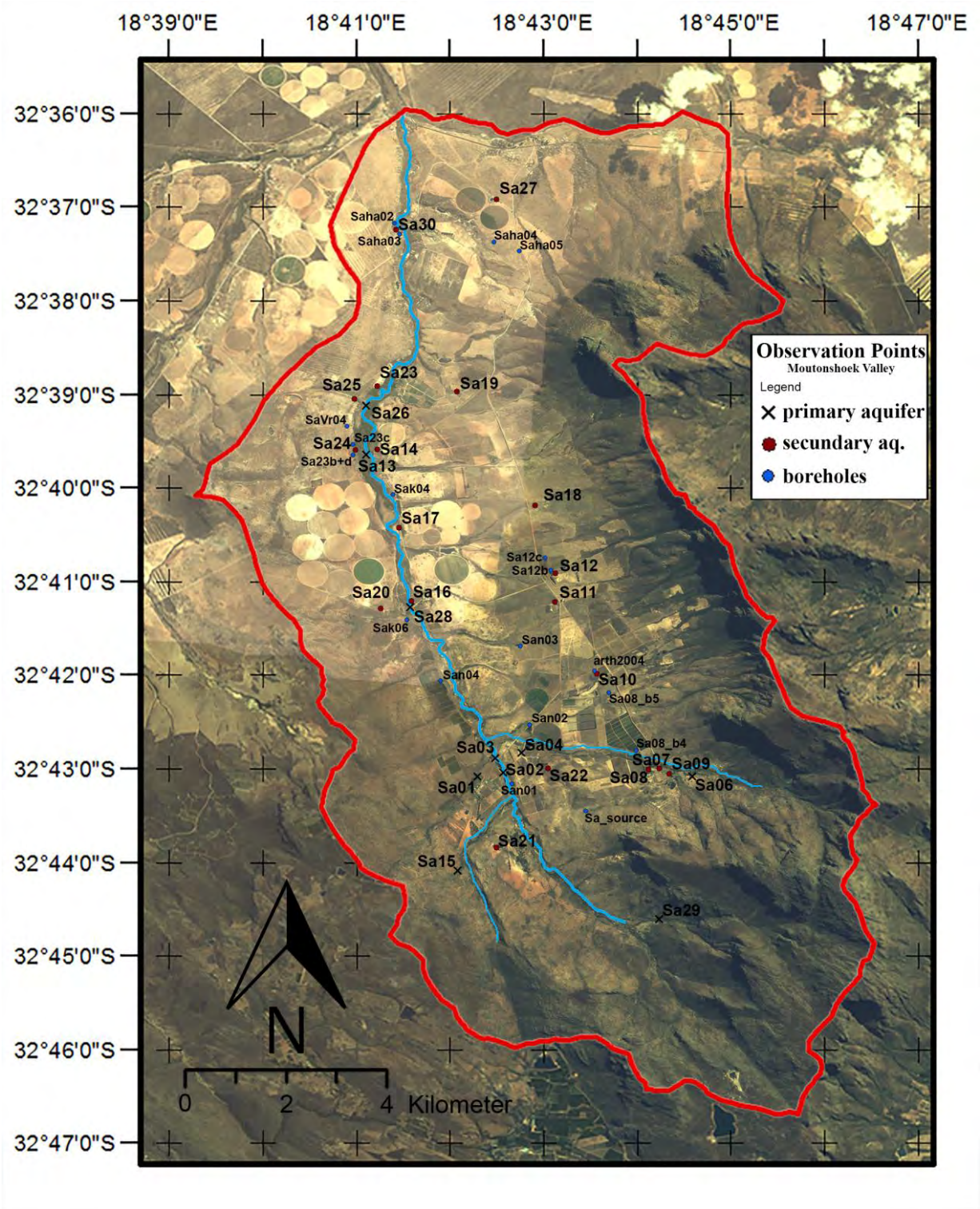

Figure 22: Observation points of the master thesis in Moutonshoek Valley (Sa01 - Sa30).

4.4.1 Conductivity

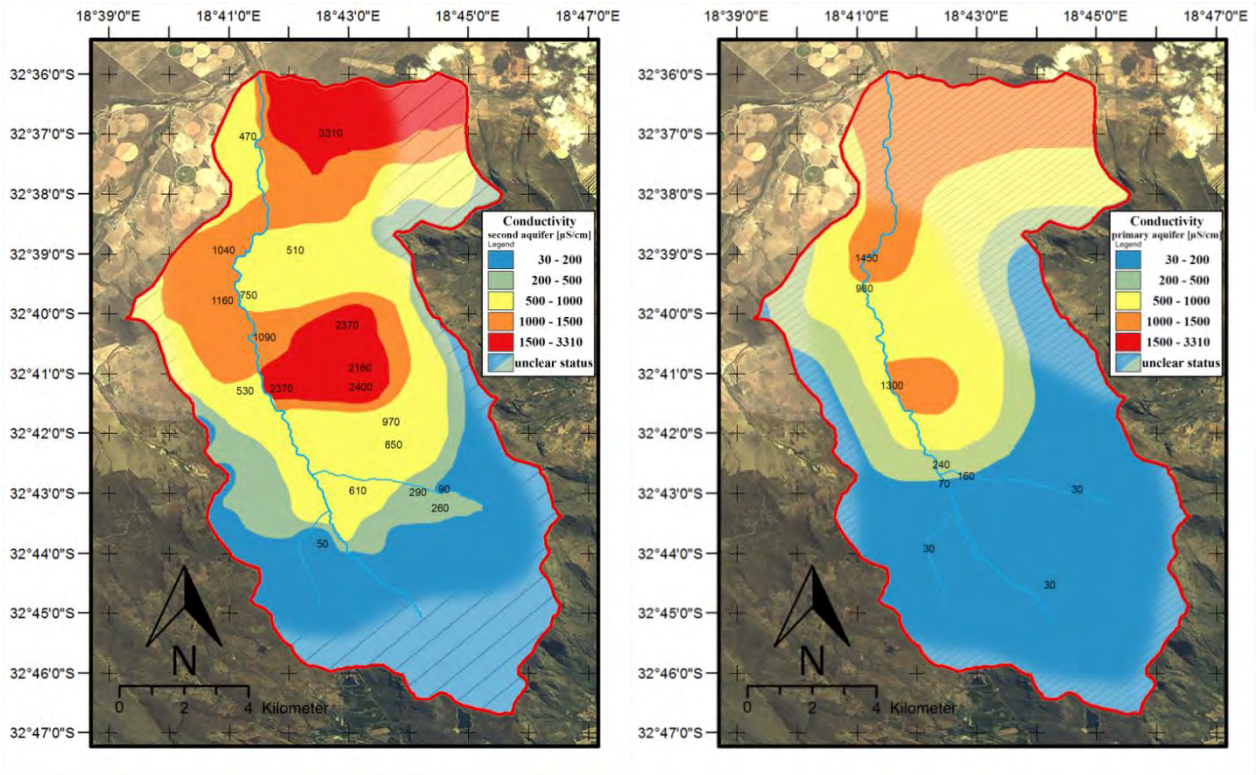

Figure 23 and 24: Spatial distribution maps of the conductivity in the second- (left) and primary (right) aquifer.

The conductivity in the catchment ranges from about 30 µS/cm in topographically higher areas and upstream in the primary aquifer, up to 3310 µS/cm in specific locations. Probably influenced by surface runoff, the conductivity in the first aquifer increases slowly (Fig.24) up to 1450 µS in the last measured sample downstream. The second aquifer (Fig.23) got a conspicuous hot spot near the Riviera Granite Dome as well as in the direction of its groundwater flow. Four samples, namely Sa11, Sa12, Sa16 and Sa18 with an electrical conductivity > 2000 µS/cm leads to brackish waters in this area. Another hot spot further north (Sa27) with the top conductivity in the study area of more than 3300 µS/cm is present, too. On the western side of the catchment medium grade conductivities could be measured. Samples Sa24 and Sa25, both in the north-western part got conductivities of more than 1000 µS/cm. Comparing to the geological map (Fig.6) the mentioned samples are all present in Malmesbury Rock aquifers. Conductivities in the Table Mountain aquifer for example in the south-east of the study area (Sa21), come up with conductivities below 500 µS/cm. Due to the influent behavior of the Krom Antonies River, the downstream conductivity in the second aquifer decreases again.

4.4.2 pH

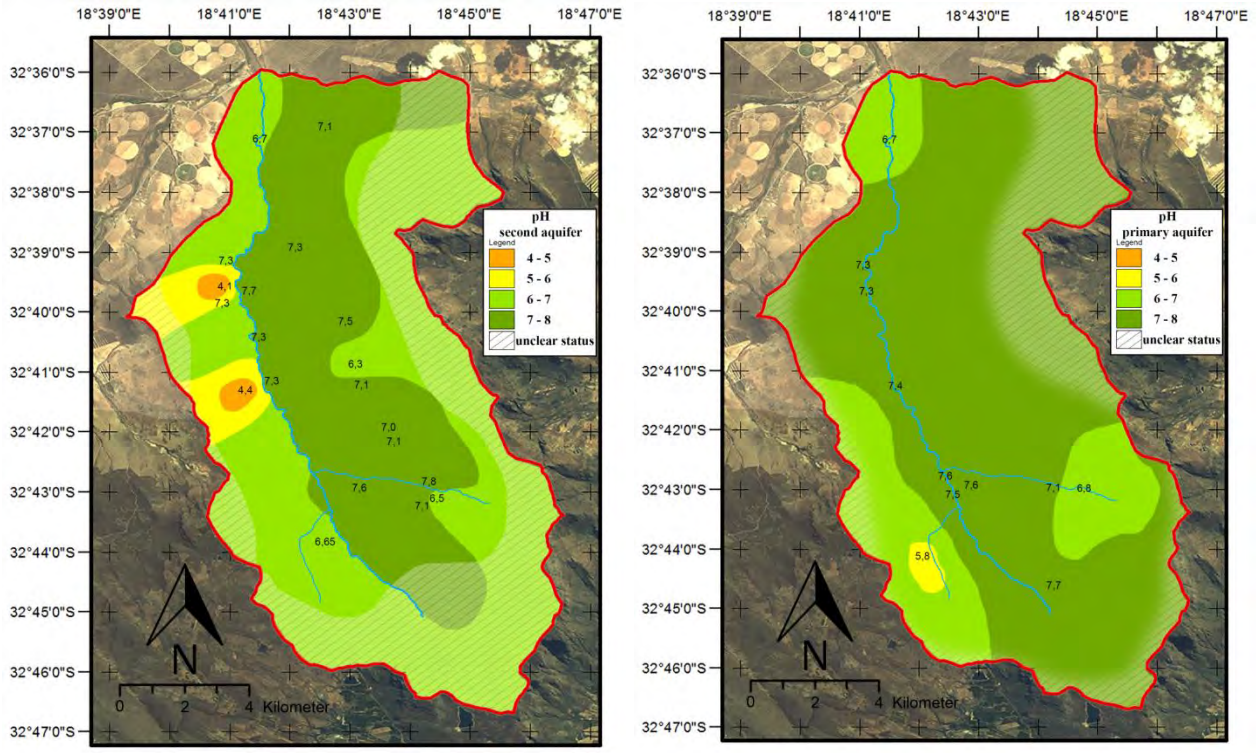

Figure 25 and 26: Spatial distribution maps of the pH in the second- (left) and primary (right) aquifer.

The pH values of the waters in the study area is bound to its position either east or west to the Krom Antonies River. East of the Krom Antonies River, the pH value ranges from 6,3 to 7,8- averagely in an neutral state of about 7,3. On the western side more acidic waters are present. PH-values of 4,1 and 4,4 in the second aquifer samples Sa24 and Sa25 could be detected. Mixed up downstream, the surface water as well as the water of the second aquifer drains into the Verlorenvlei with an pH value of about 6,7. Low pH values in the primary aquifer can be explained to the influence of rain water.

4.4.3 Sodium

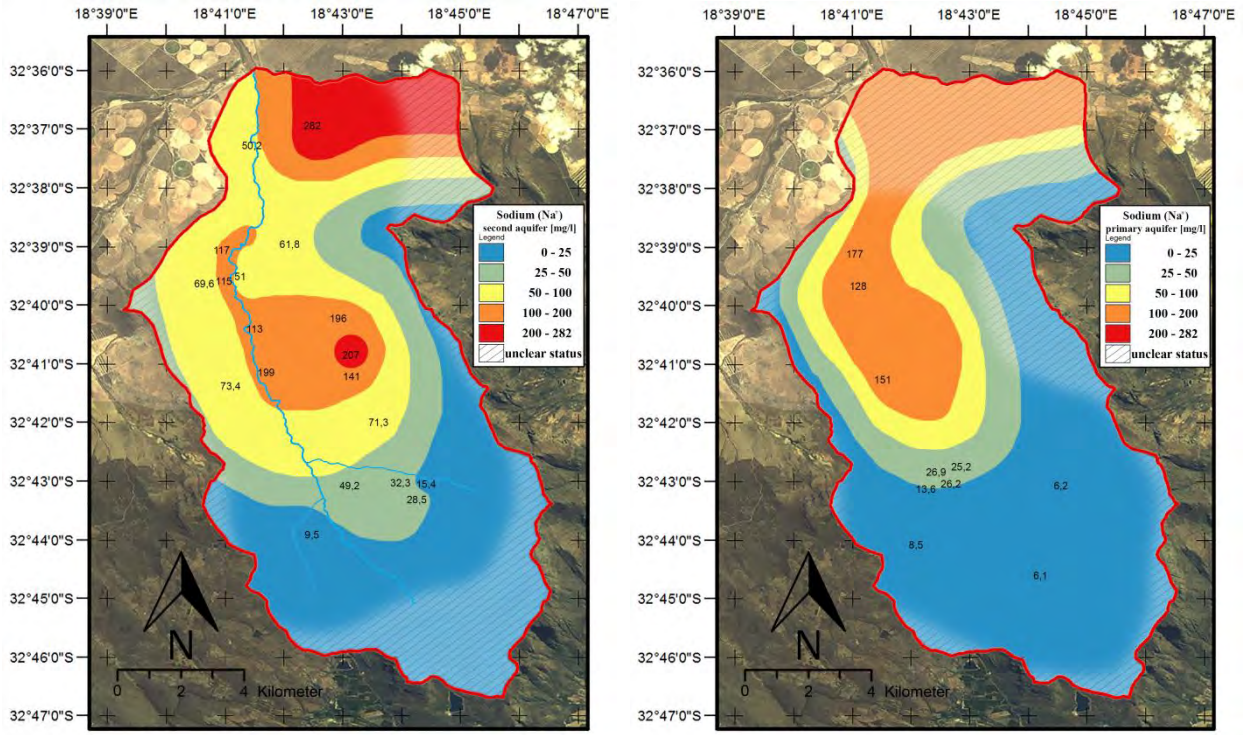

Figure 27 and 28: Spatial distribution maps of sodium in the second- (left) and primary (right) aquifer.

The amounts of sodium ranges between 9,5 mg/l to 282 mg/l in the second- and between 6,1 mg/l to 177 mg/l in the primary aquifer. The distribution in the primary aquifer seemingly rising due to the amount of infiltrating groundwater of the second aquifer in the area of the artesian borehole Sa14 in the middle of the catchment. In the second aquifer the location near the Riviera Granite Dome as well as in the direction of its groundwater flow shows higher amounts of sodium as well. All four samples, Sa11, Sa12, Sa16 and Sa18 contains sodium between 140 mg/l and 207 mg/l.

4.4.4 Calcium

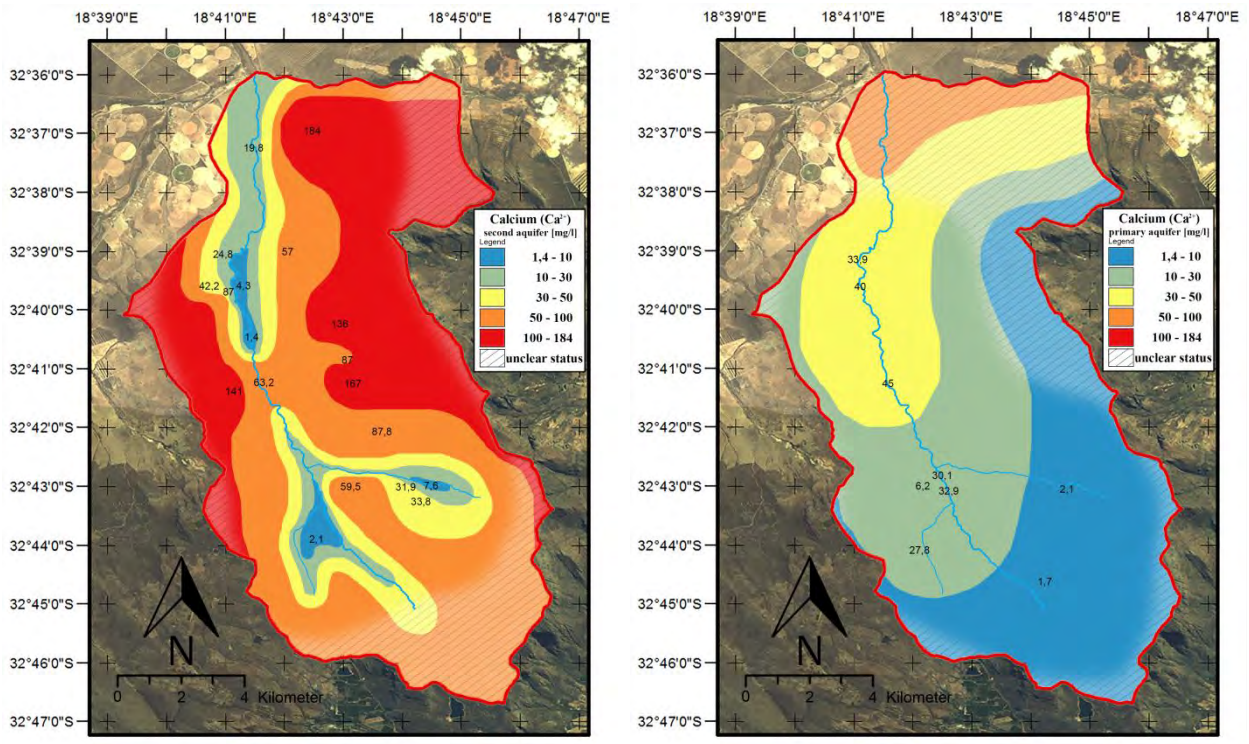

Figure 29 and 30: Spatial distribution maps of calcium in the second- (left) and primary (right) aquifer.

The distribution of calcium in the primary aquifer looks quite normal. From up- to downstream the concentration rises slowly from about 1,7 mg/l in the south to about 40 mg/l in the north. Due to a interpolation it is supposed that the concentration rises onwards up to about 60 mg/l. The second aquifer is kind of inverted. The concentration of calcium decreases from up- to downstream either on the eastern and on the western side of the valley. About 140 mg/l to 180 mg/l on the flanks of the valley down to 4,3 mg/l below the Krom Antonies River were measured.

4.4.5 Chlorine

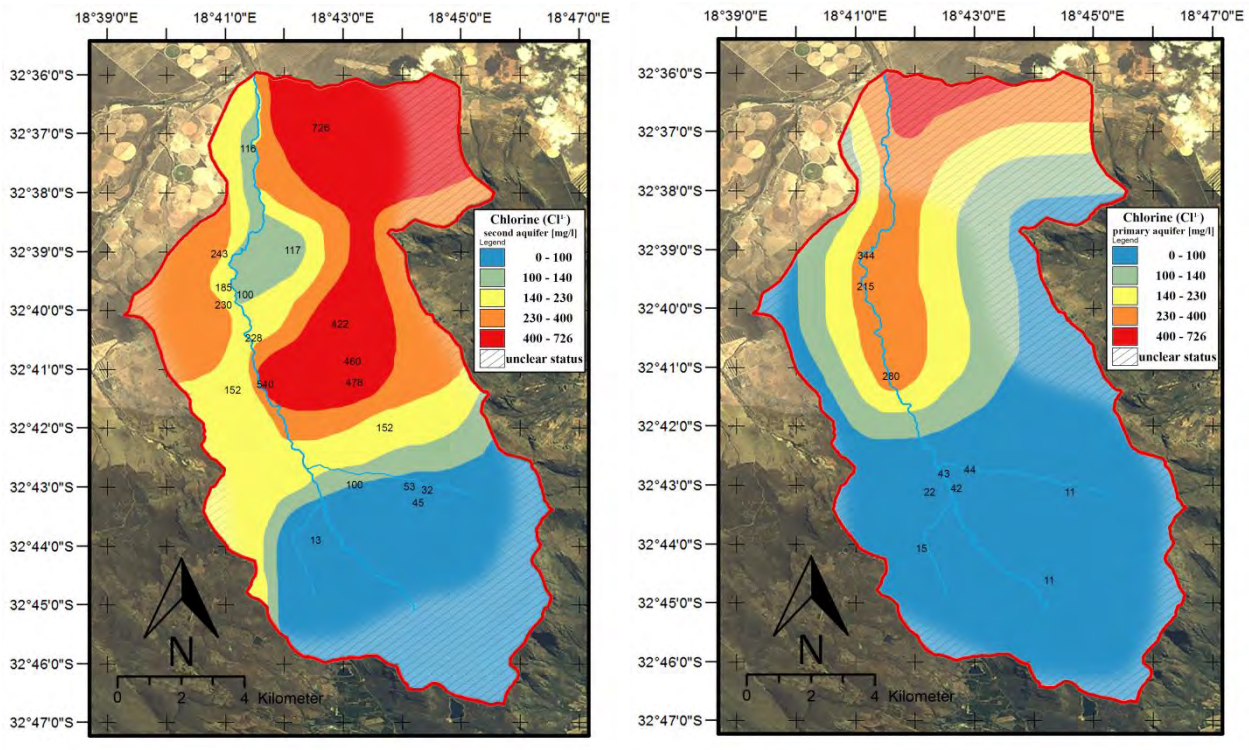

Figure 31 and 32: Spatial distribution maps of chlorine in the second- (left) and primary (right) aquifer.

The concentration of chlorine in the primary aquifer ranges between 11 mg/l upstream up to 344 mg/l downstream. The concentration probably rises due to the mix with waters coming out of the aquifer of the Malmesbury Group with concentrations between 230 mg/l in the western part up to 540 mg/l in the western part with the highest peak of about 720 mg/l in the north (Sa27) in the second aquifer. A hot spot of Chlorine is near the Riviera Granite Dome, including the samples Sa11, Sa12, Sa16 and Sa18.

4.4.6 Bicarbonate

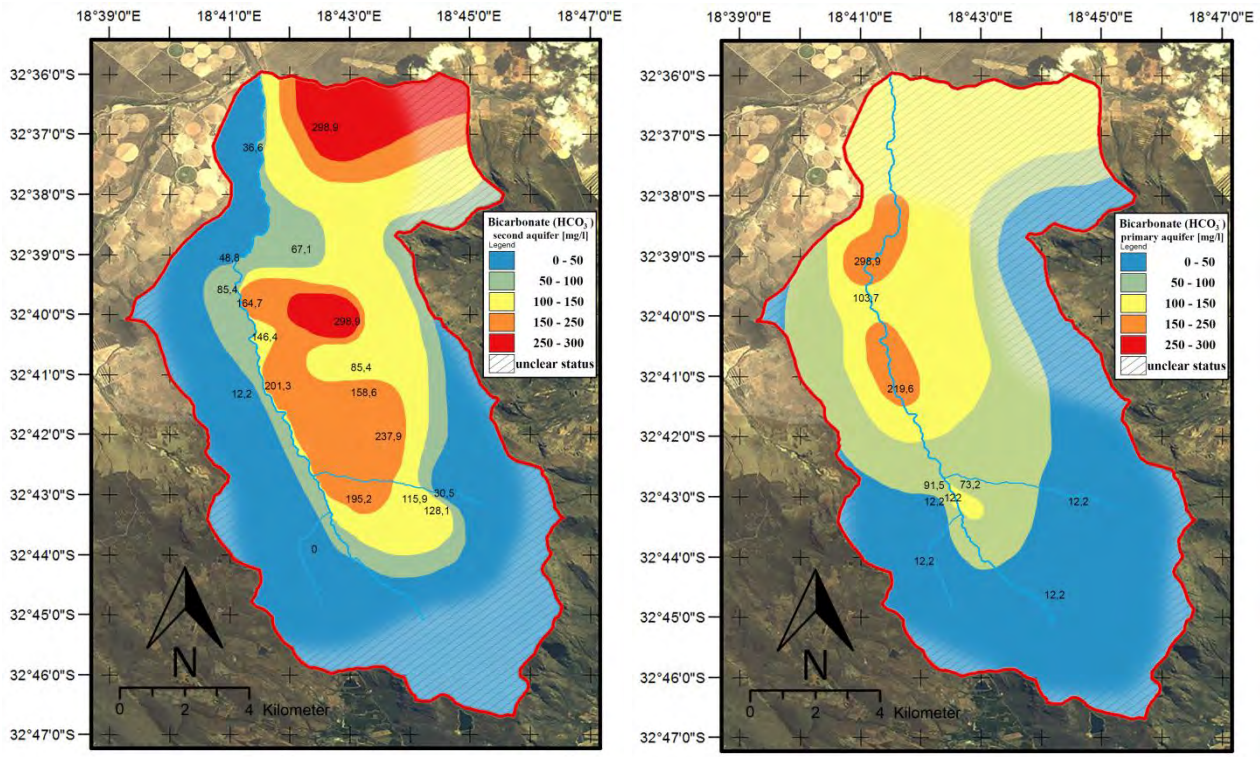

Figure 33 and 34: Spatial distribution maps of bicarbonate in the second- (left) and primary (right) aquifer.

The bicarbonate concentration in the study area ranges between the undetectable minimum in areas of low pH in the south-west up to 298,9 mg/l in the eastern and north-eastern part of the study area in the second aquifer. Waters influenced by rain in the primary aquifer contains about 12,2 mg/l. Downstream the concentration rises probably due to infiltrating waters of the second aquifer up to 298,9 mg/l in sample Sa26. A spot of medium concentration of bicarbonate is present in the area of the Riviera Granite dome in the second aquifer with concentrations about 150 mg/l and 240 mg/l.

4.4.7 Magnesium

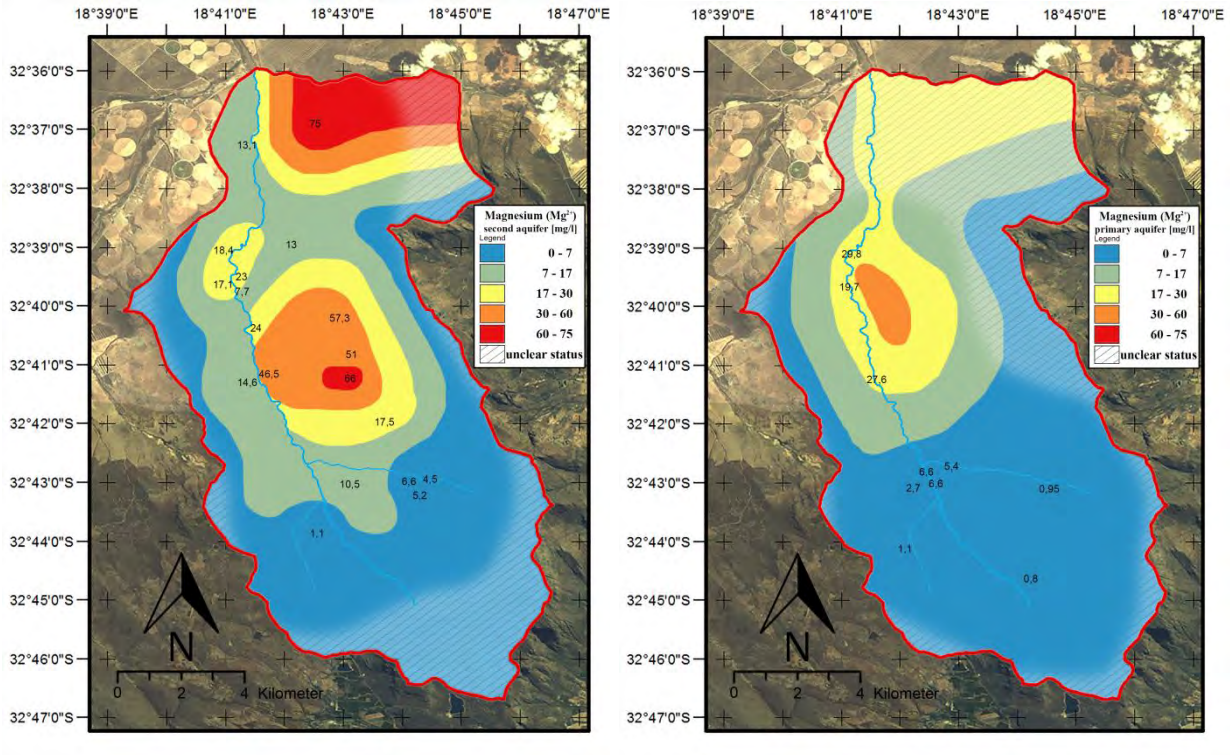

Figure 35 and 36: Spatial distribution maps of magnesium in the second- (left) and primary (right) aquifer.

The concentration of magnesium in the study area ranges between 0,8 mg/l and 30 mg/l in the primary aquifer and between 1,1 mg/l up to 75 mg/l in the second aquifer. A hotspot of up to 66 mg/l can be located at sample Sa11 near the Riviera Granite Dome, as well as up to 75 mg/l in the north at sample Sa27, both located in the second aquifer.

4.4.1 Ammonium

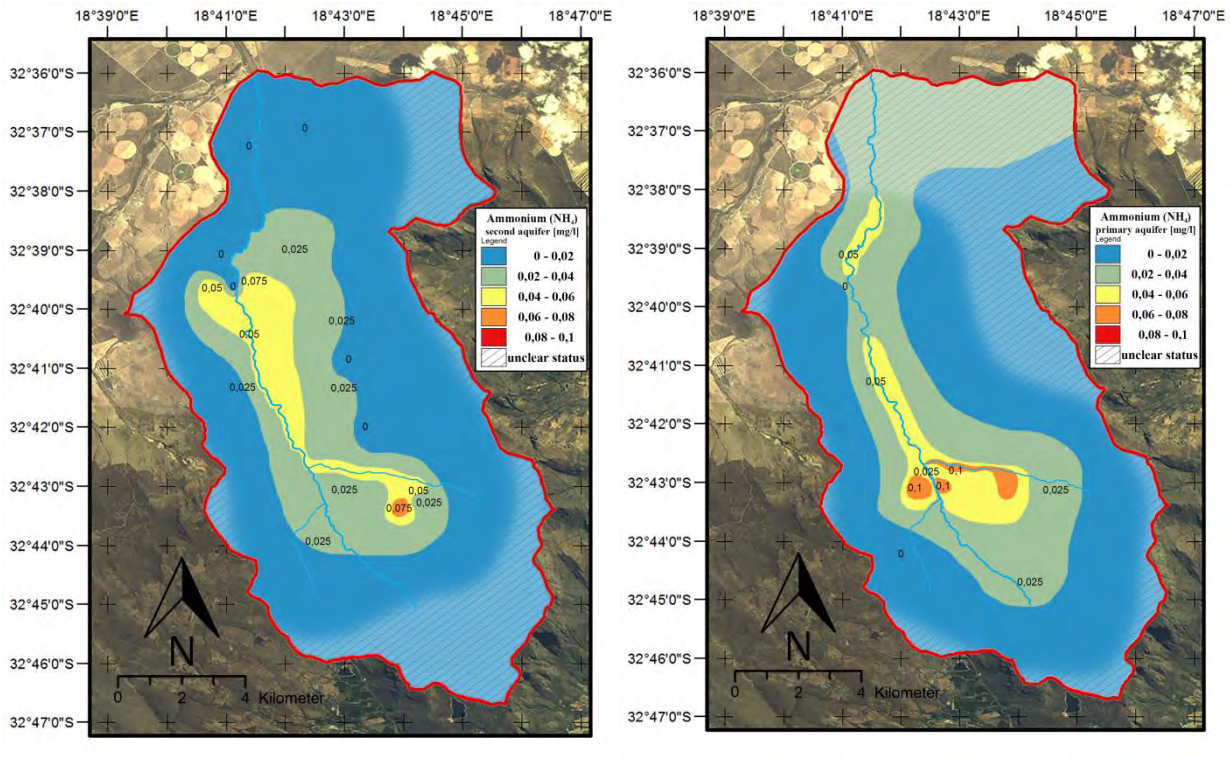

Figure 37 and 38: Spatial distribution maps of ammonium in the second- (left) and primary (right) aquifer.

The concentration of ammonium in the study area is quite low. The primary aquifer involves the samples with the highest concentrations of up to 0,1 mg/l in the samples Sa01, Sa02 and Sa04 which all three are surface water samples and accordingly indicating a man-made influence on these waters (as described on page 69) due to concentrations in the second aquifer of not more than 0,025 mg/l in sample Sa21. The concentrations in the second aquifer ranges between 0,025 mg/l and 0,05 mg/l with a peak of about 0,075 mg/l at sample Sa08. Downstream the concentrations in both, the primary- and secondary aquifer decreases due to the mix of low concentrated waters of the northern flanks of the study area.

4.4.2 Nitrite

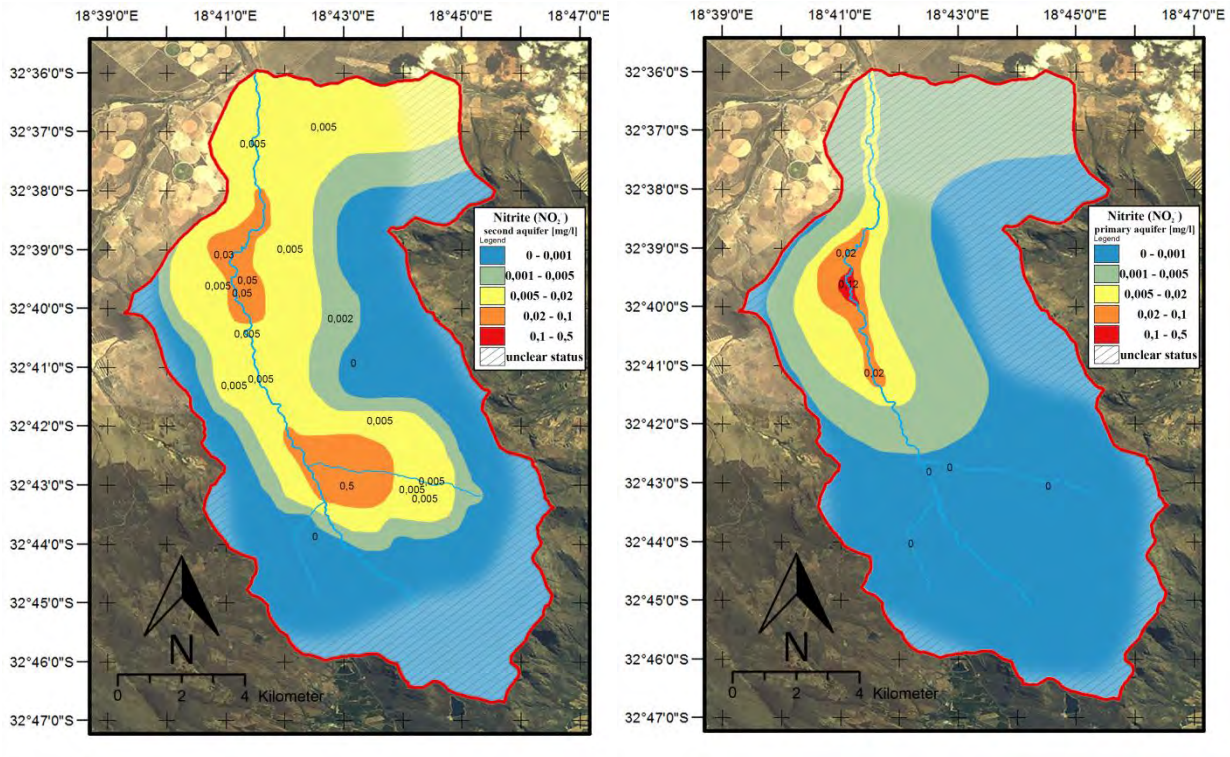

Figure 39 and 40: Spatial distribution maps of nitrite in the second- (left) and primary (right) aquifer.

Areally the second aquifer contains a larger amount of nitrite than the primary aquifer. Detectable concentrations in the second aquifer can be seen upstream of the Eselshoek River near the Kromvlei farm in the south-eastern part of the study area. Downstream concentrations up to 0,5 mg/l at second aquifer sample Sa22 could be detected, an area were the primary aquifer contains concentrations below the detectable minimum. In the primary aquifer nitrite concentrations above the detectable minimum can only be seen further downstream, beginning with the sample Sa28 with an concentration of about 0,02 mg/l. A peak of nitrite can be seen at sample Sa13 (about 0,12 mg/l) in close proximity to the artesian borehole Sa14 of the second aquifer and downstream of intense agricultural used areas on the western flank of the valley. Those amount clearly exceeds the WHO maximum permissible value of nitrite for drinking water of about 0,1 mg/l.

4.4.1 Nitrate

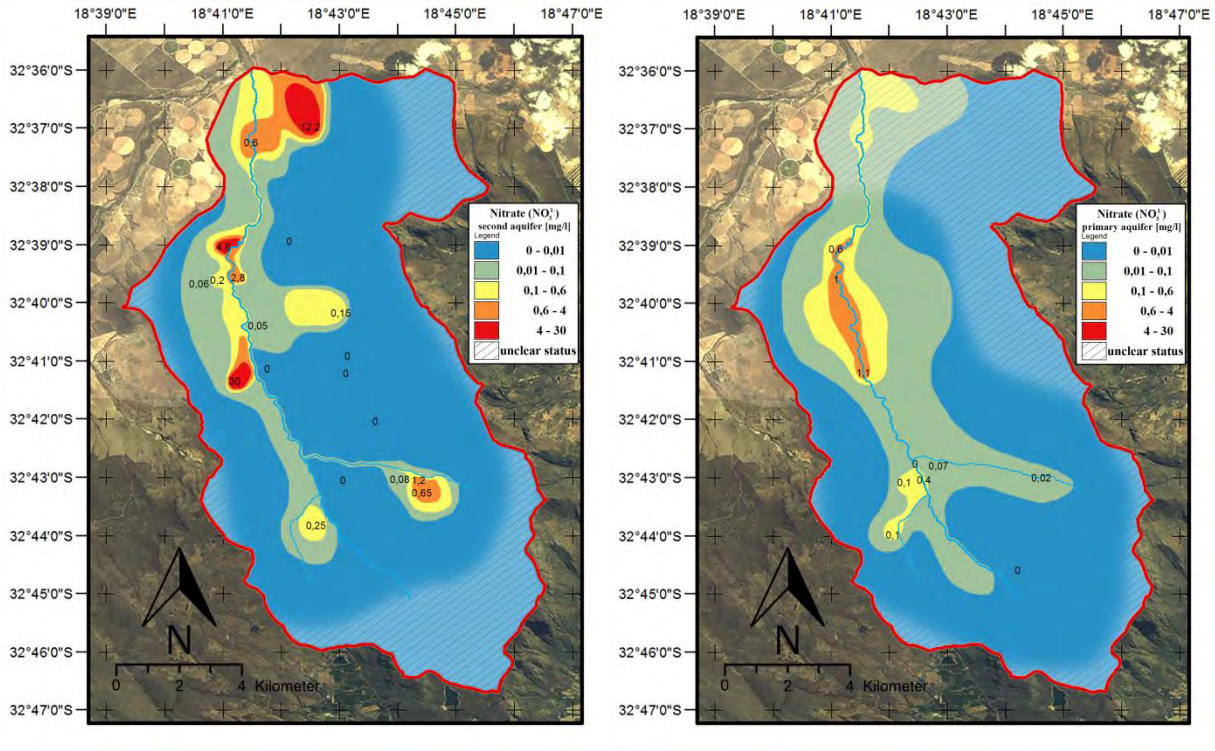

Figure 41 and 42: Spatial distribution maps of nitrate in the second- (left) and primary (right) aquifer**.**

The nitrate concentrations of the second aquifer ranges between the undetectable limit (< 0,02 mg/l) on the flanks of the valley up to 4,6 mg/l downstream. Two hotspots catch the eye in the second aquifer: Sa20 on the eastern side with a peak of about 30 mg/l and in the north Sa27 with up to 12,2 mg/l. Compared to the second- the concentrations in the primary aquifer are quite low. Concentrations of about 0,02 mg/l upstream, up to 1,1 mg/l in the central valley at sample Sa13 and Sa28. It is supposed that the nitrate concentrations continue to rise further downstream due to the occurrence of a nitrate source which also influences sample Sa27.

4.4.2 Manganese

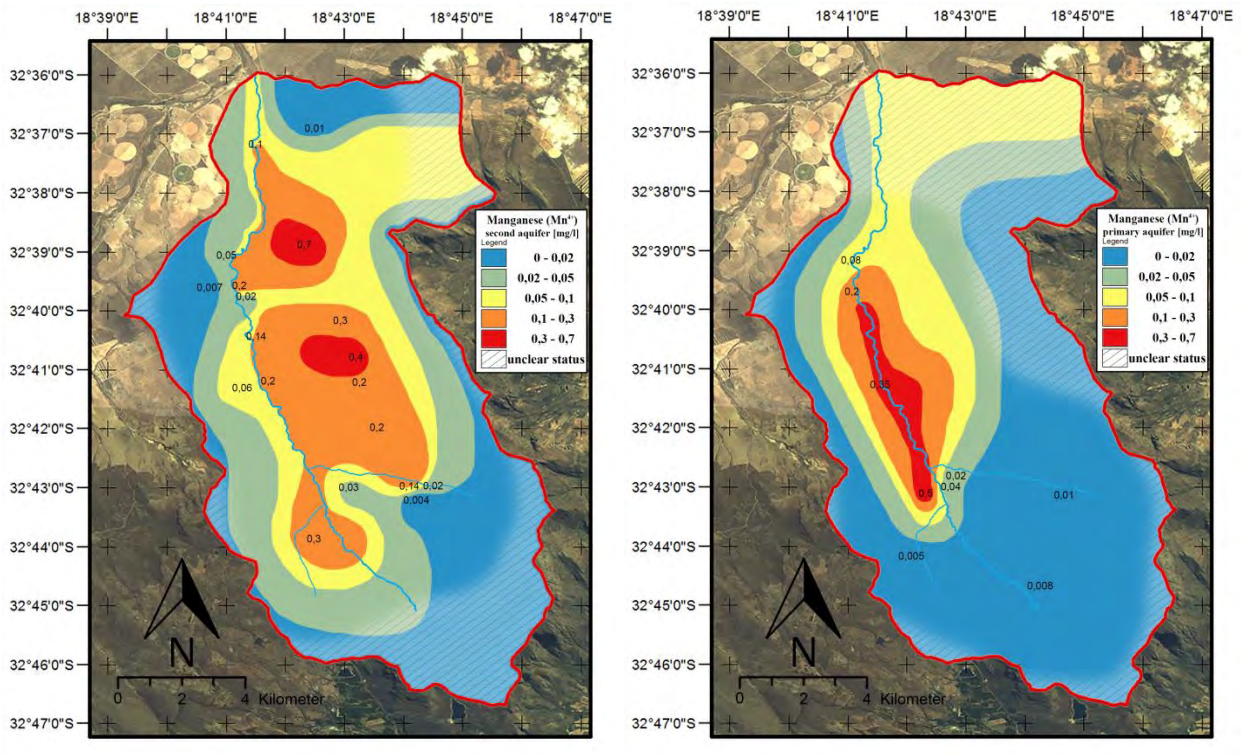

Figure 43 and 44: Spatial distribution maps of manganese in the second- (left) and primary (right) aquifer.

The concentration of manganese in the second aquifer ranges between 0,007 mg/l up to 0,3 mg/l with peaks of 0,4 mg/l and 0,7 mg/l in the samples Sa12 and Sa19. In the area of the Riviera Granite dome concentrations of about 0,2 mg/l were detected. Except for a source of manganese of about 0,5 mg/l at sample Sa03 which obviously influences the downstream samples as well, the concentration in the study area did not exceed 0,01 mg/l in the primary aquifer. The concentration downstream of sample Sa03 steadily deceases from 0,5 mg/l at sample Sa03 to 0,35 mg/l at sample Sa28 to 0,2 mg/l at sample Sa13 to finally 0,08 mg/l at sample Sa26 in the north.

4.4.3 Fluorine

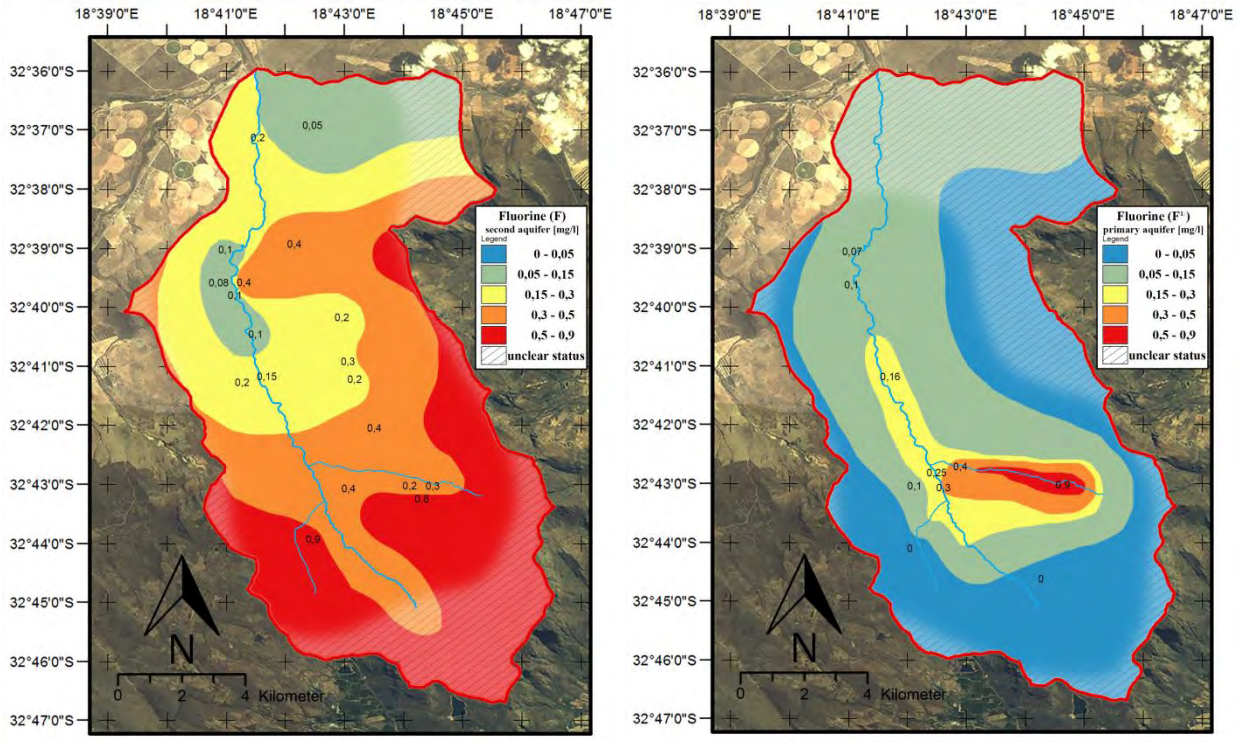

Figure 45 and 46: Spatial distribution maps of fluorine in the second- (left) and primary (right) aquifer.

The distribution of fluorine in the second aquifer decreases from up- to downstream. Concentrations of up to 0,9 mg/l in the south-eastern part at sample Sa21 and 0,8 mg/l in the south-western part at sample Sa09 are steadily decreasing below 0,1 mg/l at sample Sa25. Therefore the concentrations on the flanks of the valley are proposed to be greater than 0,5 mg/l, even there aren´t measuring points available to confirm these assumption. Except for an hotspot of fluorine at sample Sa06 with a detected concentration of about 0,9 mg/l and decreasing concentrations downstream of this sample, there is hardly any fluorine in the primary aquifer. This might lead to the lowering of the concentration in the second aquifer due to infiltrating surface waters.

4.4.4 Sulfur

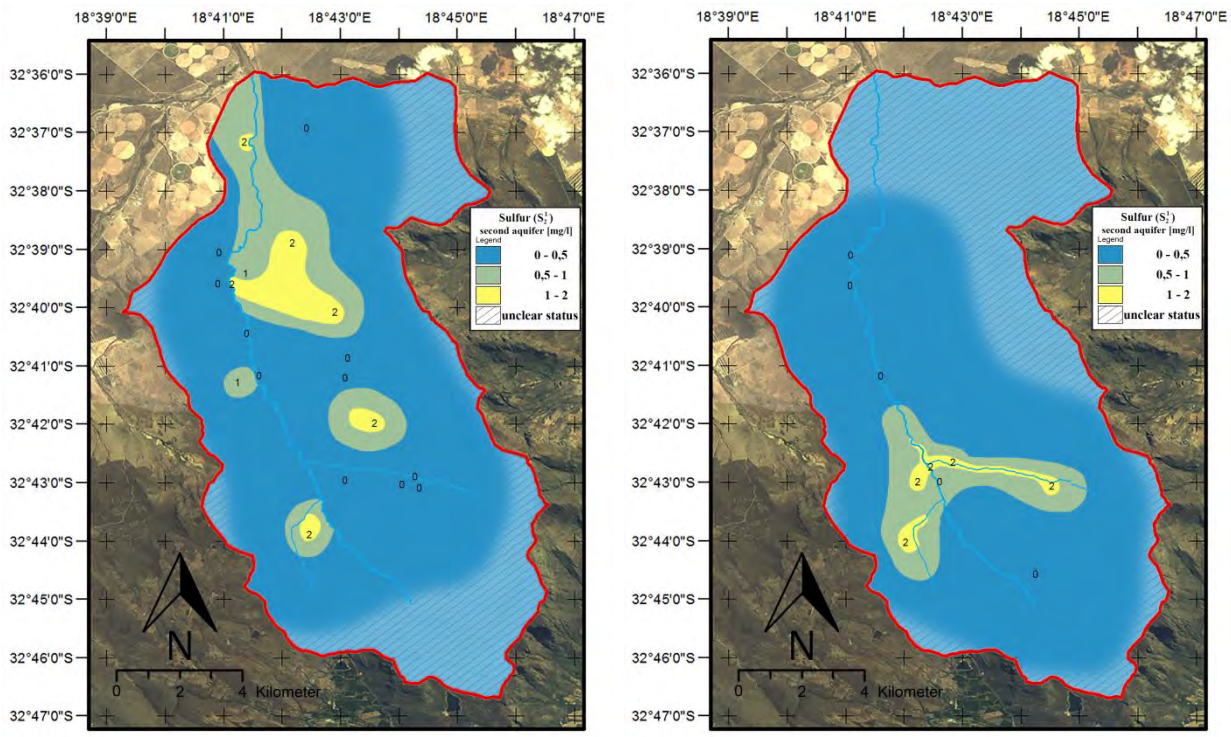

Figure 47 and 48: Spatial distribution maps of sulfur in the second- (left) and primary (right) aquifer.

The concentration of sulfur, meaning the measured concentration of HS^--Ions, in the study area ranges between the undetectable limit (< 1 mg/l) and at maximum about 2 mg/l in the primary as well as the secondary aquifer. The sources in the primary aquifer are detected upstream at samples Sa01, Sa03, Sa04, Sa06 and Sa15 with concentrations of 2 mg/l and randomly distributed in the second aquifer.

4.4.5 Sulfate

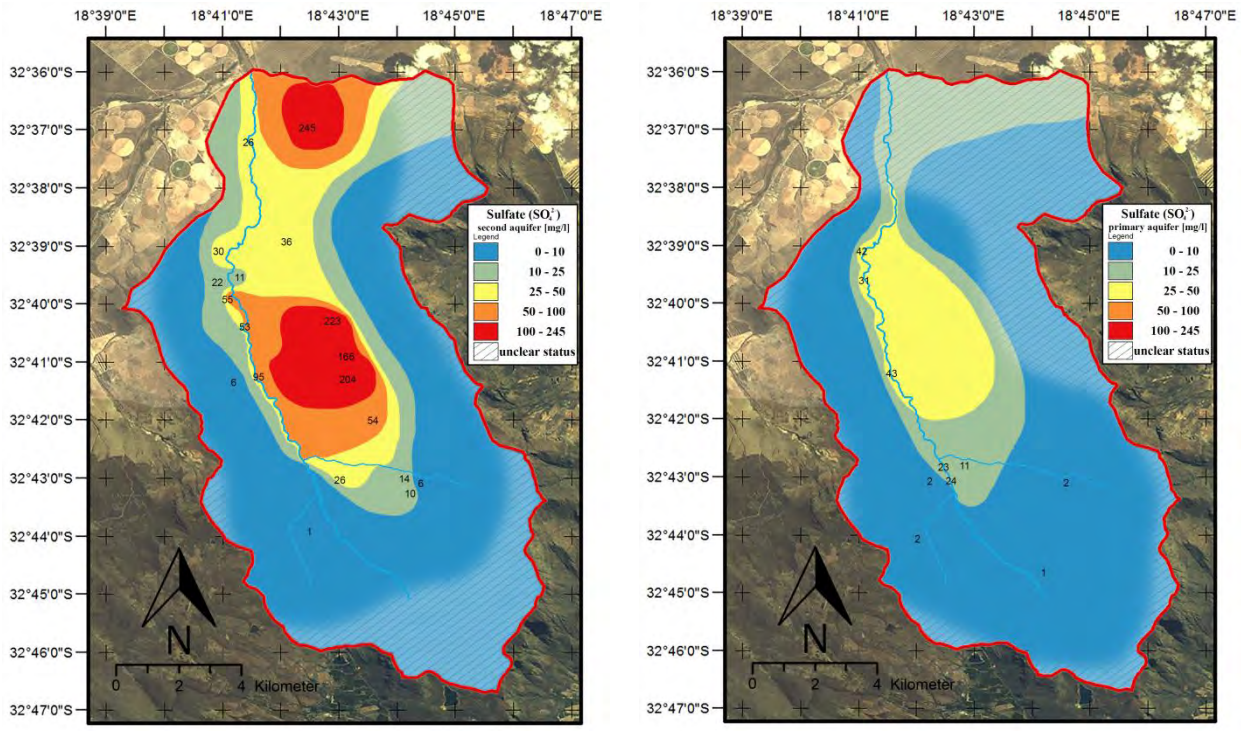

Figure 49 and 50: Spatial distribution maps of sulfate in the second- (left) and primary (right) aquifer.

The concentration of sulfate in the second aquifer ranges between 1 mg/l upstream and in the flanks of the valley to 200 mg/l in samples Sa11, Sa12 and Sa18 up to a peak of about 245 mg/l in sample Sa27. The hotspots in the second aquifer are matching with the peaks of the EC. The concentrations of the primary aquifer are considerable lower. With a concentration of about 1 mg/l to 2 mg/l upstream, the concentration does not exceeds 43 mg/l downstream. It is conspicuous that the concentration in the primary aquifer rises at the point the high concentrated waters of the second aquifer come across due to the groundwater flow.

4.4.6 Phosphate

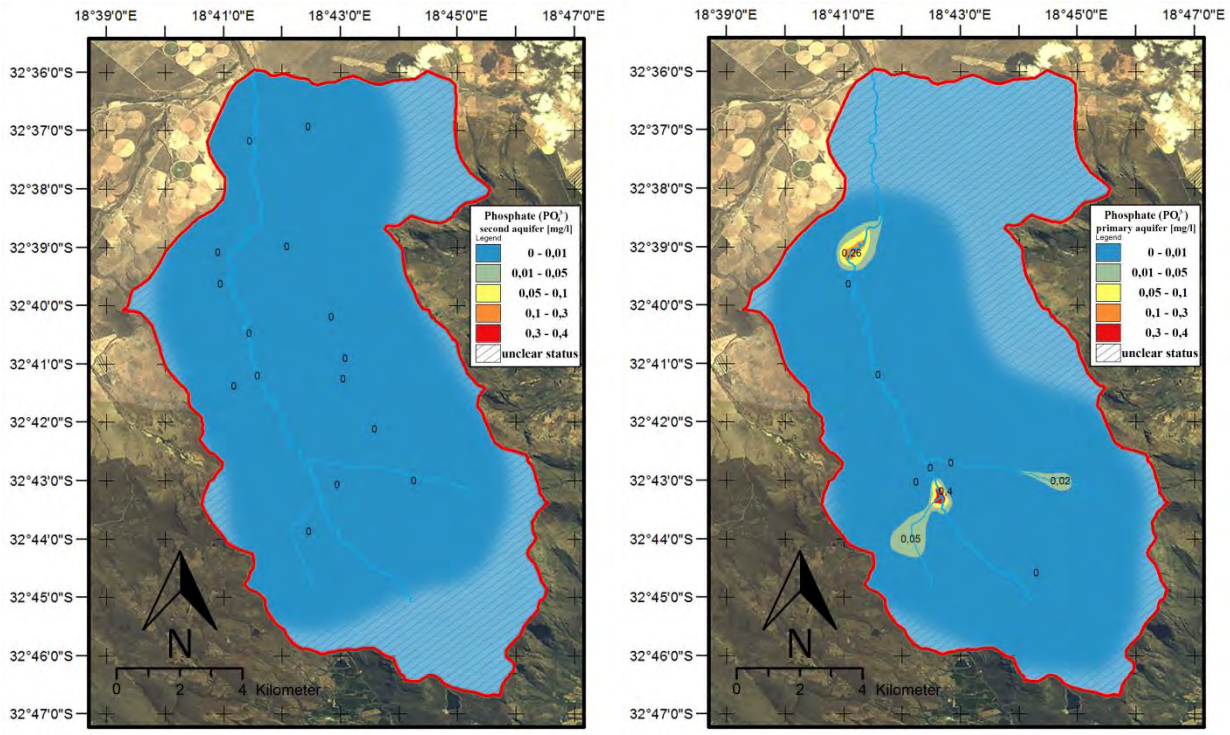

Figure 51 and 52: Spatial distribution maps of phosphate in the second- (left) and primary (right) aquifer.

Phosphate could only be detected in the first aquifer. Concentrations of 0,02 mg/l up to 0,4 mg/l matches with areas of increased agricultural usage and the presence of buildings.

4.4.7 Arsenic

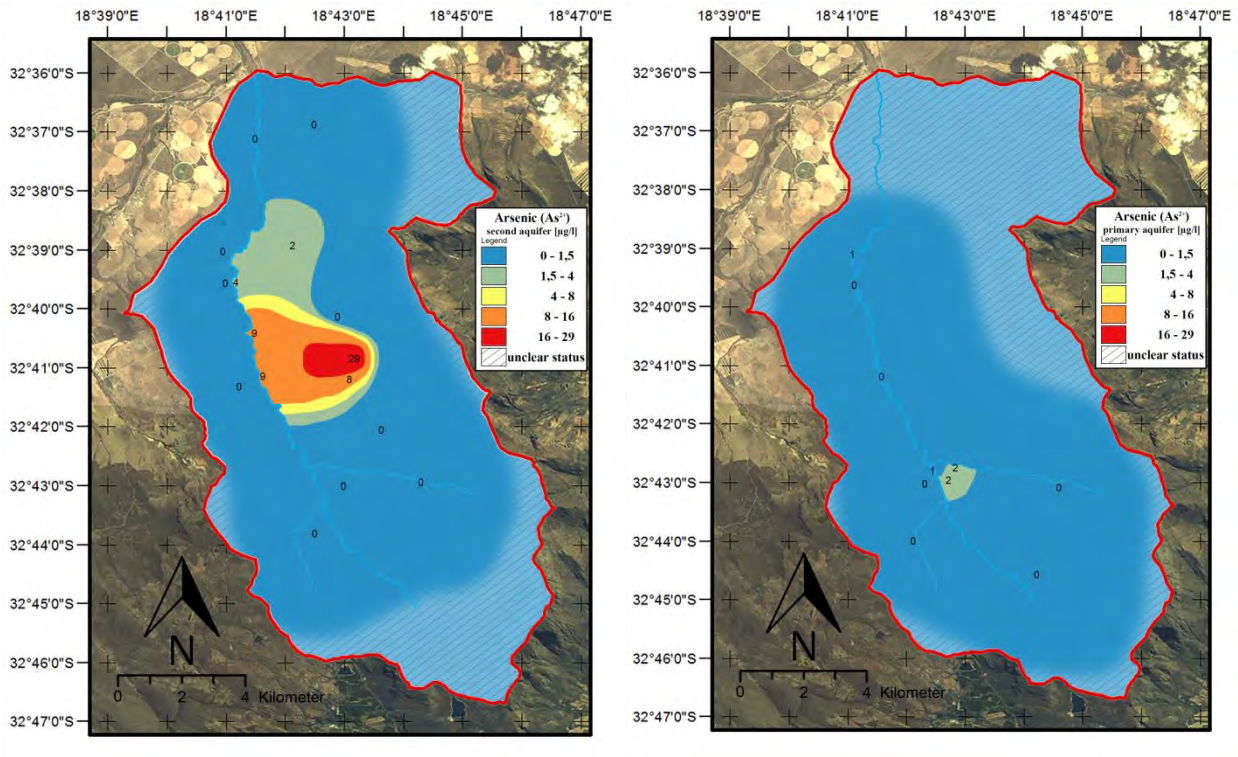

Figure 53 and 54: Spatial distribution maps of arsenic in the second- (left) and primary (right) aquifer.

A single source of arsenic bonds could be detected in the study area of about 29 µg or 0,029 mg/l at sample Sa12 in the second aquifer. Marginal grades of about 2 µg/l or 0,002 mg/l of arsenic bonds in the primary aquifer could be found in samples Sa02 and Sa04. These two are river samples out of the Krom Antonies River as well as the Eselshoek River. The WHO maximum permissible value for drinking water is about 0,01 mg/l.

4.4.8 Bromine

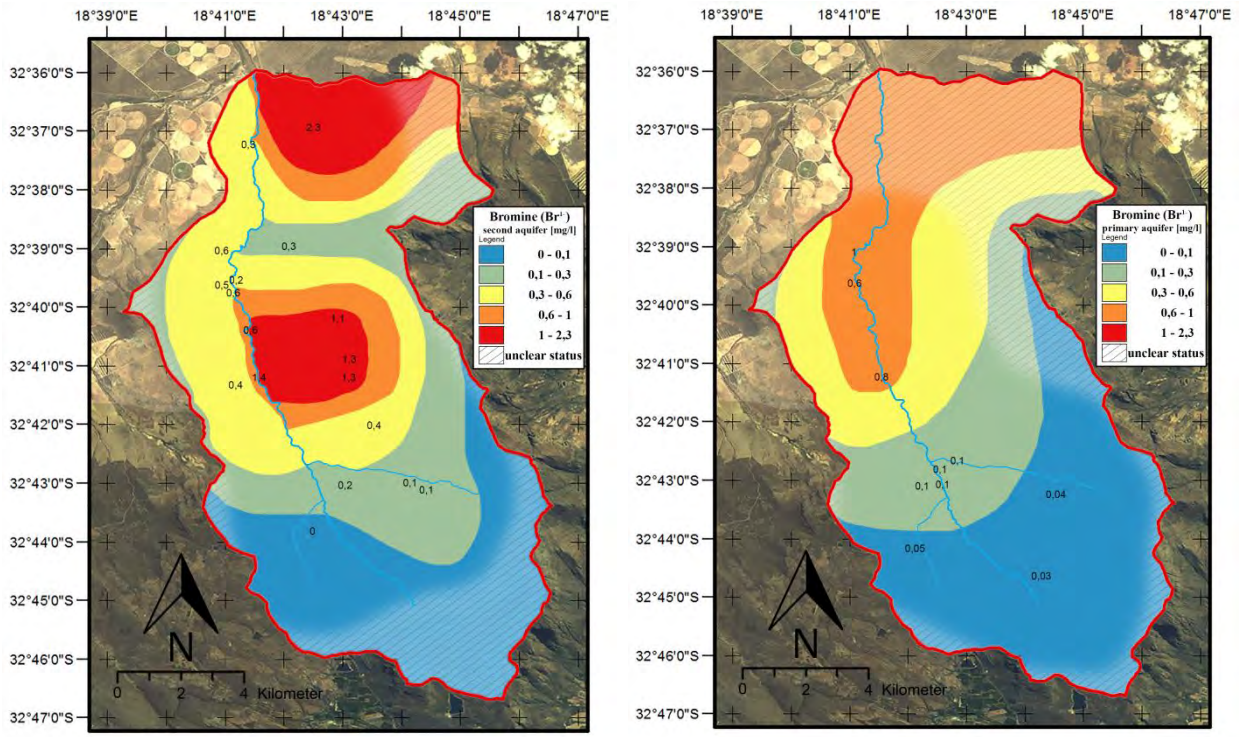

Figure 55 and 56: Spatial distribution maps of bromine in the second- (left) and primary (right) aquifer.

The concentration of bromine in the second aquifer ranges from 0,1 mg/l to 0,6 mg/l, in hot spots up to 1,3 mg/l in the samples near the Riviera Granite dome and up to 2,3 mg/l in sample Sa27 in the north. The primary aquifer contains steadily rising concentrations from up- to downstream in concentrations of about 0,03 mg/l to 0,8 mg/l.

4.4.9 Potassium

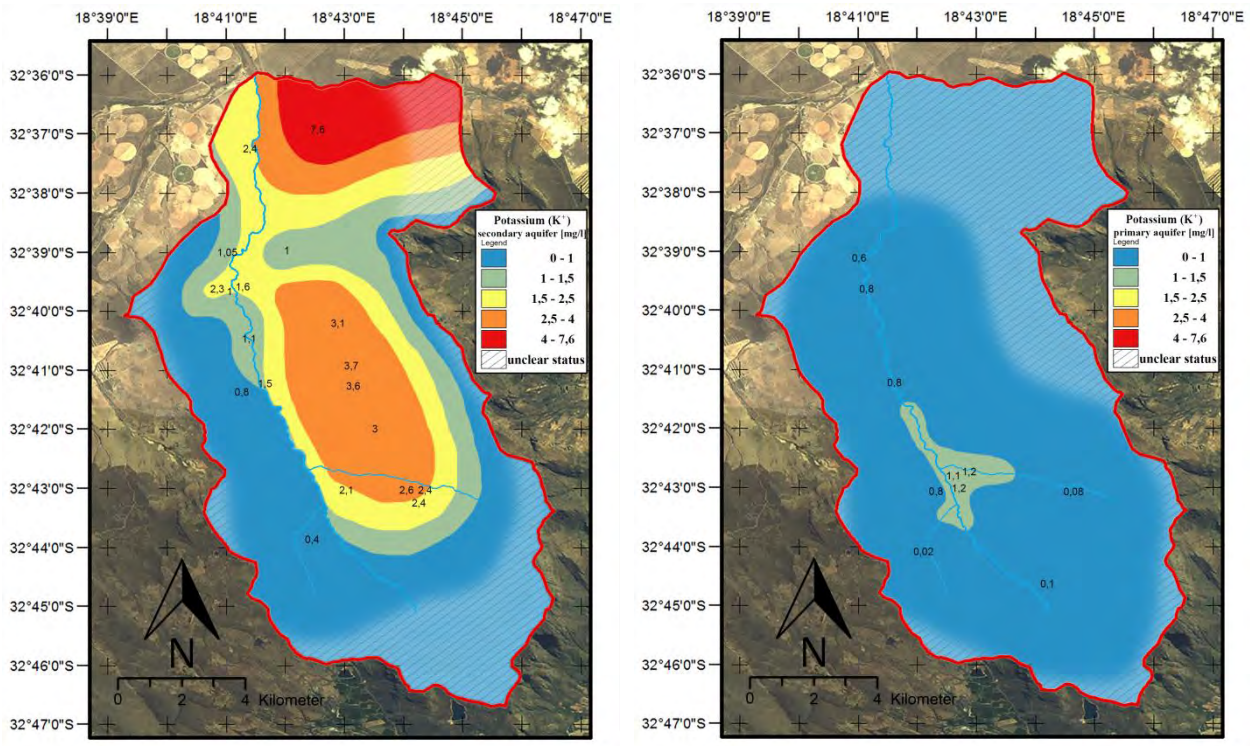

Figure 57 and 58: Spatial distribution maps of potassium in the second- (left) and primary (right) aquifer.

In the second aquifer low concentrations of not more than 1 mg/l potassium is shown in the western part of the Krom Antonies River as well as upstream and on the flanks of the valley. On the eastern side the concentrations ranges up to 3,7 mg/l near the Riviera granite and northerly. The highest concentrations of potassium were detected in sample Sa27 with 7,6 mg/l. The primary aquifer rarely exceeds concentrations of more than 1 mg/l distributed over the whole area.

4.4.10 Iron

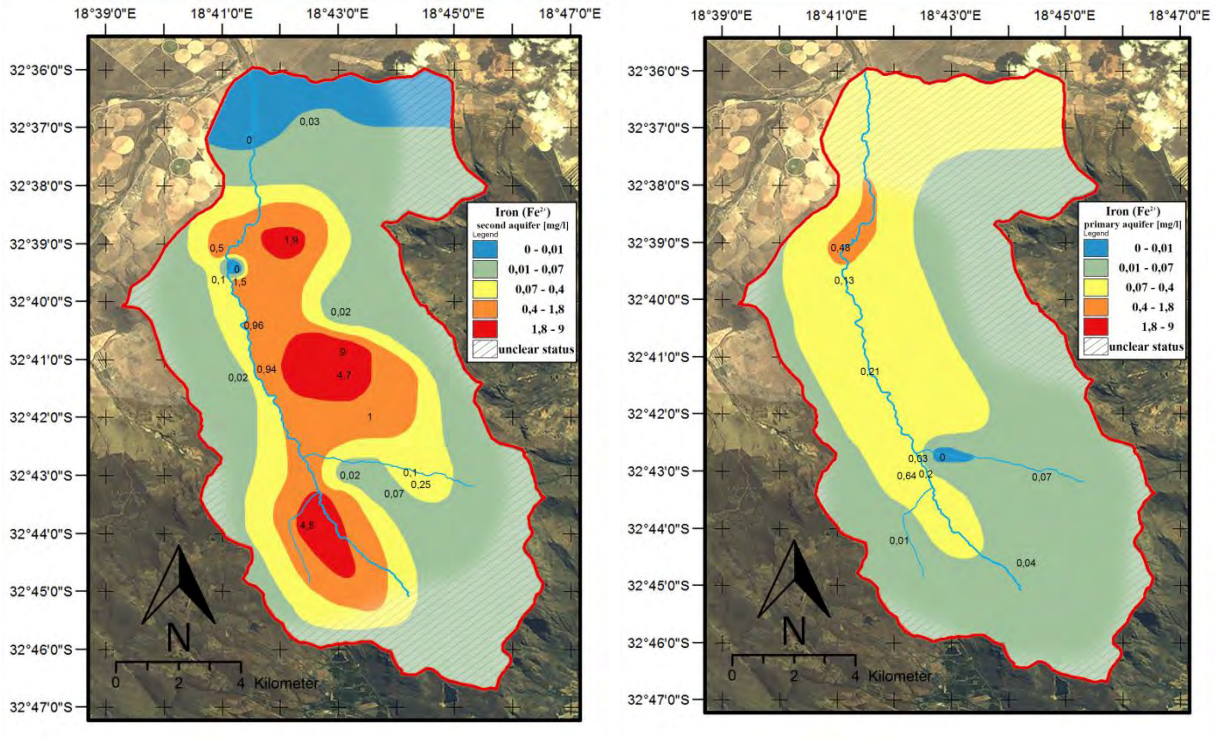

Figure 59 and 60: Spatial distribution maps of iron in the second- (left) and primary (right) aquifer.

The concentrations of dissolved iron ranges between 0,02 mg/l up to 4,8 mg/l in the second aquifer. Samples with low pH in the western part of the valley are showing both low (0,02 mg/l at sample Sa21) and high (4,8 mg/l at sample Sa20) concentrations. Upstream and on the flanks concentrations of not more than 0,07 mg/l were detected as well as interpolated. The highest amounts of dissolved iron in the secondary aquifer of about 9 mg/l could be found in sample Sa12. The concentration in the primary aquifer rises from up- to downstream from 0,01 mg/l and 0,07 mg/l in the rain dominated samples up to 0,45 mg/l in the last measuring point sample Sa26 in the north.

4.4.11 Strontium

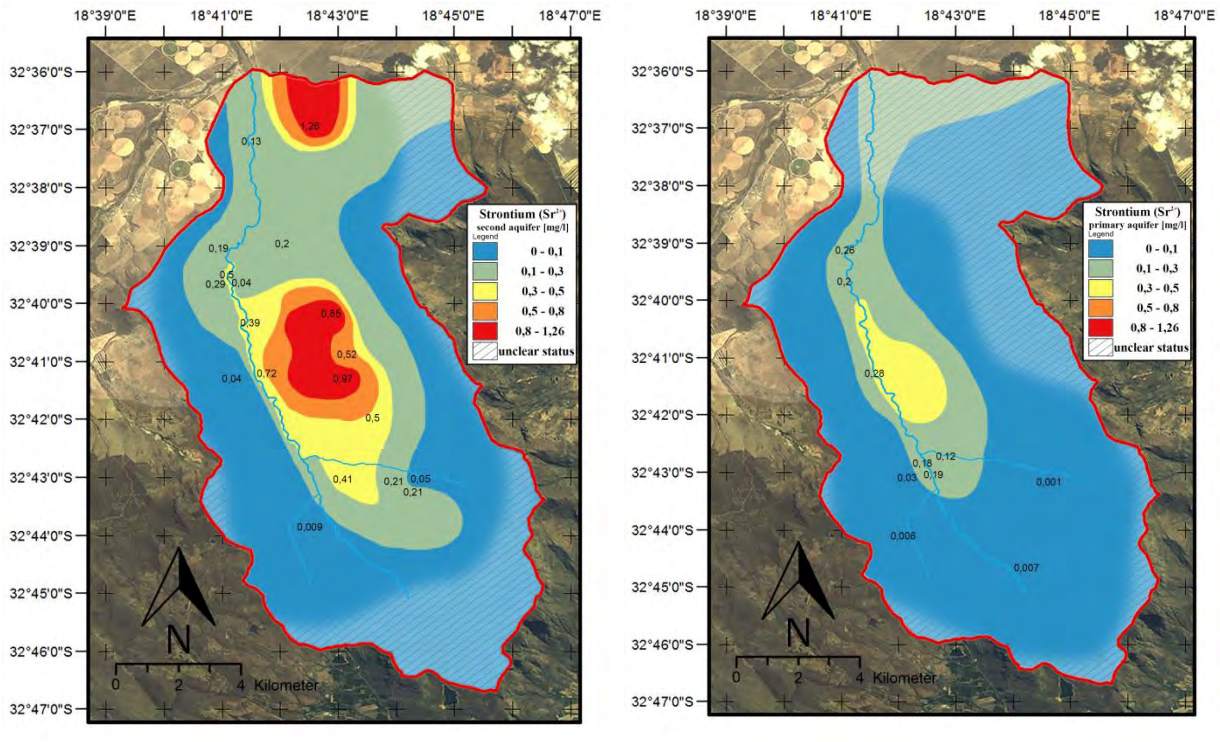

Figure 61 and 62: Spatial distribution maps of strontium in the second- (left) and primary (right) aquifer.

The concentrations of strontium in the second aquifer builds up two hot spots of about 0,9 mg/l at samples Sa11 and Sa18 and 1,26 mg/l at sample Sa27. The primary aquifer contains concentrations up to 0,28 mg/l. The concentration rises at the point the high concentrated waters of the second aquifer come across due to the groundwater flow.

4.4.12 Silicon

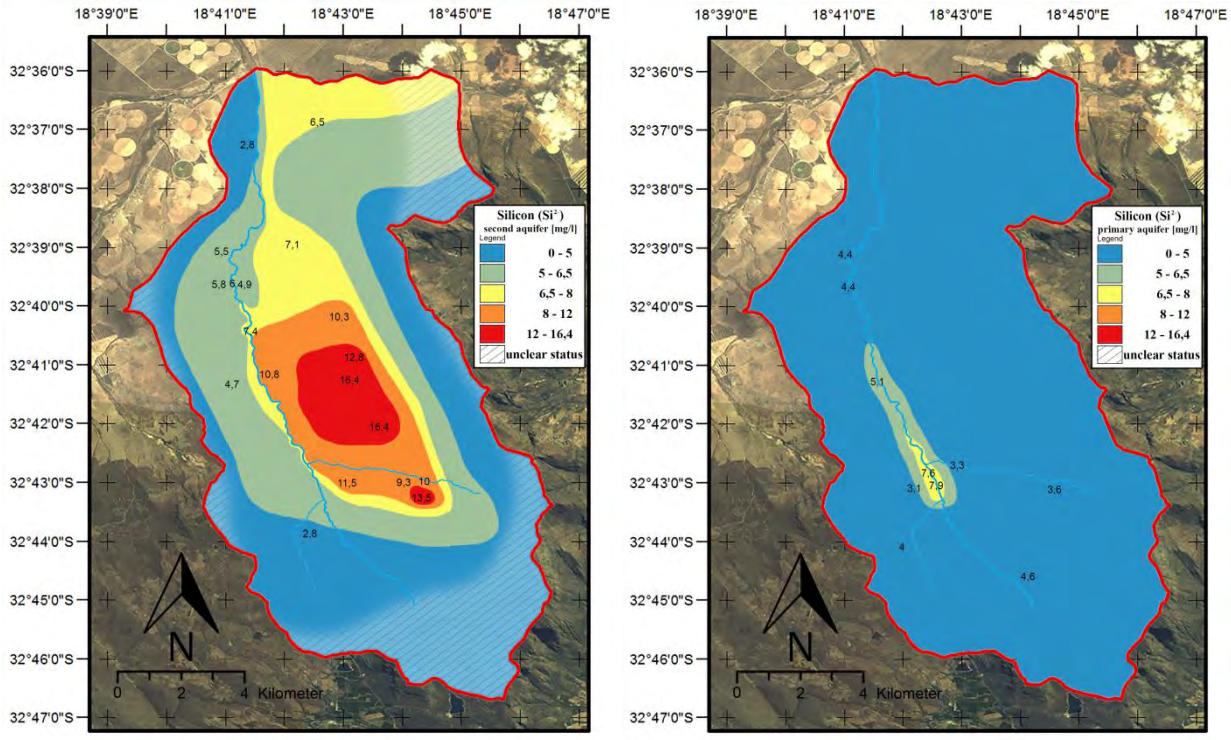

Figure 63 and 64: Spatial distribution maps of silicon in the second- (left) and primary (right) aquifer.

The secondary aquifer contains lower concentrations of silicon on the western part of the study area as well as upstream and on the flanks of the valley (between 2,8 mg/l and below up to about 5 mg/l). A hot spot can be identified in the area of the Riviera Granite dome with concentrations up to 16,4 mg/l. Silicon in the primary aquifer does not exceed concentrations of 7,9 mg/l. An average of not more than about 4 mg/l distributed over the catchment is more prominent.

4.5 Piper- and Schoeller plots

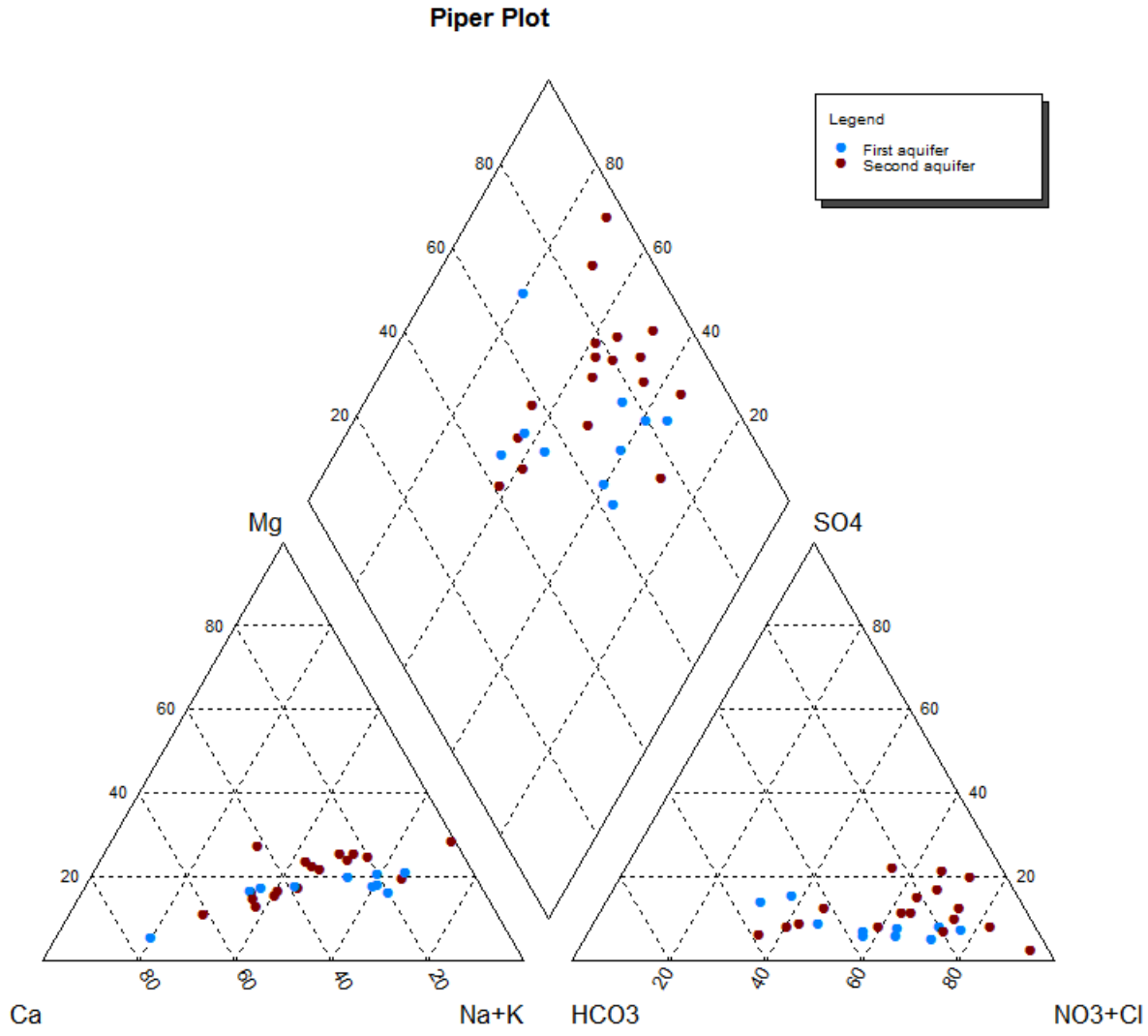

Figure 65: Piper Plot of the measuring points divided in the first and second aquifer samples.

As can be seen in the Piper Plot, the second aquifer waters (red dots) are dominated by chlorine plus nitrate than bicarbonate or sulfate on the anion ternary plot. On the cation ternary plot sodium plus potassium equals with calcium, both dominating magnesium.

The primary (first) aquifer doesn´t differ much compared to the second aquifer. On the anion ternary plot mainly even less sulfate comes into account and chlorine plus nitrates dominating the bicarbonate.

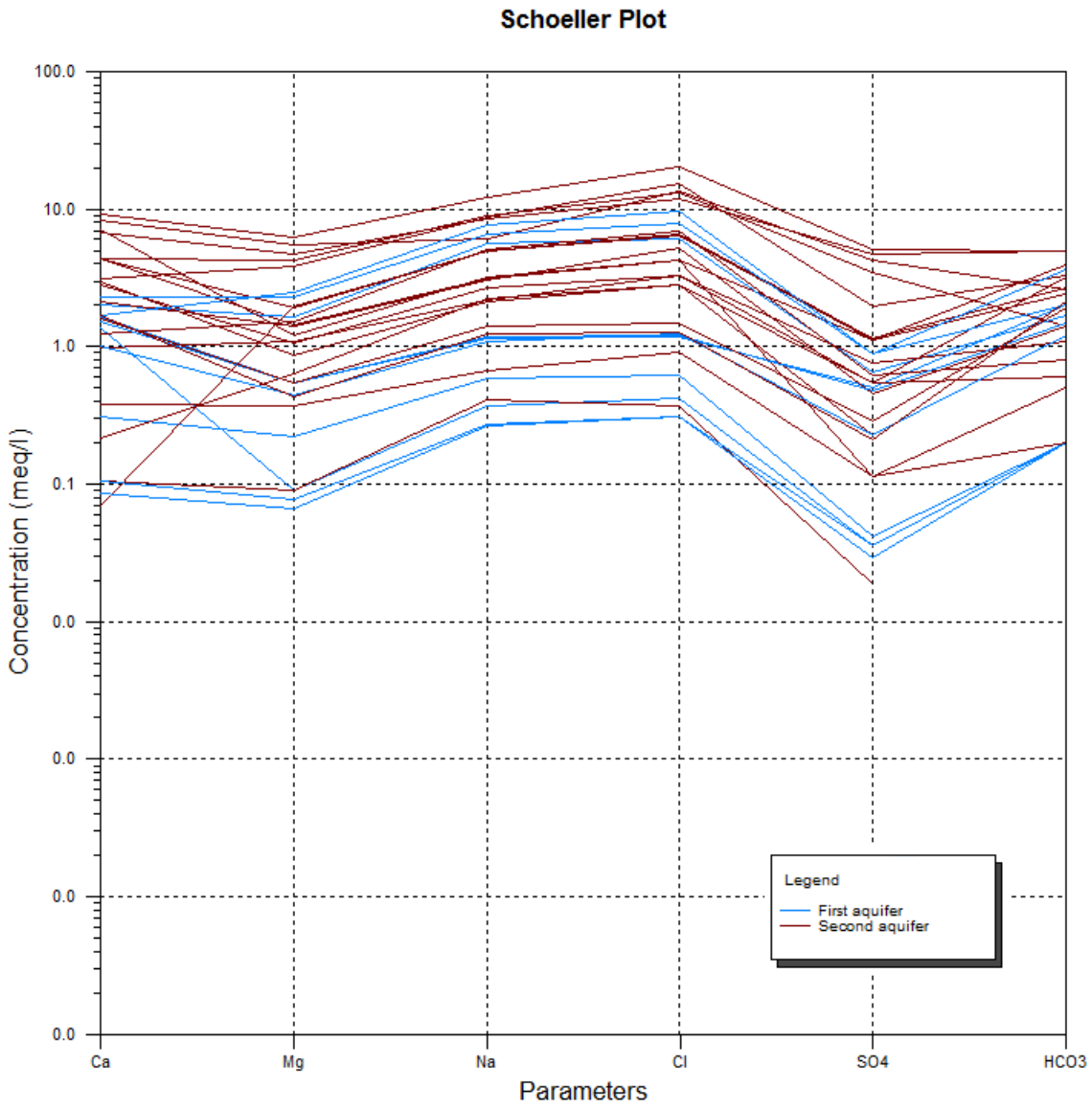

Figure 66: Schoeller Plot of the measuring points divided in the first and second aquifer samples.

Due to a higher mineralization the second aquifer waters (red lines) are dominating those of the primary (first) aquifer (blue lines).

4.6 Classification of waters

Due to the classification of the waters Na-Cl-waters are predominantly (table 7).

Sample	**classification**	**Sample**	**classification**
Sa01	Na-Ca-Mg-Cl	Sa17	Na-Mg-Cl-HCO3
Sa02	Ca-Na-HCO3-Cl	Sa18	Na-Ca-Mg-Cl-HCO3-SO4
Sa03	Ca-Na-HCO3-Cl	Sa19	Ca-Na-Cl
Sa04	Na-Ca-Cl-HCO3	Sa20	Ca-Na-Cl
Sa06	Na-Cl-HCO3	Sa21	Na-Cl
Sa07	Ca-Na-HCO3-Cl	Sa22	Ca-Na-HCO3-Cl
Sa08	Ca-Na-HCO3-Cl	Sa23	Na-Mg-Cl
Sa09	Na-Ca-Mg-Cl-HCO3	Sa24	Na-Ca-Mg-Cl-HCO3
Sa10	Ca-Na-Cl-HCO3	Sa25	Na-Cl
Sa11	Ca-Na-Mg-Cl-SO4	Sa26	Na-Mg-Cl
Sa12	Na-Ca-Mg-Cl	Sa27	Na-Ca-Mg-Cl
Sa13	Na-Ca-Cl	Sa28	Na-Cl-HCO3
Sa14	Na-Ca-Cl-HCO3	Sa29	Na-Cl-HCO3
Sa15	Ca-Na-Cl	Sa30	Na-Mg-Ca-Cl
Sa16	Na-Mg-Cl		

Table 7: Water classification of the samples

5 Interpretation

The interpretation and following conclusion is structured with respect to the scientific questions of this thesis:

.1: How does the geology in the catchment look like and what kind of waters are present?

.2: Comparing the up- and downstream waters: What is the geogenic- and anthropogenic influence on the water-mineral composition?

.3: What about the water-quality, if there would be less (ground-) water available depending on climate change or other impacts and could anything be done to keep the water quality in its state?

In general the rate of the electrical conductivity (EC) in the catchment can be used as an indicator of the water quality. It extends from 30 µS/cm upstream up to 3300 µS/cm downstream. The mineralization of the water out of springs as well as out of sources from the upstream parts of Moutonshoek Valley is quite low, with an EC <80 µS/cm (oligotrophic conditions). This can be interpreted as the influence of low mineralized rain water. In the predominantly arenaceous Table Mountain Rocks there is a good groundwater quality with EC <90 µS/cm, while the EC in the area of the Riviera granite and Malmesbury rocks ranges between 600 µS/cm and 1000 µS/cm. Generally brackish the EC in these waters are partly exceeding 2000 µS/cm.

Comparing the distribution of anions and cations to the geological map leads to a confident estimation of the geogenic influence on the groundwater and based on this, the anthropogenic effect can be shown greatly.

5.1 Geology and groundwater

- How does the geology in the catchment look like and what kind of waters are present?

Due to chemical interactions between groundwater and host-rock, the rock gets weathered and its minerals dissolve into the groundwater. This means that the host-rock and the groundwater can be directly correlated. In homogeneous circumstances or "laboratory conditions" this process would continue until a chemical equilibrium would be set up which wouldn´t change over time. In contrast the boundary conditions like the host rock, the temperature or

interactions with the atmosphere in nature are changing various times and so does the mineralization of the groundwater.

In general Sodium-Chloride waters are predominantly with various amounts calcium, magnesium and bicarbonate.

pH and Bicarbonate:

The Bicarbonate values in the study area corresponds to the pH. The more HCO_3 is available, the more H^+-Ions get bounded due to the equation:

$$HCO_3^- + H^+ \rightarrow H_2CO_3 \rightarrow H_2O + CO_2 \uparrow$$

The acidity of the water in the study area is charged by the eastern part of the study area, probably originated by pyrite oxidation.

Fluorine:

Fluorine is contained in various minerals and can be released during weathering processes to get into the water. The most important are apatite, mica, fluorite and cryolite, which are present in the Penisula Formation in the southern part of Moutonshoek Valley. In the second aquifer Fluorine is present due to weathering of this host rock in low concentrations (up to 0,9 mg/l). Due to its high electronegativity the fluorine reacts very fast to chemical bounds. Therefore the concentration of fluorine downstream decreases significantly (down to 0,05 mg/l). In the first aquifer there is only one source of fluorine, located at sample Sa06 in the south-eastern part of the study area. This could either be out of a human source (products of dental hygiene for example) or out of up-streaming water of the second aquifer. Latter is unlikely, because of the lack of other minerals generated by this source on this site.

Sulfur:

Sulfates, which are a form of the element sulfur, most commonly get into the water supply when sulfite ores are oxidized. The value of Sulfur in the catchment is randomly distributed and ranges between 0,01 mg/l and 9 mg/l.

Potassium:

Potassium dissolves due to weathering processes out of rocks, mostly feldspar and clay minerals. Potassium nitrate is also used in fertilizer, which could be the source in the northern part of the study area.

Iron:

The differences in values of dissolved iron-ions in the water samples is attributed to different pH-values and state of boreholes. In some areas the water was described to be more erosive than in other regions. Mainly in the swampy area around sample Sa14, the water was described to be very aggressive.

Arsenic:

Except for a single discontinuity in the second aquifer in the middle of the catchment and a source in a river sample in the southern part, no important amounts of arsenic were present in the study area. Two sources of arsenic bonds could come into count: Geothermal waters and pesticides (see chapter specific samples: Sa12 on page 67).

5.1.1 Riviera Granite aquifer

The influence of the Riviera Granite (see geological map on page 26) onto the groundwater is most obvious in the Moutonshoek Valley and can be clearly seen in the distribution maps (page 29 and following pages). With an electrical conductivity of up to 2400 µS in the second aquifer, it contains the highest concentration of dissolved minerals in the area. Extraordinary amounts of sulfate (up to 220 mg/l, see on page 32), silicon (up to 16,4 mg/l, see on page 33), chlorine (up to 478 mg/l, see on page 31), bromine (up to 1,3 mg/l, see on page 34), magnesium (up to 66 mg/l, see on page 36) and strontium (up to 0,97 mg/l, see on page 38) characterizes these waters. Directly affected measuring points for the second aquifer are Sa11, Sa12 and Sa18. Like these, the second- and the primary aquifer further downstream of this source contains higher concentrations of mentioned minerals as well. Affected samples downstream are Sa16 and Sa17 for the second aquifer and Sa28 for the first aquifer. As the sample Sa28 is a river sample with an EC= 1300 µS, and the river samples upstream, like Sa02, Sa03 and Sa04 contains significantly less minerals (EC=70 µS, 240 µS and 160 µS), there has to be a good connectivity between the first- and second aquifer in this area. The groundwater on the western part of the Krom Antonies River, which could influence sample Sa28 too, just got an EC of 530 µS. Based on this, the groundwater flow direction (page 26) could be approved as well.

The presence of strontium in this area can be seen as an indicator for geothermal water raising upwards through faults triggered by the granite dome. A circumstance, which should be take into account, when the origin of the clay layer is discussed.

5.1.2 Malmesbury Rock aquifer

Comparisons of the geological map and the distribution of dissolved minerals of the samples in the north-eastern- (Sa24 and Sa25) and north-western (Sa11, Sa12, Sa18 and Sa27) part of the study area, where rocks of the Malmesbury Group (Piketberg Formation) are present, shows, that chlorine and calcium are generated from these rocks. This is consistent with the Malmesbury rock properties described in the literature. The chlorine probably dissolves from the quartz-chlorite schist of the Malmesbury Series and the calcium out of calcite and gypsum. The lower concentration of calcium further downstream, could be explained due to a mix up with unaffected and low mineralized rainwater. The question remains why the host rock is not leached out and "sweetened" over time and if the dissolved ingredients maybe were transported allochthonous, originated at some other source (see also on page 73). The Malmesbury Rock aquifer is generally brackish with an EC up to 1160 µS.

5.1.3 Table Mountain Rock aquifer

Due to they are mostly composed out of weathered quartz sandstones, the Table Mountain Rocks do not have a large impact on the chemical composition in the study area. On the other hand they have a good permeability to transfer rainwater fast to the underlying rock layers and enrich the groundwater.

5.1.4 Special locations

Some discontinuities were discovered in specific samples which are listed below.

Sample Sa12:

The arsenic bonds in sample Sa12 could be present due to pest control in grape regions, because sometimes arsenic is used to preserve the plants from rot and decay. The fact that it was only detected in the second aquifer leads to two assumptions: first that it was used in the past and since then washed away by fresh water in the primary aquifer and second that fractures are limited in the second aquifer, leading to a slow flow through of groundwater in this area. Dry and therefore abandoned boreholes in this area supporting the latter.

Sample Sa14:

The artesian character of this borehole verifies the presence and position of the clay layer in cross section C-D (page 30). Groundwater of the second aquifer is upwelling into the Krom Antonies River in this area. This can be approved with the related chemical composition to

sample Sa13, a river sample near Sa14. The higher nitrate concentration in Sa13 could be triggered out of fertilizer used at the flanks at the valley.

Sample Sa15:

The not satisfying Ionic balance error of -47,35 is supported by the low mineralization of the sample Sa15. The less dissolved minerals are in a sample, the greater is its effect on the IB. So due to the electrical conductivity of just 31,4 µS/cm, only small inaccuracies in the analyzes were responsible and it was decided do use the results nevertheless. The sample shows a pH value of about 5,8. Because of dissolved carbon dioxide, unpolluted rain water has a pH of 5,6. That for sample Sa15 is exclaim to be made up of rainwater.

5.1.5 Krom Antonies River

Related to how they interact with the groundwater system, there are two fundamentally different types of rivers. Effluent rivers are streams which get their water from the groundwater. The surface of the stream directly relates to the surface of the groundwater and the stream will rise and fall as the water table rises and falls. Effluent streams are common in temperate to tropical climates, and generally become both wider and deeper downstream due to increased discharge: the continual addition of water from tributaries and groundwater. Effluent streams also commonly run year round, because of their relationship to the groundwater.

The second type of stream is called an influent stream, which are most commonly found in arid climates. Most of them actually lose water as they flow towards their destiny. There can be several reasons for the loss of water: Seepage into the ground, evaporation, and use by plants and animals are common causes of discharge reduction.

The Krom Antonies River apparently shows both types, depending on where it is examined in the valley. In general it should be called to be influent, because of its general loss of water downstream, probably effected by seepage triggered by irrigation and evaporation. On the other hand, there are spots of swampy lands around the river in the middle of the catchment in between samples Sa13 and Sa26 and around sample Sa21, with the groundwater head apparently near the surface. Due to there is a great connectivity between groundwater head and river, it is partly in an effluent state. Latter could also originated out of the clay layer, which prevents the water from seepage.

5.2 Anthropogenic influence on the groundwater

- Comparing the up- and downstream waters: What is the geogenic- and anthropogenic influence on the water-mineral composition?

In the study area geogenic- as well as human influences on the ground- and surface water could be verified due to the correlation of the chemical distribution of anions and cations of the geology to agriculture use and settlements.

The nitrogen compounds ammonium, nitrite and nitrate are considered to be the rate of the nitrogen load of the water. If nitrogen polluted water is present within reducing conditions, it can be identified by high amounts of ammonium and low amounts of nitrate. This reduction of nitrate is mostly caused by bacteria and fungi, which reduces the NO_3 to nitrite (NO_2) and further to elemental nitrogen gas or ammonium ions (NH_4^+), in case the amount of oxygen is lower than 5 mg/l. In unaffected, oxygen-rich groundwater, it is the opposite: Ammonium and nitrite ions are oxidized by nitrogen bacteria to nitrate or nitrogen. Therefore the ratio of ammonium - nitrite - nitrate provides information on the electrochemical conditions in the water.

5.2.1 Ammonium

Ammonium is usually not present in drinking water or groundwater. So based on the occurrence of ammonium of up to 0,1 mg/l in the first- and 0,075 mg/l in the second aquifer (see on page 39), statements can be made to the degree of domestic and agricultural influence. The highest concentration of ammonium in the first aquifer is downstream to populated and intensively agriculturally used areas in the southern part of the study area. The samples Sa01, Sa02 and Sa04 have got concentrations of 0,1 mg/l, but are still far below the WHO maximum permissible value of 1,5 mg/l. Downstream of this sources the concentration decreases slowly because of the absorption of ammonium and the mix with unloaded waters, to rise again in areas of farms further downstream. Due to the influent flow of the Krom-Antonies River and the drain away of the surface water into the second aquifer, the concentration of ammonium in the second aquifer ranges between 0,025 mg/l and 0,075 mg/l, too. Higher values of ammonium in the second aquifers are located below the more populated areas.

5.2.2 Nitrate

Most probably the occurring nitrate originates from droppings of animals, detergents in populated areas and agriculture land-use, the latter for the nitrogen fertilizer used there. The concentration of nitrate in agricultural used areas in the first aquifer ranges from 0,02 mg/l to 1,1 mg/l and up to 30 mg/l in the second aquifer (see on page 32). Even if the WHO maximum permissible concentration of 50 mg/l is not reached, concentrations of over 20 mg/l may be harmful to infants, if it is consumed regularly, for example in case of breast milk substitutes.

5.2.3 Phosphate

Phosphate levels <0,05 mg/l are mostly originated geogenic. Higher phosphate levels indicate anthropogenic influences. Concentrations up to 0,4 mg/l, probably out of animal droppings or detergents were detected in the samples Sa03 and Sa26 within the primary aquifer. The WHO maximum permissible value of phosphate was 6,7 mg/l until 2003. Nowadays it is told that phosphate is proved to be "not of health concern at levels found in drinking water".

5.2.4 Manganese

The distribution of manganese in the second aquifer can be attributed to normal weathering of the host rocks, maybe with a small influence of surface water infiltrating to the second aquifer in the southern part of the study area. A high value of manganese in the surface-water in the southern part at sample Sa01 of the study area is interpreted as additives to animal feed, which is most common in feeding horses. Sample Sa01 as a dam sample was described to be fed only by rainwater out of the flanks of the valley, therefore the second aquifer as a source for manganese can be excluded.

5.2.5 Arsenic

Due to the fact, that arsenic bonds could only be detected in a single spot, the arsenic bonds in sample Sa12 are most probably present due to the usage of pest control, preserving plants from rot and decay. Two assumptions were made in this case: first that it was used in the past and since then washed away by fresh water in the primary aquifer and second that fractures are limited in the second aquifer, leading to a slow flow through of groundwater in this area.

6 Conclusion

30 ground- and surface water samples have been analyzed for pH, temperature, conductivity, nitrite, nitrate, ammonium, sulfur, hydrogen-carbonate and additive anions and cations (anions: chloride, sulfate, phosphate, fluorine, bromine, silicon, sulfur; cations: calcium, magnesium, sodium, potassium, iron, manganese, arsenic, strontium). Of these 15 were irrigation wells, eight drinking water sources, six river spots and one dam sample.

The comparison of the primary and secondary aquifer along with the given geology has proven to be a great indicator to distinguish between human and geogenic impact on the ground- and surface water. The quality of the ground water in the catchment is high variable. This depends mostly on the host rock and the increased infiltration of fertilizer downstream. The rate of the electrical conductivity, used as an indicator for water quality, extends from 30µS/cm upstream to 3300 µS/cm downstream. Downstream increased values of Chloride, Nitrate and Arsenic bonds caused by human and natural sources have been identified.

6.1 Geology and groundwater

The mineralization of the water out of springs as well as out of sources from the upstream parts of the primary aquifer is mainly influenced by low mineralized rain water. During the way to its destination, these waters are influenced by the host rocks. The groundwater in the area of the Riviera Granite and downstream is characterized by high amounts of sulfate silicon, chlorine, bromine, magnesium and strontium, with an EC up to 2400 µS. Malmesbury Rock waters, which are present in large parts of the catchment, are generally brackish with high amounts of chlorine and calcium and an EC up to 1160 µS. The Table Mountain aquifers are generally low mineralized due to its composition out of quartzitic sandstone.

6.2 Anthropogenic influence on the groundwater

Ammonium, nitrate, phosphate and manganese could be verified to be out of human sources. The detection of ammonium ions indicates critical contamination with wastewater, manure or compost, even if the WHO maximum value of ammonium in the study area is not reached. The amounts of nitrate and phosphate are mostly originated out of fertilizers in the agriculture land-use and detergents and wastewater in populated areas.

6.3 Henceforward water quality

The assessment of the quality of groundwater only refers to the measured ingredients compared to the WHO guidelines. Whether a sample corresponds to the drinking water standards in all aspects (for example biology or other contaminants), cannot be provided in this thesis.

Except for the single source of arsenic at Sa12 of about 29 mg/l, the measured concentrations of the ions are currently below the WHO maximum permissible values (table 8) and the groundwater as well as the surface water quality seems to be in a good state. Particular increased values of chloride at the Malmesbury Rock aquifer and nitrate downstream of agricultural used areas stays below the maximum permissible value, but should be monitored at regular intervals.

Ion	**WHO-Guideline value**	**Maximum value in the study area**
Ammonium	1,5 mg/l	0,1 mg/l
Arsenic	0,01 mg/l	0,029 mg/l
Chlorine	no value (detectable taste: 250 mg/l)	726 mg/l
Fluoride (Fluorine)	1,5 mg/l	0,9 mg/l
Nitrate	50 mg/l	30 mg/l
Phosphate	no value (6,7 mg/l until 2003)	0,4 mg/l

Table 8: WHO maximum permissible values of drinking water (2015) compared to the maximum values in the study area.

With refer to CONRAD 2012, climate change models for the Sandveld-Area are indicating warmer and drier conditions also resulting in reduced groundwater recharge. Less groundwater recharge would lead to higher concentrations of man-made ingredients like ammonium, nitrate, phosphate, manganese and arsenic bonds out of fertilizers and pest control. Other reasons that could lead to a reduced amount of groundwater and thus to higher concentrations in the study area are the usage of the center pivot irrigation systems and probably the presence of dams. Center pivot systems leads to an great loss of water from the aquifers triggered by an increased evaporation and could result in closed water circles, were

the mineralization is further increased over time. Dams are known to increase the evaporation, too. Studies in Australia have shown that the loss of water in a dam due to evaporation and seepage is up to 40% (CRAIG ET AL 2007). On the other hand, excessive amounts of water during heavy rain events could be collected and used in times of less water. If the one or the other is reasonable for this specific area, should be further investigated, but couldn´t be implemented within this thesis.

With respect to the decreasing amount of groundwater recharge due to predicted climate changes, the usage of fertilizer and pest control should be handled even more carefully, keeping the water quality in mind.

6.4 Discussion

Clay deposits in the study area:

Two different origins of the clay layer are discussed in the literature. The first assumption implies, that the clay layer emerged due to leaching of the overlying alluvium (CONRAD 2012). The second and not insignificant statement is, that the clay occurs due to uprising thermal waters and was identified about 150 km south of the study area by PEROLD AND THEART 2007: The shrinking of the Aghulas Sea around 310 My ago leads to great pressure and rising thermal waters out of the Swartland Group. Gravels of the Swartland Group are present in the basement of the Malmesbury Group (Belcher und Kisters 2003) and overlain by clay, which rises up within the thermal waters to be filtered gradually inside the Malmesbury Group. "The intrusion of the approximately 550 to 510 Ma syn- to post tectonic granitoids of the Cape Granite Suite into micaceous, feldspathic shale of the Malmesbury Group created a hydrothermal vein structure. These veins developed along pre-existing zones of weakness such as fault or shear zones. Hydrothermal fluids migrating along these fractures were initially dominated by magmatic water and later by meteoric or seawater." (PEROLD AND THEART 2007). In this manner it could possibly happened in the Moutonshoek valley as well. The presence of geothermal fluids could also be the allochthonous source of the mineralized waters in the Malmesbury Group.

Different days of sampling and time of the year:

A great challenge of the analysis of the chemical distribution maps was to consider the different days of sampling, where especially the surface waters could be strongly influenced by rain water. Even if it was ensured that the sampling preceded several dry days, there have

sometimes been low precipitation at night. Furthermore, it has turn out to be difficult to satisfactorily estimate the seasonal differences, due it was the running out dry season the fieldtrip have taken place.

A greater than presumed catchment area:

As mentioned in the description of cross-section E - F on page 31, the groundwater recharge area is greater than the topographically developed study area itself and reaches in the Hol River valley for nearly one kilometer. This is due to the graben-horst structures on the western part of the valley and leads to an approximated larger area for the groundwater recharge of about 6000 m^2. Due to the geological map after DE BEER 1990 AND ROZENDAAL 1994 (Fig. 5) and as illustrated in the cross-sections (pages 29 to 33), the overlaying rocks of the Table Mountain Series lies flat on the basement or dips in low angels and does not have an effect onto the size of the groundwater recharge area.

6.5 Recommendations for future research

It was missed to take enough groundwater heads out of the boreholes, due to their were in use for irrigation. Unfortunately, these are necessary to construct an area wide depth to groundwater map. Although the estimation of the groundwater flow direction could be implemented on the basis of chemical data, a more accurate description would have been useful.

Long term measurements of the measuring points would provide a closer look at the hydrochemistry, especially when more groundwater is available in the system. At least another field trip in the running out wet season would be most profitable compared with gathered results.

An age determination with an $\Delta^{18}O$ analyses in the Malmesbury rock aquifer could clarify whether the waters are transported allochthonous or autochthonous and thereof the origin of the clay layer.

It would be useful to establish groundwater protection zones in areas of abstraction for drinking water and therefore get into contact with the water users of the Hol river valley in the west.

7 Appendix

7.1 Appendix A: Glossary of Terms

Abiotic Not pertaining to living organisms; environmental features such as temperature, rainfall etc. (Parson 2004).

Anisotropic Having some physical property that varies with direction (Parson 2004).

Aquifer A geological formation which has structures or textures that hold water or permit appreciable water movements through them. [from National Water Act South Africa (Act No. 36 of 1998)]

Artesian an adjective referring to groundwater under hydrostatic pressure (Parson 2004)

Baseflow sustained low flow in a river during dry or fair weather conditions, but not necessarily all contributed by groundwater; includes contributions from delayed interflow and groundwater discharge (Parson 2004).

Borehole In respect to the South African notification a "borehole" is the same as a groundwater measuring point (German nomenclature). Includes a well, exavation, or any other artificially constructed or improved groundwater cavity which can be uses for the purpose of intercepting, collecting or storing water from an aquifer; observing or collectiong data and information on water in an aquifer; or recharging an aquifer [from National Water Act South Africa (Act No. 36 of 1998)]

Catchment The area from which any rainfall will drain into the watercourse, contributing to the runoff at a particular point in a river system (Parson 2004).

Discharge area An area in which subsurface water, including water in the unsaturated and saturated zones, is discharged at the land surface (Parson 2004).

Electrical conductivity Is a measurement of the ease with which water conducts electricity. Distilled water conducts electricity poorly, while sea water, with its very high salt content, is a very good conductor of electricity (Parson 2004).

Fault A zone of displacement in rock formations resulting from forces of tension or compression in the earth's crust (Parson 2004).

Geohydrology The study of the properties, circulation and distribution of groundwater, in practise used interchangeably with hydrogeology; but in theory hydrogeology is the study of geology from the perspective of its role and influence in hydrology, while geohydrology is the study of hydrology from the perspective of the influence on geology (Parson 2004).

Groundwater Water found in the subsurface in the saturated zone below the water table or piezometric surface, i.e. the water table marks the upper surface of groundwater systems (Parson 2004).

Hydraulic conductivity Measure of the ease with which water will pass through porous material; defined as the rate of flow through a cross-section of one square metre under a unit hydraulic gradient at right angles to the direction of flow (in m/d) (Parson 2004).

Hydraulic gradient The slope of the water table or piezometric surface; is a ratio of the change of hydraulic head divided by the distances between the two points of measurement (Conrad 2012).

Permeability The ease with which a fluid can pass through a porous medium and is defined as the volume of fluid discharged from a unit area of an aquifer under unit hydraulic gradient in unit time (expressed as m3/m2/d or m/d); it is an intrinsic property of the porous medium and is independent of the properties of the saturating fluid; not to be confused with hydraulic conductivity which relates specifically to the movement of water (Parson 2004).

Porosity The percentage of void space that a rock or sediment contains, which is an index of how much groundwater can be stored per volume when saturated. The effective porosity, also called the kinematic porosity, of a porous medium is defined as the ratio of the part of the pore volume where the water can circulate to the total volume of a representative sample of the medium (Parson 2004).

Recharge The addition of water to the zone of saturation, either by the downward percolation of precipitation or surface water and / or the lateral migration of groundwater from adjacent aquifers (Parson 2004).

Recharge area An area over which recharge occurs (Parson 2004).

7.2 Appendix B: Timeline

11.02. - 17.02. 2013

- Get prepared for a first survey of the catchment
- Meeting with Mashudu J. Murovhi, the Deputy Director of Olifants-Doorn Proto CMA of the Department of Water Affairs at Elandsbay
- Get into contact with several Geohydrologists, members of the Department of Water Affairs and employees at the University of Cape Town
- Looking for an accommodation near or inside the catchment and figure out a way of transportation

18.02. - 24.02.2013

- Survey of the catchment, looking for boreholes, dams and springs
- Getting into contact with staff of the Department of Water Affairs to get data, maps, contacts and scientific papers of interest
- Adapt the master thesis to the local circumstances
- Get equipment for field work and literature at the Fresh Water Research Unit at the University of Cape Town
- Meeting at the Department of Water Affairs in Cape Town
- Prepare and print an overview of my topic and contact as an hand-out

25.02. - 03.03.2013

- Meeting with the Water User Association of Krom Antonies catchment: introduce myself and my working thesis, get contacts of the farmers, requesting information. For example: rainfall data (Fig.2), borehole locations, permission to go onto their land, arranging personal meetings.
- Taking part at a conference of the Verlorenvlei Coalition
- Get more equipment for the field work (f.e. acid, multimeter) at the Fresh Water Research Unit at the University of Cape Town and organized a car
- Survey the catchment

04.03. - 10.03.2013

- Meeting with the farmer Innis Brynard and getting water samples at *Kromvlei-farm*
- Meeting with the farmer Danni Coetzee and getting water samples at *Twisnikt-farm*
- Meeting with the farmer Halmar Enderstein and getting water samples at *Hamerkop/Wilgerboschrift*
- Personal meeting with Jocobus Smit (Head of the WUA)
- Get access to random residents and getting water samples out of private boreholes
- Getting water samples out of Krom Antonies River
-

11.03. - 17.03.2013

- Meeting with Brian of the Department of Water Affairs in the catchment
- Meeting with the farmer Jacobus Smit and getting water samples at *Karookop*
- Meeting with the farmer Jacquie van der Merwe and getting water samples at *Namaquas Fontaine*
- Meeting with the farmer Herman Coetzee and getting water samples at his farm
- Meeting with the farmer Matthys Bothma and getting water samples at *Karsten Boerdery*

18.03. - 23.3.2013

- Meeting with the farmer Louw Smit and getting water samples at *HP Smit&Seurs*
- Mountain trip to get samples out of springs
- Bundle soil samples
- Taking part at the conference of the National Water Week in Clanwilliam

7.3 Appendix C: Measuring points

Sample Sa01

Image Sa01: Sample Sa01 at the Moutonshoek rainwater-dam, line of sight: W, 25.02.2013.

Coordinates (WGS84):

E: 18,704944 N: -32,717472

On site parameters:

conductivity	**pH**	**NH_4^+**	**S_2^-**	**temperature**
µS		mg/l	mg/l	°C
66	7,51	0,1	0,02	30,9

Anions:

Cl^-	**$SO4^{2-}$**	**$NO3^-$**	**$PO4^{3-}$**	**F**	**Br^-**	**Si^{2-}**	**HCO3-**
mg/l	mg/l	mg/l	mg/l	mg/l	mg/l	mg/l	mg/l
22	2	0,1	0	1	0,1	3,1	12,2

Cations:

Ca^{2+}	**Mg^{2+}**	**Na^+**	**K^+**	**Fe^{2+}**	**Mn^{4+}**	**As^{2+}**	**Sr^{2+}**
mg/l	mg/l	mg/l	mg/l	mg/l	mg/l	µg/l	mg/l
6,2	2,7	13,6	0,8	0,64	0,5	0	0,03

Sample Sa02

Image Sa02: Krom-Antonies River near Moutonshoek, line of sight: S, 27.02.2013.

Coordinates (WGS84):

E: 18,709444 N: -32,716694

On site parameters:

conductivity	pH	NH_4^+	S_2^-	temperature
µS		mg/l	mg/l	°C
248	7,61	0,1	0	30,9

Anions:

Cl^-	$SO4^{2-}$	$NO3^-$	$PO4^{3-}$	F	Br^-	Si^{2-}	HCO3-
mg/l	mg/l	mg/l	mg/l	mg/l	mg/l	mg/l	mg/l
42	24	0,4	0,4	0,3	0,1	7,9	122

Cations:

Ca^{2+}	Mg^{2+}	Na^+	K^+	Fe^{2+}	Mn^{4+}	As^{2+}	Sr^{2+}
mg/l	mg/l	mg/l	mg/l	mg/l	mg/l	µg/l	mg/l
32,9	6,6	26,2	1,2	0,2	0,04	2	0,19

Sample Sa03

Image Sa03: Krom-Antonies River near Moutonshoek, line of sight: S, 28.02.2013.

Coordinates (WGS84):

E: 18,708111 N: -32,71425

On site parameters:

conductivity	**pH**	**NH_4^+**	**S_2^-**	**temperature**
µS		mg/l	mg/l	°C
248	7,64	0,025	0,02	22,8

Anions:

Cl^-	**$SO4^{2-}$**	**$NO3^-$**	**$PO4^{3-}$**	**F**	**Br^-**	**Si^{2-}**	**HCO3-**
mg/l	mg/l	mg/l	mg/l	mg/l	mg/l	mg/l	mg/l
43	23	0	0	0,25	0,1	7,6	91,5

Cations:

Ca^{2+}	**Mg^{2+}**	**Na^+**	**K^+**	**Fe^{2+}**	**Mn^{4+}**	**As^{2+}**	**Sr^{2+}**
mg/l	mg/l	mg/l	mg/l	mg/l	mg/l	µg/l	mg/l
30,1	6,7	26,9	1,1	0,03	0,02	1	0,18

Sample Sa04

Image Sa04: Dam near Moutonshoek, line of sight: SE, 01.03.2013.

Coordinates (WGS84):

E: 18,712722 N: -32,713278

On site parameters:

conductivity	pH	NH_4^+	S_2^-	temperature
µS		mg/l	mg/l	°C
163,3	-	0,08	0,02	24,9

Anions:

Cl^-	$SO4^{2-}$	$NO3^-$	$PO4^{3-}$	F	Br^-	Si^{2-}	HCO3-
mg/l	mg/l	mg/l	mg/l	mg/l	mg/l	mg/l	mg/l
44	11	0,07	0	0,4	0,1	3,3	73,2

Cations:

Ca^{2+}	Mg^{2+}	Na^+	K^+	Fe^{2+}	Mn^{4+}	As^{2+}	Sr^{2+}
mg/l	mg/l	mg/l	mg/l	mg/l	mg/l	µg/l	mg/l
20,2	5,4	25,2	1,2	0	0,003	2	0,12

Sample Sa06

Image Sa06: Tributary of the Krom-Antonies River, line of sight: E, 05.03.2013.

Coordinates (WGS84):

E: 18,742944 N: -32,716444

On site parameters:

conductivity	pH	NH_4^+	S_2^-	temperature
µS		mg/l	mg/l	°C
29,2	6,8	0,025	0,02	25,1

Anions:

Cl^-	$SO4^{2-}$	$NO3^-$	$PO4^{3-}$	F	Br^-	Si^{2-}	HCO3-
mg/l	mg/l	mg/l	mg/l	mg/l	mg/l	mg/l	mg/l
11	1,7	0,02	0,02	0,9	0,04	3,6	12,2

Cations:

Ca^{2+}	Mg^{2+}	Na^+	K^+	Fe^{2+}	Mn^{4+}	As^{2+}	Sr^{2+}
mg/l	mg/l	mg/l	mg/l	mg/l	mg/l	µg/l	mg/l
2,1	0,95	6,2	0,08	0,07	0,01	0	0,21

Sample Sa07

Image Sa07: Kromvlei irrigantion well, Boorgat I, line of sight: NE, 05.03.2013.

Coordinates (WGS84):

E: 18,737361 N: -32,716444

On site parameters:

conductivity	**pH**	**NH_4^+**	**S_2^-**	**temperature**
µS		mg/l	mg/l	°C
261	7,07	0,075	0	24,8

Anions:

Cl^-	**$SO4^{2-}$**	**$NO3^-$**	**$PO4^{3-}$**	**F**	**Br^-**	**Si^{2-}**	**HCO3-**
mg/l	mg/l	mg/l	mg/l	mg/l	mg/l	mg/l	mg/l
45	10	1,02	0	0,8	0,1	13,5	128,1

Cations:

Ca^{2+}	**Mg^{2+}**	**Na^+**	**K^+**	**Fe^{2+}**	**Mn^{4+}**	**As^{2+}**	**Sr^{2+}**
mg/l	mg/l	mg/l	mg/l	mg/l	mg/l	µg/l	mg/l
33,8	5,2	28,5	2,4	0,07	0,14	0	0,21

Sample Sa08

Image Sa08: Kromvlei irrigantion well, Boorgat II, 06.03.2013.

Coordinates (WGS84):

E: 18,735472 N: -32,716528

On site parameters:

conductivity	pH	NH_4^+	S_2^-	temperature
µS		mg/l	mg/l	°C
288	7,84	0,05	0	24,4

Anions:

Cl^-	$SO4^{2-}$	$NO3^-$	$PO4^{3-}$	F	Br^-	Si^{2-}	HCO3-
mg/l	mg/l	mg/l	mg/l	mg/l	mg/l	mg/l	mg/l
53	13,7	0,08	0	0,2	0,1	9,3	115,9

Cations:

Ca^{2+}	Mg^{2+}	Na^+	K^+	Fe^{2+}	Mn^{4+}	As^{2+}	Sr^{2+}
mg/l	mg/l	mg/l	mg/l	mg/l	mg/l	µg/l	mg/l
31,9	6,6	32,3	2,6	0,1	0,04	0	0,21

Sample Sa09

Image Sa09: Jan´s irrigantion well, line of sight: N, 06.03.2013.

Coordinates (WGS84):

E: 18,738972 N: -32,717306

On site parameters:

conductivity	pH	NH_4^+	S_2^-	temperature	Borehole depth
µS		mg/l	mg/l	°C	M
91,4	6,49	0,025	0	22,2	130

Anions:

Cl^-	$SO4^{2-}$	$NO3^-$	$PO4^{3-}$	F	Br^-	Si^{2-}	HCO3-
mg/l	mg/l	mg/l	mg/l	mg/l	mg/l	mg/l	mg/l
32	5,5	0,65	0	0,3	0,07	10	30,5

Cations:

Ca^{2+}	Mg^{2+}	Na^+	K^+	Fe^{2+}	Mn^{4+}	As^{2+}	Sr^{2+}
mg/l	mg/l	mg/l	mg/l	mg/l	mg/l	µg/l	mg/l
7,6	4,5	15,4	2,4	0,25	0,02	0	0,05

Sample Sa10

Image Sa10: Kromvlei irrigantion well, Boorgat VI, line of sight: W, 06.03.2013.

Coordinates (WGS84):

E: 18,726222 N: -32,699639

On site parameters:

conductivity	**pH**	**NH_4^+**	**S_2^-**	**temperature**
µS		mg/l	mg/l	°C
972	7,01	0	0,02	25,5

Anions:

Cl^-	**$SO4^{2-}$**	**$NO3^-$**	**$PO4^{3-}$**	**F**	**Br^-**	**Si^{2-}**	**HCO3-**
mg/l	mg/l	mg/l	mg/l	mg/l	mg/l	mg/l	mg/l
152	54	0	0	0,4	0,4	16,4	237,9

Cations:

Ca^{2+}	**Mg^{2+}**	**Na^+**	**K^+**	**Fe^{2+}**	**Mn^{4+}**	**As^{2+}**	**Sr^{2+}**
mg/l	mg/l	mg/l	mg/l	mg/l	mg/l	µg/l	mg/l
87,8	17,5	71,3	3	1	0,2	0	0,5

Sample Sa11

Image Sa11: Rugby-field irrigantion well, line of sight: SW, 07.03.2013.

Coordinates (WGS84):

E: 18,718750 N: -32,686889

On site parameters:

conductivity	**pH**	**NH_4^+**	**S_2^-**	**temperature**
µS		mg/l	mg/l	°C
2400	7,09	0,025	0	22,4

Anions:

Cl^-	**$SO4^{2-}$**	**$NO3^-$**	**$PO4^{3-}$**	**F**	**Br^-**	**Si^{2-}**	**HCO3-**
mg/l	mg/l	mg/l	mg/l	mg/l	mg/l	mg/l	mg/l
478	204	0	0	0,2	1,3	16,4	158,6

Cations:

Ca^{2+}	**Mg^{2+}**	**Na^+**	**K^+**	**Fe^{2+}**	**Mn^{4+}**	**As^{2+}**	**Sr^{2+}**
mg/l	mg/l	mg/l	mg/l	mg/l	mg/l	µg/l	mg/l
167	66	141	3,6	4,7	0,2	8	0,97

Sample Sa12

Image Sa12: Karookop irrigantion well, line of sight: W, 07.03.2013.

Coordinates (WGS84):

E: 18,71883 N: -32,681694

On site parameters:

conductivity	**pH**	**NH_4^+**	**S_2^-**	**temperature**
µS		mg/l	mg/l	°C
2160	6,3	0	0	23,2

Anions:

Cl^-	**$SO4^{2-}$**	**$NO3^-$**	**$PO4^{3-}$**	**F**	**Br^-**	**Si^{2-}**	**HCO3-**
mg/l	mg/l	mg/l	mg/l	mg/l	mg/l	mg/l	mg/l
460	166	0	0	0,3	1,3	12,8	85,4

Cations:

Ca^{2+}	**Mg^{2+}**	**Na^+**	**K^+**	**Fe^{2+}**	**Mn^{4+}**	**As^{2+}**	**Sr^{2+}**
mg/l	mg/l	mg/l	mg/l	mg/l	mg/l	µg/l	mg/l
87	51	207	3,7	9	0,4	29	0,52

Sample Sa13

Image Sa13: Krom Antonies River, line os sight: W, 08.03.2013.

Coordinates (WGS84):

E: 18,685194 N: -32,660333

On site parameters:

conductivity	**pH**	**NH_4^+**	**S_2^-**	**temperature**
µS		mg/l	mg/l	°C
976	7,28	0	0	20,2

Anions:

Cl^-	**$SO4^{2-}$**	**$NO3^-$**	**$PO4^{3-}$**	**F**	**Br^-**	**Si^{2-}**	**HCO3-**
mg/l	mg/l	mg/l	mg/l	mg/l	mg/l	mg/l	mg/l
215	31	1	0	0,1	0,6	4,4	103,7

Cations:

Ca^{2+}	**Mg^{2+}**	**Na^+**	**K^+**	**Fe^{2+}**	**Mn^{4+}**	**As^{2+}**	**Sr^{2+}**
mg/l	mg/l	mg/l	mg/l	mg/l	mg/l	µg/l	mg/l
40	19,7	128	0,8	0,13	0,2	0	0,2

Sample Sa14

Image Sa14: Arthesian borehole near the Krom Antonies River, 08.03.2013.

Coordinates (WGS84):

E: 18,685889 N: -32,660083

On site parameters:

conductivity	**pH**	**NH_4^+**	**S_2^-**	**temperature**	**borehole depth**
µS		mg/l	mg/l	°C	m
1157	7,38	0	0,02	20,6	60

Anions:

Cl^-	**$SO4^{2-}$**	**$NO3^-$**	**$PO4^{3-}$**	**F**	**Br^-**	**Si^{2-}**	**HCO3-**
mg/l	mg/l	mg/l	mg/l	mg/l	mg/l	mg/l	mg/l
230	55	0,6	0	0,1	0,6	6	167,7

Cations:

Ca^{2+}	**Mg^{2+}**	**Na^+**	**K^+**	**Fe^{2+}**	**Mn^{4+}**	**As^{2+}**	**Sr^{2+}**
mg/l	mg/l	mg/l	mg/l	mg/l	mg/l	µg/l	mg/l
87	23	115	1	1,5	0,2	4	0,5

Others: Arthesian

Sample Sa15

Image Sa15: Little brook near Namaquasfontaine, line of sight: W, 09.03.2013.

Coordinates (WGS84):

E: 18,701417 N: -32,734278

On site parameters:

conductivity	**pH**	**NH_4^+**	**S_2^-**	**temperature**
m		mg/l	mg/l	°C
31,4	5,76	0	0,02	22,3

Anions:

Cl^-	**$SO4^{2-}$**	**$NO3^-$**	**$PO4^{3-}$**	**F**	**Br^-**	**Si^{2-}**	**HCO3-**
mg/l	mg/l	mg/l	mg/l	mg/l	mg/l	mg/l	mg/l
15	1,7	0,1	0,05	0	0,05	4	12,2

Cations:

Ca^{2+}	**Mg^{2+}**	**Na^+**	**K^+**	**Fe^{2+}**	**Mn^{4+}**	**As^{2+}**	**Sr^{2+}**
mg/l	mg/l	mg/l	mg/l	mg/l	mg/l	µg/l	mg/l
27,8	1,1	8,5	0,02	0,01	0,005	0	0,006

Sample Sa16

Image Sa16: Konkelbos irrigation well 1, line of sight: N, 11.03.2013.

Coordinates (WGS84):

E: 18,701417 N: -32,734278

On site parameters:

conductivity	pH	NH_4^+	S_2^-	temperature	borehole depth
m		mg/l	mg/l	°C	m
2370	7,25	0,025	0	23,6	120

Anions:

Cl^-	$SO4^{2-}$	$NO3^-$	$PO4^{3-}$	F	Br^-	Si^{2-}	HCO3-
mg/l	mg/l	mg/l	mg/l	mg/l	mg/l	mg/l	mg/l
540	95	0	0	0,15	1,4	10,8	201,3

Cations:

Ca^{2+}	Mg^{2+}	Na^+	K^+	Fe^{2+}	Mn^{4+}	As^{2+}	Sr^{2+}
mg/l	mg/l	mg/l	mg/l	mg/l	mg/l	µg/l	mg/l
63,2	46,5	199	1,5	0,94	0,02	9	0,72

Others:Pumping at about 70 m

Sample Sa17

Image Sa17: Konkelbos irrigation well 2, line of sight: NE, 11.03.2013.

Coordinates (WGS84):

E: 18,691056 N: -32,673778

On site parameters:

conductivity	**pH**	**NH_4^+**	**S_2^-**	**temperature**	**borehole depth**
µS		mg/l	mg/l	°C	m
1086	7,29	0,05	0	23,1	120

Anions:

Cl^-	**$SO4^{2-}$**	**$NO3^-$**	**$PO4^{3-}$**	**F**	**Br^-**	**Si^{2-}**	**HCO3-**
mg/l	mg/l	mg/l	mg/l	mg/l	mg/l	mg/l	mg/l
228	53	0,05	0	0,1	0,6	7,4	146,4

Cations:

Ca^{2+}	**Mg^{2+}**	**Na^+**	**K^+**	**Fe^{2+}**	**Mn^{4+}**	**As^{2+}**	**Sr^{2+}**
mg/l	mg/l	mg/l	mg/l	mg/l	mg/l	µg/l	mg/l
1,4	24	113	1,1	0,96	0,14	9	0,39

Others:Pumping at about 70 m

Sample Sa18

Image Sa18: Konkelbos animal drinking water, line of sight: NE, 11.03.2013.

Coordinates (WGS84):

E: 18,715111 N: -32,669639

On site parameters:

conductivity	pH	NH_4^+	S_2^-	temperature	Borehole depth
µS		mg/l	mg/l	°C	m
2370	7,52	0,025	0,02	23,9	48

Anions:

Cl^-	$SO4^{2-}$	$NO3^-$	$PO4^{3-}$	F	Br^-	Si^{2-}	HCO3-
mg/l	mg/l	mg/l	mg/l	mg/l	mg/l	mg/l	mg/l
422	223	0,15	0	0,2	1,1	1,03	298,9

Cations:

Ca^{2+}	Mg^{2+}	Na^+	K^+	Fe^{2+}	Mn^{4+}	As^{2+}	Sr^{2+}
mg/l	mg/l	mg/l	mg/l	mg/l	mg/l	µg/l	mg/l
136	57,3	196	3,1	0,02	0,3	0	0,85

Others:Pumping at about 48 m

Sample Sa19

Konkelbos well, 12.03.2013.

Coordinates (WGS84):

E: 18,701710 N: -32,649320

On site parameters:

conductivity	**pH**	**NH_4^+**	**S_2^-**	**temperature**	**borehole depth**
µS		mg/l	mg/l	°C	m
513	7,26	0,025	0,02	22,5	120

Anions:

Cl^-	**$SO4^{2-}$**	**$NO3^-$**	**$PO4^{3-}$**	**F**	**Br^-**	**Si^{2-}**	**HCO3-**
mg/l	mg/l	mg/l	mg/l	mg/l	mg/l	mg/l	mg/l
117	36	0	0	0,4	0,3	7,1	67,1

Cations:

Ca^{2+}	**Mg^{2+}**	**Na^+**	**K^+**	**Fe^{2+}**	**Mn^{4+}**	**As^{2+}**	**Sr^{2+}**
mg/l	mg/l	mg/l	mg/l	mg/l	mg/l	µg/l	mg/l
57	13	61,8	1	1,9	0,7	2	0,2

Others:Pumping at about 100 m

Sample Sa20

Riviera well, 12.03.2013.

Coordinates (WGS84):

E: 18,687806 N: -32,688028

On site parameters:

conductivity	**pH**	**NH_4^+**	**S_2^-**	**temperature**
µS		mg/l	mg/l	°C
528	4,39	0,025	0,01	23,8

Anions:

Cl^-	**$SO4^{2-}$**	**$NO3^-$**	**$PO4^{3-}$**	**F**	**Br^-**	**Si^{2-}**	**HCO3-**
mg/l	mg/l	mg/l	mg/l	mg/l	mg/l	mg/l	mg/l
152	5,5	30	0	0,2	0,4	4,7	12,2

Cations:

Ca^{2+}	**Mg^{2+}**	**Na^+**	**K^+**	**Fe^{2+}**	**Mn^{4+}**	**As^{2+}**	**Sr^{2+}**
mg/l	mg/l	mg/l	mg/l	mg/l	mg/l	µg/l	mg/l
141	14,6	73,4	0,8	0,02	0,06	0	0,04

Sample Sa21

Image Sa21: Irrigation well, line of sight: N, 13.03.2013.

Coordinates (WGS84):

E: 18,708444 N: -32,730417

On site parameters:

conductivity	**pH**	**NH_4^+**	**S_2^-**	**temperature**	**borehole depth**
µS		mg/l	mg/l	°C	m
46,1	6,65	0,025	0,02	28,0	75

Anions:

Cl^-	**$SO4^{2-}$**	**$NO3^-$**	**$PO4^{3-}$**	**F**	**Br^-**	**Si^{2-}**	**HCO3-**
mg/l	mg/l	mg/l	mg/l	mg/l	mg/l	mg/l	mg/l
13	0,9	0,25	0	0,9	0	0,02	0

Cations:

Ca^{2+}	**Mg^{2+}**	**Na^+**	**K^+**	**Fe^{2+}**	**Mn^{4+}**	**As^{2+}**	**Sr^{2+}**
mg/l	mg/l	mg/l	mg/l	mg/l	mg/l	µg/l	mg/l
2,1	1,1	9,5	0,4	4,8	0,3	0	0,009

Others: Hydraulic head at 2,81 m

Sample Sa22

Irrigation well, 13.03.2013.

Coordinates (WGS84):

E: 18,717500 N: -32,716444

On site parameters:

conductivity	pH	NH_4^+	S_2^-	temperature
µS		mg/l	mg/l	°C
613	7,55	0,025	0	24,0

Anions:

Cl^-	$SO4^{2-}$	$NO3^-$	$PO4^{3-}$	F	Br^-	Si^{2-}	HCO3-
mg/l	mg/l	mg/l	mg/l	mg/l	mg/l	mg/l	mg/l
100	26	0	0	0,4	0,2	11,5	195,2

Cations:

Ca^{2+}	Mg^{2+}	Na^+	K^+	Fe^{2+}	Mn^{4+}	As^{2+}	Sr^{2+}
mg/l	mg/l	mg/l	mg/l	mg/l	mg/l	µg/l	mg/l
59,5	10,5	49,2	2,1	0,02	0,03	0	0,41

Others:Pumping at about 20 m, efficiency approximately 100qm/h

Sample Sa23

Image Sa23: Volgersbosdrift well, line of sight: NE, 21.03.2013.

Coordinates (WGS84):

E: 18,689310 N: -32,659806

On site parameters:

conductivity	**pH**	**NH_4^+**	**S_2^-**	**temperature**	**borehole depth**
µS		mg/l	mg/l	°C	m
751	7,73	0,075	0,01	23,9	150

Anions:

Cl^-	**$SO4^{2-}$**	**$NO3^-$**	**$PO4^{3-}$**	**F**	**Br^-**	**Si^{2-}**	**HCO3-**
mg/l	mg/l	mg/l	mg/l	mg/l	mg/l	mg/l	mg/l
100	10,8	2,8	0	0,4	0,2	4,9	-

Cations:

Ca^{2+}	**Mg^{2+}**	**Na^+**	**K^+**	**Fe^{2+}**	**Mn^{4+}**	**As^{2+}**	**Sr^{2+}**
mg/l	mg/l	mg/l	mg/l	mg/l	mg/l	µg/l	mg/l
4,3	7,7	51	1,6	0	0,02	0	0,04

Others:2 Pumps in charge

Sample Sa24

Image Sa24: Vrede Farm well, line of sight: NE, 14.03.2013.

Coordinates (WGS84):

E: 18,683361 N: -32,659806

On site parameters:

conductivity	pH	NH_4^+	S_2^-	temperature	borehole depth
µS		mg/l	mg/l	°C	m
318	4,13	0,05	0	25,7	15

Anions:

Cl^-	$SO4^{2-}$	$NO3^-$	$PO4^{3-}$	F	Br^-	Si^{2-}	HCO3-
mg/l	mg/l	mg/l	mg/l	mg/l	mg/l	mg/l	mg/l
185	22	0,06	0	0,08	0,5	5,8	85,4

Cations:

Ca^{2+}	Mg^{2+}	Na^+	K^+	Fe^{2+}	Mn^{4+}	As^{2+}	Sr^{2+}
mg/l	mg/l	mg/l	mg/l	mg/l	mg/l	µg/l	mg/l
42,2	17,1	69,6	2,3	0,1	0,007	0	0,29

Sample Sa25

Image Sa25: Vrede Farm irrigation well, line of sight: N, 21.03.2013.

Coordinates (WGS84):

E: 18,683200 N: -32,650870

On site parameters:

conductivity	**pH**	**NH_4^+**	**S_2^-**	**temperature**
µS		mg/l	mg/l	°C
1040	7,33	0	0	22,3

Anions:

Cl^-	**$SO4^{2-}$**	**$NO3^-$**	**$PO4^{3-}$**	**F**	**Br^-**	**Si^{2-}**	**HCO3-**
mg/l	mg/l	mg/l	mg/l	mg/l	mg/l	mg/l	mg/l
243	30	4,6	0	0,1	0,6	5,5	48,8

Cations:

Ca^{2+}	**Mg^{2+}**	**Na^+**	**K^+**	**Fe^{2+}**	**Mn^{4+}**	**As^{2+}**	**Sr^{2+}**
mg/l	mg/l	mg/l	mg/l	mg/l	mg/l	µg/l	mg/l
24,8	18,4	117	1,05	0,5	0,05	0	0,19

Others:Pumping at about 80 m

Sample Sa26

Image Sa26: Vrede Farm irrigation pumps inside Krom Antonies River, line of sight: W, 21.03.2013.

Coordinates (WGS84):

E: 18,685120 N: -32,651680

On site parameters:

conductivity	**pH**	**NH_4^+**	**S_2^-**	**temperature**
µS		mg/l	mg/l	°C
1450	7,25	0,05	0	21,0

Anions:

Cl^-	**$SO4^{2-}$**	**$NO3^-$**	**$PO4^{3-}$**	**F**	**Br^-**	**Si^{2-}**	**HCO3-**
mg/l	mg/l	mg/l	mg/l	mg/l	mg/l	mg/l	mg/l
344	42	0,6	0,26	0,07	1	4,4	122

Cations:

Ca^{2+}	**Mg^{2+}**	**Na^+**	**K^+**	**Fe^{2+}**	**Mn^{4+}**	**As^{2+}**	**Sr^{2+}**
mg/l	mg/l	mg/l	mg/l	mg/l	mg/l	µg/l	mg/l
33,9	29,8	177	0,6	0,48	0,08	1	0,26

Sample Sa27

Image Sa27: Pumping well of the northest borehole inside the study area, line of sight: NNW, 14.03.2013.

Coordinates (WGS84):

E: 18,708278 N: -32,615417

On site parameters:

conductivity	**pH**	**NH_4^+**	**S_2^-**	**temperature**
µS		mg/l	mg/l	°C
3310	7,09	0	0	25,6

Anions:

Cl^-	**$SO4^{2-}$**	**$NO3^-$**	**$PO4^{3-}$**	**F**	**Br^-**	**Si^{2-}**	**HCO3-**
mg/l	mg/l	mg/l	mg/l	mg/l	mg/l	mg/l	mg/l
726	245	12,2	0	0,05	2,3	6,5	298,9

Cations:

Ca^{2+}	**Mg^{2+}**	**Na^+**	**K^+**	**Fe^{2+}**	**Mn^{4+}**	**As^{2+}**	**Sr^{2+}**
mg/l	mg/l	mg/l	mg/l	mg/l	mg/l	µg/l	mg/l
184	75	282	7,6	0,03	0,01	0	1,26

Sample Sa28

Image Sa28: Krom Antonies passage at the Riviera Farm, line of sight: SW, 15.03.2013.

Coordinates (WGS84):

E: 18,693056 N: -32,687278

On site parameters:

conductivity	**pH**	**NH_4^+**	**S_2^-**	**temperature**
µS		mg/l	mg/l	°C
1294	7,38	0,05	0	23,0

Anions:

Cl^-	**$SO4^{2-}$**	**$NO3^-$**	**$PO4^{3-}$**	**F**	**Br^-**	**Si^{2-}**	**HCO3-**
mg/l	mg/l	mg/l	mg/l	mg/l	mg/l	mg/l	mg/l
280	43	1,1	0	0,16	0,8	5,1	219,6

Cations:

Ca^{2+}	**Mg^{2+}**	**Na^+**	**K^+**	**Fe^{2+}**	**Mn^{4+}**	**As^{2+}**	**Sr^{2+}**
mg/l	mg/l	mg/l	mg/l	mg/l	mg/l	µg/l	mg/l
45,7	27,6	151	0,8	0,21	0,35	0	0,28

Sample Sa29

Image Sa29: Krom Antonies upstream, line of sight: S, 17.03.2013.

Coordinates (WGS84):

E: 18,737028 N: -32,742750

On site parameters:

conductivity	pH	NH_4^+	S_2^-	temperature
µS		mg/l	mg/l	°C
25,3	7,65	0,025	0	22,7

Anions:

Cl^-	$SO4^{2-}$	$NO3^-$	$PO4^{3-}$	F	Br^-	Si^{2-}	HCO3-
mg/l	mg/l	mg/l	mg/l	mg/l	mg/l	mg/l	mg/l
11	1,4	0	0	0	0,03	4,6	12,2

Cations:

Ca^{2+}	Mg^{2+}	Na^+	K^+	Fe^{2+}	Mn^{4+}	As^{2+}	Sr^{2+}
mg/l	mg/l	mg/l	mg/l	mg/l	mg/l	µg/l	mg/l
1,7	0,8	6,1	0,1	0,04	0,008	0	0,007

Sample Sa30

Image Sa30: Volgersbosdrift well, 19.03.2013.

Coordinates (WGS84):

E: 18,690389 N: -32,620750

On site parameters:

conductivity	**pH**	**NH_4^+**	**S_2^-**	**temperature**	**borehole depth**
µS		mg/l	mg/l	°C	m
467	6,74	0	0,02	24,1	40

Anions:

Cl^-	**$SO4^{2-}$**	**$NO3^-$**	**$PO4^{3-}$**	**F**	**Br^-**	**Si^{2-}**	**HCO3-**
mg/l	mg/l	mg/l	mg/l	mg/l	mg/l	mg/l	mg/l
116	26	0,6	0	0,2	0,3	2,8	36,6

Cations:

Ca^{2+}	**Mg^{2+}**	**Na^+**	**K^+**	**Fe^{2+}**	**Mn^{4+}**	**As^{2+}**	**Sr^{2+}**
mg/l	mg/l	mg/l	mg/l	mg/l	mg/l	µg/l	mg/l
19,8	13,1	50,2	2,4	0	0,1	0	0,13

7.4 Appendix D: Maps

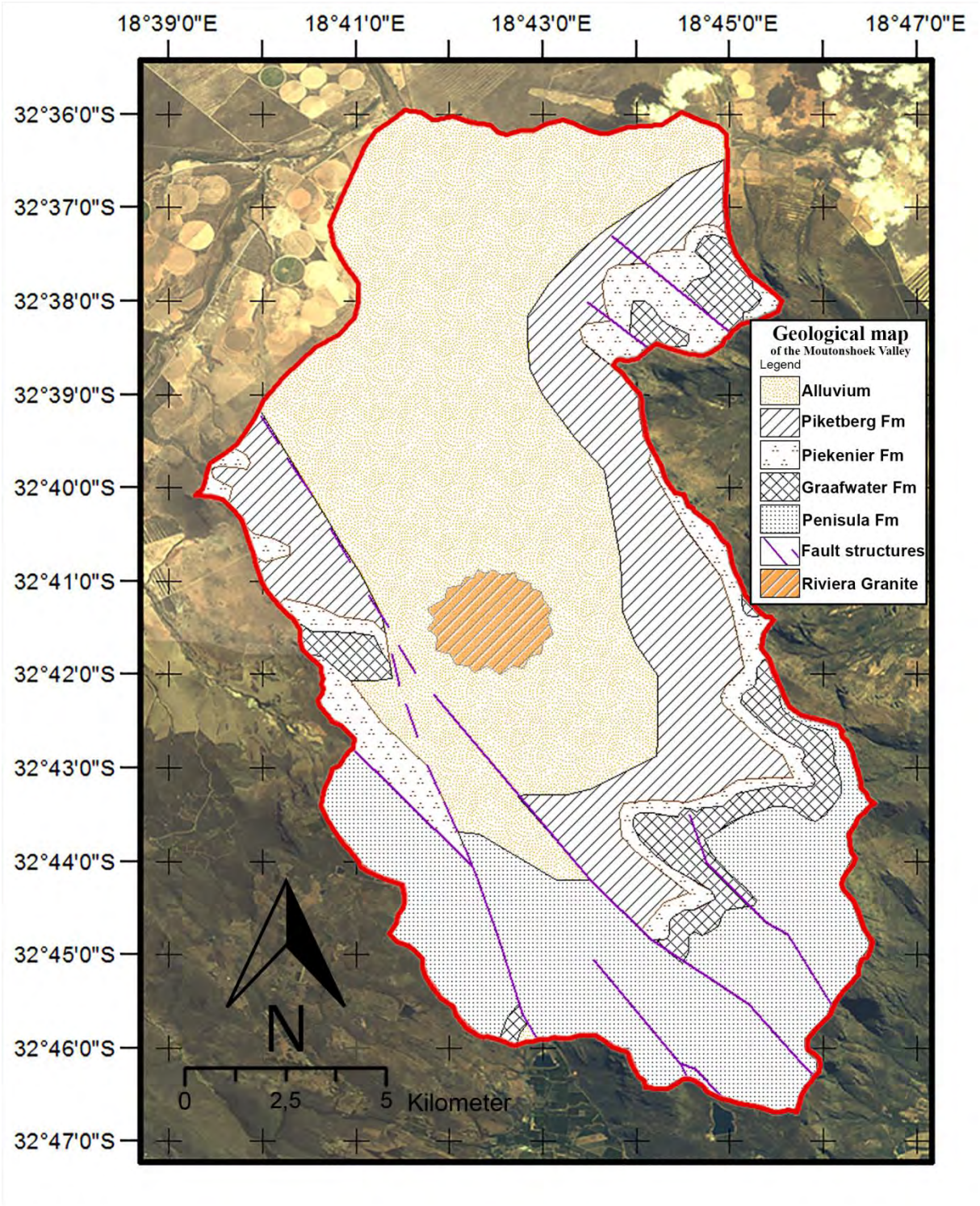

Figure 6: Geological map of the Moutonshoek Valley (after DE BEER 1990 and ROZENDAAL 1994). The estimated shape of the Riviera Granite is not representative. Imagery: LANDSAT prepared with ARCGIS 10.1.

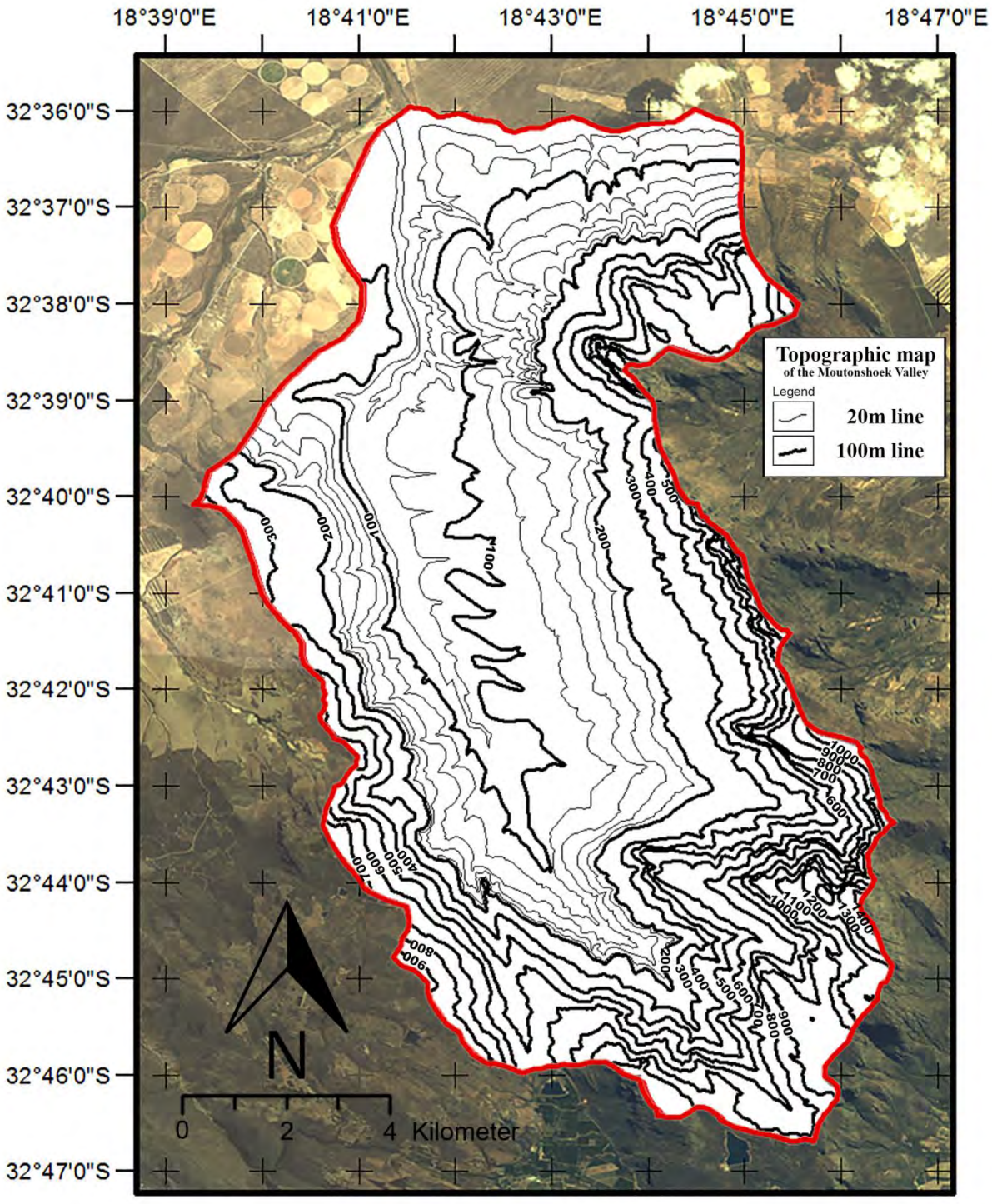

Figure.7: Topographic map of the Moutonshoek Valley. Imagery: LANDSAT prepared with ARCGIS 10.1.

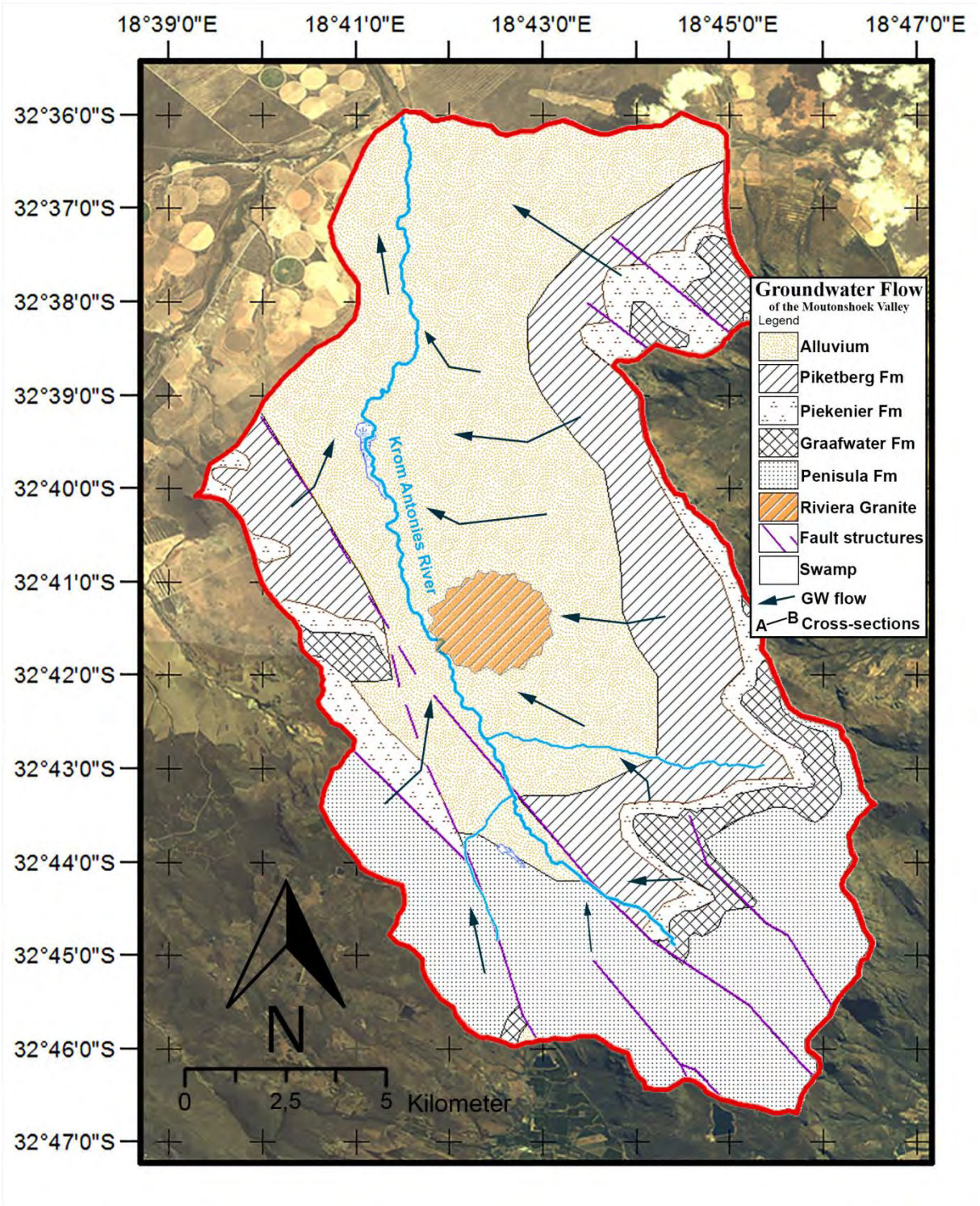

Figure 21: Map of the estimated groundwater flow in Moutonshoek Valley.

7.5 Appendix E: Acknowledgments

Taking samples in the Krom Anonies Catchment in South Africa was successful. The owners of the farms and their employees were hospitable, friendly, helpful and interested in my work at all time. The cooperation with the project partners at Cape Town University was quite nice. They gave me all the equipment I couldn´t bring myself from Germany as it was discussed and helped me out with acid, multimeters, literature and contacts of farm owners and government.

I like to thank my advisor Prof. Dr. Michael Schneider for giving me this interdisciplinary topic in cooperation with the Institute of Geographical Sciences for my master thesis and for his support. Also I want to thank my second advisor Prof. Dr. Brigitta Schütt for giving me the opportunity as a hydrogeoligist to participate in the project *Integrated Watershed Management, Research & Development Capacity Building* of the DAAD. Many thanks to Anette Stumptner, Dr. Stefan Thiemann and Christian, who accompanied me in the catchment, for the help to get in contact with the stakeholders, the great advices and moral support.

Thanks to the staff of the Cape Town University, first of all Prof. Jenny Day as well as Liesl from the laboratory and Soraya of the Traffic department, for the technical support, advices, literature and rent-a-car-support.

The close collaboration with the residents is necessary for a successful data collection. I like to say "Dankie!" to the water user association of the Moutonshoek Valley: Jocobus Smit, for the great trip through the mountains, the interesting conversations with you and your wife in the evenings, the brai and lemon ice tea and the fun we had with your dogs. Jacquie and Bennie van der Merwe for the hospitable residence made us feel at home. Innis Brynard, Danni Coetzee, Halmar Enderstein, Herman Coetzee, Matthys Bothma and Louw Smit as well as their co-workers for the time, support and trustfulness in me and Christian. Thank you for let us make our science on your property and feel so comfortable in our stay. Thanks to Johannes and his wife for the great Roibos tea and Feliciti Strange for let us participating at the conference of the Verlorenvlei Coalition. Many thanks to the staff of the Department of Water Affairs: Mashudu J. Murovhi, Deputy Director of the Department of Water Affairs and his secretary Timbisa for the permission to make studies and take samples in the study area and for the invitation to the conference of the National Water Week. Thanks to Bryan Dysson and Johann van Sale for the interesting conversations and data.

I would also like to thank Dr. Andreas Winkler for his support, especially in relation to hydro-chemical issues and Elke Heyde for the performed laboratory analyzes. Thanks to my fellow students for the funny and inspiring hours in the computer room.

Last but not least I like to thank my friends and family for the moral support you gave me in exhausting times and in years of studying.

7.6 Appendix F: References

Published literature

[Belcher and Kisters 2003] Belcher, Richard W.; Kisters, Alexander F.M.:
Lithostratigraphic correlations in the western branch of the Pan-African Saldania belt, South Africa: the Malmesbury Group revisited. South African Journal of Geology, 2003, Volume 106, pages 327-342, doi:10.2113/106.4.327

[Compton 2004] Compton, John S.:
The Rocks & Mountains of Cape Town. Cape Town: Double Story. 2004. ISBN 978-1-919930-70-1

[Conrad 2004] Conrad, Julian; Nel, Jaco; Wentzel, Johan:
The challenges and implications of assessing groundwater recharge: A case study - northern Sandveld, *Western Cape, South Africa*. Water SA Vol. 30 No. 5 (Special Edition), ISSN 0378-4738

[Craig et al 2007] Craig, Ian; Aravinthan, Vasantha; Baillie, Craig, Beswick, Alan; Barnes, Geoff; Bradbury, Ron; Connell, Luke; Coop, Paul; Fellows, Christopher; Fitzmaurice, Li; Foley, Joe; Hancock, Nigel; Lamb, David; Morrison, Pippa; Misra, Rabi; Mossad, Ruth; Pittaway, Pam; Prime, Emma; Rees, Steve; Schmidt, Erik; Solomon, David; Symes, Troy; Turnbull, David:
Evaporation, Seepage and Water Quality Management in Storage Dams: A Review of Research Methods. Environmental Health, Vol. 7, No . 32007

[Etzold 2012] Etzhold, Cay; Weiler-Wohlfarth, Margot:
Welcome to Africa, The cooperation of African and German universities at a glance. DAAD leaflet, 27 pages, Köllen Druck & Verlag GmbH, Bonn

[Förch and Schütt 2004] Förch, Gerd; Schütt, Brigitta:
Watershed Management - an Introduction. FWU, Vol. 4, Lake Abaya Research Symposium 2004 - Proceedings

[Frimmel and Fölling 2004] Frimmel, Hartwig E.; Fölling, Peter G.:
Late Vendian Closure of the Adamastor Ocean: Timing of Tectonic Inversion and Syn-orogenic Sedimentation in the Gariep Basin. Gondwana Research
2004 | 7 | 3 | 685-699

[McCarthy and Rubridge 2005] McCarthy, T.; Rubridge, B.:

The Story of Earth and Life. A Southern African Perspective on a 4.6-Billion-Year Journey. 334 pp. Cape Town: Struik Publishers/Johnnic Publishing Group, 2005. ISBN 1 77007 148 2.

[Nölte 2002] Nölte, Joachim:

ICP Emissionsspektrometrie für Praktiker: Grundlagen, Methodenentwicklung, Anwendungsbeispiele. Wiley-VHC-Verlag, 271 pages., Germany 2002, ISBN: 978-3-527-66076-6

[Perold and Theart 2007] Perold, J.; Theart, H.F.J.:

Genetic model for a residual brick clay deposit, western Cape Province, South Africa. South African Journal of Geology, 2007, Volume 110, pages 561-574, doi: 10.2113/gssajg.110.4.561

[Parsons 2004] Parsons, Roger

Surface Water - Groundwater Interaction in a Southern African Context -A Geohydrological Perspective- Water Research Commission Report No. TT 218/03, January 2004

[Rozendasl et al 1994] Rozendasl, A.; Gresse, P.G.; De Beer, C.:

Structural setting of the Riviera W-Mo deposit, Western Cape, South Africa. South African Journal of Geology, June 1994, v. 97, p. 184-195

[Rozendaal et al 2009] Rozendaal, A.; Moyen, J.:

The Riviera Deposit: Endo-skarn and Vein-hosted W-MO-REE Mineralization in I-type Granites of the Cape Granite Suite, South Africa. American Geophysical Union, Spring Meeting 2009, abstract #V13B-02

[Schulze 1997] Schulze, Roland:

South African Atlas of Agrohydrology and –Climatology, Water Research Commission, Report TT82/96, Pretoria, ISBN: 1-86845-271-9.

[Theron et al 1992] Theron, J.N.; Gresse, P.G.; Siegfried, H.P; Rogers, J.:

Explanation sheet 3318 – The Geology of the Cape Town Area. Geological Survey, Department of Mineral and Energy Affairs, Government Printer, Pretoria 1992. ISBN 978-0-621-14284-6

[Vos and Tankard 1980] Vos, Richard G.; Tankard, Anthony J.:
Braided fluvial sedimentation in the lower paleozoic Cape basin, South Africa. Sedimentary Geology Vol. 29 p.171-193, 1981. Elsevier Scientific Publishing Company, Amsterdam

[WHO 2011] World Health Organisation:
Guidelines for Drinking-water Quality. Fouth Edition, 264 pages, ISBN 978 92 4 154815 1

[Weiss 1995] Weiss, Joachim:
Ion Chromatography. Second Edition, 476 pages. John Wiley & Sons, 2008. ISBN 3-527-28698-5

Unpublished reports

[Belcher 2003] Belcher, Richard W.:
Tectonostratigraphic evolution of the Swartland region and aspects of orogenic lode-gold mineralisation in the Pan-African Saldania Belt, Western Cape, South Africa. Unpublished Ph.D thesis, University of Stellenbosch, South Africa, 302pp.

[Conrad, 2012] Conrad, Julien:
Geohydrological assessment of the Moutonshoek Area and environs – Sandveld, Western Cape. GEOSS Report No: G2012/08-01, GEOSS Project No: 2011_08-769

[Kanen 2001] Kanen, R.A.:
Distinguishing between "S" and "I" type granites. Internet-source 28.11.2014: http://www.geologynet.com/granitetypes.htm

[Villaros, 2006] Villaros, Amaud:
The Cape Granite Suit. a short introduction. Internet source (July 2014): http://academic.sun.ac.za/earthSci/undergraduate/G314/The%20Cape%20Granite%20Suite.doc

[Visser, 2009] Visser, D.; Goes, M.; Dennis, I.:
Preliminary Assessment of Impact of the Proposed Riviera Tungsten Mine on Groundwater Resources. Report No 392947 Draft V2.

Internet sources:

[Council for Geoscience SA]:

http://www.geoscience.org.za/ (January 2015)

Statement of authorship - Selbstständigkeitserklärung

Hiermit erkläre ich, dass ich die vorliegende Masterarbeit selbstständig verfasst habe. Es wurden keine anderen als die in der Arbeit angegebenen Quellen und Hilfsmittel benutzt. Die wörtlichen oder sinngemäß übernommenen Zitate habe ich als solche kenntlich gemacht.

I hereby confirm that this thesis is my own work and none but the mentioned sources have been used.

Heinrich Hecht

_____

Berlin, der 28.02.2015